UNIVERSITÉ DU QUÉBEC

MÉMOIRE

PRÉSENTÉ À

L'UNIVERSITÉ DU QUÉBEC À CHICOUTIMI

COMME EXIGENCE PARTIELLE

DE LA MAÎTRISE EN SCIENCES DE LA TERRE

PAR

DANY SAVARD

ÉTUDE DU COMPORTEMENT GÉOCHIMIQUE DU SÉLÉNIUM, SA RELATION AVEC LE SOUFRE DANS LE BUSHVELD (AFRIQUE DU SUD) ET DÉVELOPPEMENT DES TECHNIQUES ANALYTIQUES

FÉVRIER 2010

Bibliothèque
Paul-Émile-Boulet

UQAC
Université du Québec
à Chicoutimi

Mise en garde/Advice

Afin de rendre accessible au plus grand nombre le résultat des travaux de recherche menés par ses étudiants gradués et dans l'esprit des règles qui régissent le dépôt et la diffusion des mémoires et thèses produits dans cette Institution, **l'Université du Québec à Chicoutimi (UQAC)** est fière de rendre accessible une version complète et gratuite de cette œuvre.

Motivated by a desire to make the results of its graduate students' research accessible to all, and in accordance with the rules governing the acceptation and diffusion of dissertations and theses in this Institution, the **Université du Québec à Chicoutimi (UQAC)** is proud to make a complete version of this work available at no cost to the reader.

L'auteur conserve néanmoins la propriété du droit d'auteur qui protège ce mémoire ou cette thèse. Ni le mémoire ou la thèse ni des extraits substantiels de ceux-ci ne peuvent être imprimés ou autrement reproduits sans son autorisation.

The author retains ownership of the copyright of this dissertation or thesis. Neither the dissertation or thesis, nor substantial extracts from it, may be printed or otherwise reproduced without the author's permission.

RÉSUMÉ

L'étude du comportement géochimique du sélénium et sa relation avec le soufre dans les roches du complexe du Bushveld (Afrique du Sud) sont présentées dans ce mémoire. La détermination quantitative de ces deux éléments chimiques a été réalisée dans 157 échantillons provenant de la suite litée de Rustenberg (Bushveld) et des roches de la marge de l'intrusion représentant les magmas parentaux. Étant donné que la plupart des roches analysées contiennent de très faibles teneurs en soufre et en sélénium, il a d'abord été nécessaire de mettre au point les techniques d'analyses appropriées. Au cours du développement de ces techniques, des matériaux de références géologiques internationales (MRGI) ont été analysés pour valider les résultats afin d'assurer une qualité constante et traçable lorsque cela est possible. Vingt-six MRGI ont été analysés pour le sélénium et vingt-neuf pour le soufre. Chaque technique développée a été publiée dans un journal scientifique arbitré et les résultats sont en accord avec ceux disponibles dans la littérature et/ou sur les certificats d'analyses. De plus, les résultats des analyses du sélénium obtenus à l'UQAC dans les MRGI ont été greffés aux données disponibles dans la littérature et des traitements statistiques ont été réalisés pour produire un nouvel article décrivant les MRGI utiles, en termes de Se, servant à valider et à contrôler les déterminations. Une fois établies les bases analytiques, les résultats obtenus dans l'étude du Bushveld ont mené à l'élaboration de trois modèles pour expliquer les relations géochimiques observées. Le premier modèle suggère que les sulfures qui étaient présents dans l'empilement cristallin aient pu migrer dans les roches encaissantes ou au centre de l'intrusion. Le deuxième modèle suggère quant à lui que le magma ait été saturé en soufre en profondeur et que, durant le transport, des sulfures aient été emprisonnés dans de petites cavités présentes dans la matrice cristalline-visqueuse. Finalement, le troisième modèle suggère que les roches aient été appauvries en S et en Se à température élevée après la solidification de l'intrusion. À ce jour, il est impossible d'évaluer lequel de ces modèle est le plus plausible, mais les deux premiers modèles ont une implication importante pour l'exploration de nouvelles ressources. En effet, si l'un des modèles s'avère être exact, cela signifierait qu'il y a dans le centre de l'intrusion ou à sa périphérie une réserve en métaux de base importante et possiblement aussi en métaux précieux, associée aux sulfures. Il a également été possible de calculer un coefficient de partage du Se dans les sulfures à partir des roches de la portion supérieure de l'intrusion. Les proportions Se/Cu augmentent avec la stratigraphie, ce qui suggère que le coefficient de partage du Se dans les sulfures est plus bas que celui du Cu (1,200 versus 1,700). Le coefficient de partage aide à comprendre le comportement géochimique des éléments et leur relation avec les sulfures et les autres phases présents dans les roches.

AVANT-PROPOS

Le modèle de ce mémoire de maîtrise en sciences de la Terre est sous forme de publications. Quatre manuscrits ont été publiés dans des journaux scientifiques internationaux avec un comité de lecteurs: Savard *et al.* (publié dans la revue *Talanta* en 2006); Bédard *et al.* (publié dans *Journal of Geostandards and Geoanalytical Research* en 2008), Barnes *et al.* (publié dans la revue Mineralium *Deposita* en 2009) et Savard *et al.* (publié dans *Journal of Geostandards and Geoanalytical Research* en 2009). L'ensemble de ces quatre publications forme le corps de ce mémoire. Les manuscrits ont été rédigés et publiés en anglais et sont fournis en annexe. Une introduction générale en français est présentée pour mettre en perspective l'ensemble du projet à travers chacune des quatre parties. Un résumé est présenté pour chaque manuscrit ainsi que les contributions scientifiques relatives du candidat à la maîtrise et de ses collaborateurs. Les contributions intellectuelles et physiques de chacun des auteurs sont énumérées afin de souligner les connaissances et les habiletés acquises lors de chacun de ces projets. Une conclusion générale en français est également présentée.

TABLE DES MATIÈRES

LISTE DES ANNEXES

ÉQUIPE DE SUPERVISION

Les travaux liés au présent ouvrage scientifique ont été réalisés au Laboratoire d'analyse des Matériaux Terrestres (LabMaTer) de l'Université du Québec à Chicoutimi (UQAC) sur une période de quatre années (2004-2008). La supervision a été assurée par madame Sarah-Jane Barnes, professeure-chercheure à l'UQAC et titulaire de la Chaire de Recherche Canada en Métallogénie Magmatique, monsieur Paul Bédard (Ing. PhD), responsable du laboratoire LabMaTer de l'UQAC ainsi que monsieur Wolfgang Maier (PhD), professeur-chercheur à l'Université Western Australia lors de la réalisation des travaux et aujourd'hui professeur-chercheur à l'Université d'Oulu (Finlande).

INTRODUCTION GÉNÉRALE

L'ensemble de ce projet touche deux grandes sphères du domaine des sciences de la Terre, c'est-à-dire l'analyse quantitative en laboratoire et l'interprétation géochimique des résultats obtenus. Le soufre (S) et le sélénium (Se) sont les deux principaux éléments qui ont été analysés et étudiés au cours de ce projet.

Le S et le Se peuvent servir de traceurs économiques. Les propriétés physico-chimiques des deux éléments sont discutées dans les publications, selon le contexte. Brièvement, les deux éléments font partie de la famille *VIA* du tableau périodique et sont tous deux classifiés comme des éléments chalcophiles (Goldschmidt, 1954). De façon générale, les deux éléments ont des comportements géochimiques similaires (valence et rayon ionique compatible) et peuvent notamment former des complexes volatiles, ce qui explique en partie leur faible abondance sur la Terre. Le sélénium que l'on retrouve, en nanogrammes par gramme sur l'ensemble de la Terre, est environ 3000 fois moins abondant que le soufre (McDonough et Sun, 1995). En géologie magmatique, les concentrations les plus élevées de soufre et de sélénium se retrouvent dans les minéraux sulfurés (les sulfures) comme élément essentiel et comme élément trace, respectivement. Dans les systèmes magmatiques, la compatibilité du soufre dans les minéraux silicatés et les oxydes est très faible. De plus, le soufre s'associe avec les métaux de base tels que le fer, le nickel, le cuivre, l'or et les métaux précieux du groupe du platine (ÉGP) lors du refroidissement des magmas.

En géologie économique, ces minéraux sont d'une importance capitale puisqu'ils concentrent les métaux précieux qui, à leur tour, peuvent être accumulés dans un volume restreint qui pourra éventuellement devenir un gisement économique si leur quantité est assez importante. De plus, les métaux précieux tels que l'or et les éléments du groupe du platine tendent également à s'associer aux sulfures. Lorsque la quantité de métaux de base et/ou précieux est suffisamment concentrée pendant les processus magmatiques, il y a alors la formation d'un gisement de type magmatique. C'est notamment le cas du complexe du Bushveld en Afrique du Sud qui est au cœur des travaux présentés ici. Le complexe du Bushveld, formé il y a 3,5 milliards d'années, est une intrusion magmatique de taille exceptionnelle (200 km x 300 km).

Tout comme les métaux de base et les ÉGP, le sélénium s'associe aux sulfures. Le sélénium peut se substituer au soufre dans les réseaux cristallins et, comme déjà mentionné, les comportements géochimiques du soufre et du sélénium sont très similaires, excepté dans le cas de leur mobilité relative. Le sélénium pouvant être légèrement moins mobile que le soufre dans les systèmes géologiques à basse température (e.g. Dreibus et al, 1995), cette distinction peut alors devenir un outil pour étudier les transformations géochimiques que la roche a pu subir, en comparant les proportions de soufre et de sélénium présentes dans les roches du magma parent avec une roche qui a subi une transformation post-cristallisation. Si la roche étudiée montre une proportion plus élevée de S/Se que la roche mère, cela peut suggérer que la roche a subi un gain en soufre. Dans certains types de gisement de nickel, l'apport supplémentaire de soufre provient de la roche encaissante et est essentiel à la formation de gisement (e.g. Naldrett et al, 1984). Si, au contraire, la proportion S/Se est moins élevée que dans la roche mère, alors cela suggère que la roche étudiée peut avoir perdu

plus de soufre que de sélénium. Dans le cas du Bushveld, une perte de soufre importante pourrait en partie expliquer les fortes concentrations de métaux précieux par rapport à la faible quantité de soufre présent, ce qui est un des arguments de controverse de la minéralisation unique du Bushveld (Cawthorn, 1999). Malgré l'utilité du ratio S/Se, il existe très peu d'ouvrage scientifique basée sur cet argument. Ce manquement est en partie dû à la faible abondance du Se dans les matériaux géologiques. Par exemples, la teneur moyenne de sélénium dans la croûte Terrestre est de seulement 0.05 μg/g (Taylor et McLennan, 1985). Le but de cette étude est donc de faire l'analyse quantitative des concentrations de soufre et de sélénium dans une série de roches provenant du Bushveld et d'une série de roches identifiées comme représentant les magmas parentaux du Bushveld. Le but étant de vérifier si les proportions S/Se pourraient indiquer une perte de soufre. Les résultats de cette étude sont présentés dans le troisième ouvrage scientifique (Annexe A : Barnes *et al.*, 2009).

Le Bushveld est économiquement exploité depuis plusieurs décennies pour ses métaux de base variés (nickel, vanadium, chrome, titane, etc.), mais ce sont surtout les nombreux sites d'exploitation des métaux précieux du groupe du platine (ÉGP, platine, palladium, ruthénium, rhodium, iridium et osmium) qui permettent au Bushveld d'être un gisement de classe mondiale. Les ÉGP du Bushveld se retrouvent principalement dans de minces horizons, de quelques centimètres à quelques dizaines de mètres d'épaisseur, s'étalant latéralement sur presque l'entière étendue de l'intrusion. Ces horizons sont appelés « reefs » et les plus connus sont le Platreef et le Merensky Reef. Le Platreef est situé dans le lobe nord de l'intrusion et n'est pas abordé dans cette étude. Le Merensky Reef a une épaisseur moyenne d'environ 1-2 mètres et se situe à environ 2000 mètres de la base de l'intrusion. Son imposant volume et son contenu économique

exceptionnel en ÉGP font du Merensky Reef un des sites métallogénique les plus étudiés. Aucun modèle géologique ne peut complètement expliquer la formation du Merensky Reef à ce jour, ce qui en rehausse l'intérêt scientifique.

Comme les teneurs en soufre et en sélénium sont très basses dans les roches du Bushveld, les méthodes d'analyses traditionnelles (titration, activation neutronique, absorption atomique, etc.) ne peuvent convenir car elles présentent des limites de détection trop élevées. De plus, l'analyse moderne par spectrométrie de masse (ICP-MS) est difficile, car la présence d'argon, qui est utilisé pour le plasma, ainsi que d'oxygène et d'autres gaz et de particules élémentaires crée des interférences poly-atomiques qui faussent le signal du sélénium. Les deux éléments étant volatils à basse température, cela limite la préparation des échantillons pour la mise en solution en acides à haute température. C'est donc pour des raisons analytiques qu'il a d'abord été nécessaire de mettre au point des techniques d'analyse appropriées pour la quantification en basses teneurs du sélénium et du soufre dans les matériaux géologiques. Cette problématique supplémentaire a donc mené à la rédaction de deux des quatre ouvrages scientifiques présentés dans ce mémoire (Annexe B : Savard *et al.*, 2006 et Annexe C : Bédard *et al.*, 2008).

À travers le développement des techniques d'analyse, de nombreux obstacles ont dû être franchis. Un de ces obstacles est la validation des techniques puisque la disponibilité des matériaux de référence certifiés pour le soufre ou le sélénium est très limitée, voire non-disponible étant donnée les difficultés analytiques mentionnées plus haut. Il existe néanmoins des matériaux de référence qui ont été caractérisés dans divers ouvrages scientifiques disponibles dans la littérature. Ces valeurs informatives ont permis de comparer les résultats obtenus à l'UQAC afin de valider les techniques

pendant leur développement. De nombreuses analyses ont été réalisées sur divers matériaux de référence au cours du développement des techniques et également pendant les analyses sur les roches du Bushveld dans le but d'en valider les résultats (Annexe D : Savard et *al.*, 2009). Ce dernier ouvrage scientifique propose une compilation exhaustive des teneurs en sélénium disponibles dans la littérature de plusieurs matériaux de référence. Les concentrations obtenues à l'UQAC y ont été greffées. Ainsi, des traitements statistiques pour 26 matériaux de références sont présentés pour qualifier et classifier ces matériaux selon le consensus des déterminations disponibles dans la littérature. Ce quatrième ouvrage scientifique devient donc un outil essentiel pour les scientifiques ou les entreprises qui travailleront sur la détermination du sélénium dans les matériaux géologiques.

CHAPITRE I

DÉVELOPPEMENT DE LA TECHNIQUE D'ANALYSE DU SÉLÉNIUM PAR PRÉ-CONCENTRATION SUR FIBRE DE COTON THIOL ET ANALYSE PAR ACTIVATION NEUTRONIQUE (SE/TCF-INAA)

Titre du manuscrit :

TCF selenium preconcentration in geological materials for determination at sub-μg g^{-1} with INAA (Se/TCF-INAA).

Auteurs :

Dany Savard, L. Paul Bédard & Sarah-Jane Barnes

Source :

Talanta (2006), No 70 : 566–571.

Résumé :

Dans les matériaux géologiques, les concentrations de sélénium (Se) peuvent varier entre 1 ng/g et 0.1 %. Le cycle géochimique du Se dans les roches est peu connu et la difficulté à quantifier le Se en basse teneur (moins de 1 μg/g) en est la principale raison. Le développement d'une technique d'analyse appropriée pour la détermination du Se dans les matériaux géologiques devient donc une clé pour l'avancement des

connaissances sur le cycle géochimique du sélénium. La méthode qui consiste à pré-concentrer le Se sur la fibre de coton thiol (TCF) pour ensuite être quantifié par absorption atomique munie d'une fournaise au graphite (GFAAS) a été modifiée pour la détermination par activation neutronique (INAA). La technique modifiée implique la mise en solution des échantillons avec un mélange d'acides et d'oxydant (HF, HNO_3 et H_2O_2) et l'évaporation à basse température (55-60 °C) pour éviter la perte de Se par volatilisation. Le Se^{+6} est réduit en Se^{+4} en ajoutant du HCl (6M) au résidu séché, puis la solution est chauffée avec le couvercle fermé dans un bain-marie à 95-100 °C. La solution est ensuite diluée avec de l'eau distillée pour ajuster le HCl à 0.6M et est ensuite passée dans le TCF pour collecter le Se. Le TCF est rincé et placé dans une capsule de polyéthylène pour ensuite être irradié au réacteur SLOWPOKE II (École Polytechnique de Montréal) pendant 30 secondes à un flux de neutrons de $10^{15} m^{-2} s^{-1}$. Le pic à 162 keV du ^{77m}Se est lu pendant 20 secondes après un temps de décroissance de 20 secondes.

La quantité d'échantillon nécessaire à l'analyse est déterminée par deux facteurs en compétition. Pour obtenir des limites de détection plus basses, une plus grande quantité d'échantillon est utilisée. Cependant, le TCF peut devenir saturé en éléments chalcophiles quand la masse de l'échantillon est augmentée. La quantité de soufre présent dans l'échantillon est un bon indicateur de la quantité de sélénium et d'éléments chalcophiles. Dans les échantillons pauvres en soufre (<100 μg/g), des tests on été effectués avec 3g d'échantillon et la limite de détection est de 2 ng/g. Dans les échantillons riches en soufre tels que les sulfures massifs (>10 % S), une quantité de 0.05g d'échantillon permet d'éviter la saturation du TCF et offre une limite de détection convenable de 120 ng/g pour les échantillons à haute teneur en Se, en S et en éléments

chalcophiles. La technique de détermination du Se par TCF, suivie par l'INAA (Se/TCF-INAA) comporte des avantages notables : elle est plus rapide que par la technique d'absorption atomique munie d'une fournaise au graphite, possède des limites de détection plus basses, ne cause pas d'interférences majeures, si déterminée par l'ICP-MS, et l'étape de désorption du Se, qui peut être hasardeuse, n'est pas nécessaire par INAA. Le présent ouvrage scientifique porte sur la détermination du Se dans 8 matériaux géologiques de référence de diverses natures et les résultats sont en accord avec ceux disponibles dans la littérature. Au moment d'écrire ces lignes soit trois ans après la publication, l'ouvrage scientifique comportait déjà 8 citations dans d'autres ouvrages scientifiques. (Voir l'annexe B pour le manuscrit original.)

Contribution des auteurs :

1er auteur : Dany Savard :

-Développement de la technique d'analyse (projet de fin d'études du baccalauréat en génie géologique, UQAC, 2005);

-Analyses en laboratoire du sélénium;

-Rédaction du résumé, de l'introduction, de la description expérimentale de la technique d'analyse, de la discussion et de la conclusion;

-Mise en forme de l'article suivant les critères de l'éditeur.

2^{ième} auteur : L. Paul Bédard :

-Conseils au développement analytique de la technique;

-Conseils à la rédaction de l'ensemble du manuscrit.

3^{ième} auteur : Sarah-Jane Barnes :

-Planification et direction du projet;

-Aide à la rédaction de l'ensemble du manuscrit.

CHAPITRE II

DÉVELOPPEMENT DE LA TECHNIQUE D'ANALYSE DU SOUFRE DANS LES MATÉRIAUX GÉOLOGIQUES PAR SPECTROMÉTRIE INFRAROUGE AVEC UN APPAREIL HORIBA EMIA-220V S-C ANALYZER

Titre du manuscrit :

Total sulfur concentration in geological reference materials by elemental infrared analyser.

Auteurs :

L. Paul Bédard, Dany Savard & Sarah-Jane Barnes

Source :

Journal of Geostandards and Geoanalytical Research (2008), vol. 32-2 : 203-208.

Résumé :

Le soufre total est un analyte pour lequel il existe très peu de déterminations publiées, bien que cet élément soit très important. (Par exemple, c'est un élément majeur de la plupart des minerais : un gaz très important dans le problème de réchauffement global et un participant actif au problème des eaux acides). La plupart des matériaux de référence certifiés ont des données sur le soufre de très mauvaise qualité, avec des

écarts-types relatifs (RSD) de l'ordre de 30 à 50%, même pour des concentrations supérieures à 100 µg g-1, ce qui compromet leur utilisation comme calibrant. Afin de fournir des résultats assortis de très faibles RSD, le soufre a été mesuré dans vingt-neuf matériaux de référence certifiés avec un analyseur S/C élémentaire de dernière génération, en utilisant des fragments de métal (matériaux de référence certifiés ayant un lien de traçabilité) et du soufre de qualité analytique pour les échantillons les plus concentrés. Les paramètres analytiques (poids de l'échantillon, dégazage du creuset, stratégie de calibration, etc.) ont été optimisés via une série de tests. Nos résultats sont en accord avec les valeurs données pour les matériaux de référence par leurs organismes de certification respectifs. La concentration mesurée (129±13 µg g^{-1} S) pour CCRMP SY-2, qui a été proposée comme matériau de référence pour le soufre, est en accord avec la valeur actuelle de 122±3.7 µg g^{-1} S. (Voir l'annexe C pour le manuscrit original.)

Contribution des auteurs :

1er auteur : L.Paul Bédard :

-Planification et direction du projet;

-Rédaction de l'ensemble du manuscrit, tableaux et figures;

-Analyses en laboratoire des tests d'optimisation.

2ième auteur : Dany Savard :

-Analyses en laboratoire des résultats présentés;

-Élaboration de la technique d'analyse pour les matériaux de hautes teneurs;

-Aide à l'élaboration de la technique d'analyse pour les matériaux de basses teneurs;

-Contribution à la rédaction sur la partie expérimentale;

-Recherche bibliographique.

3^{ième} auteur : Sarah-Jane Barnes :

-Correction du manuscrit.

CHAPITRE III

ÉTUDE DU COMPORTEMENT GÉOCHIMIQUE DU SÉLÉNIUM DANS LE BUSHVELD (AFRIQUE DU SUD)

Titre du manuscrit :

Selenium and sulfur concentrations in the Bushveld Complex of South Africa and implications for formation of the platinum-group element deposits.

Auteurs :

Sarah-Jane Barnes, Dany Savard, Wolfgang D. Maier & L. Paul Bédard

Source :

Mineralium Deposita (2009), vol. 44 (6) : 647-663.

Résumé :

Ce troisième ouvrage scientifique porte sur les différentes relations entre le soufre (S) et le sélénium (Se) dans les roches provenant de deux forages de la suite litée de Rustenberg (complexe du Bushveld, Afrique du Sud). Leur relation avec le cuivre (Cu - un élément constituant et compatible dépendant du sulfure) et le lanthane (La - un élément incompatible dans les sulfures) est également présentée. Au total, 157 analyses de Se et 124 analyses de S ont été réalisées au LabMaTer de l'UQAC. Les

concentrations de lanthane (La), de cuivre (Cu) et une partie des concentrations en soufre ont été préalablement déterminées et sont issues d'autres ouvrages scientifiques. Le but premier de ce travail est de déterminer quelles phases contrôlent la distribution de ces éléments. Le S, le Se et le Cu montrent une corrélation positive mais le La ne montre pas de corrélation. Dans la plupart des cas, les concentrations de S, Se et Cu dans les roches contenant plus de 800 µg/g de soufre peuvent être modélisées par la ségrégation d'un liquide sulfuré de fer, de nickel et de cuivre dans un magma cristallisant en fractionnement. À mesure que le magma évolue, le Se et le Cu ont été appauvris dans le magma résiduel et les ratios S/Se et S/Cu augmentent dans la stratigraphie de ces roches. Le ratio Se/Cu est plus élevé dans les roches les plus évoluées, ce qui suggère que le Se a un coefficient de partage un peu plus élevé que le Cu (1200 versus 1700). La « Lower Zone » et la « Lower Critical Zone » du complexe contiennent en moyenne 99 µg/g de S seulement. Ces basses teneurs ont permis à certains auteurs de suggérer que ces roches ne contenaient pas de cumulats de sulfures malgré le fait que ces roches soient légèrement enrichies en éléments du groupe du platine (ÉGP). Ces échantillons ont des proportions S/Se similaires aux roches riches en S et les ratios S/La et Se/La sont plus élevés que ceux du magma source, suggérant que des cumulats de sulfures sont présents malgré les basses concentrations en S. Trois modèles sont possibles pour expliquer les basses teneurs en S des roches de la « Lower Zone » et de la « Lower Critical Zone »: a) les sulfures qui étaient présents dans l'empilement cristallin ont migré dans les roches encaissantes ou au centre de l'intrusion; b) le magma était saturé en soufre en profondeur et, durant le transport, des sulfures ont été emprisonnés dans la matrice cristalline, c) les roches ont été appauvries en S et en Se à température élevée. Il est difficile pour l'instant d'évaluer lequel de ces modèles est le

plus plausible, mais il est important de souligner que les deux premiers modèles peuvent avoir une implication économique car ils pourraient mener à la découverte d'une éventuelle réserve en métaux économiques logée au centre de l'intrusion ou à sa périphérie. (Voir l'annexe A pour le manuscrit original.)

Contribution des auteurs :

1er auteur : Sarah-Jane Barnes :

-Direction et supervision du projet;

-Rédaction de la mise en contexte régionale des résultats interprétés.

2ième auteur : Dany Savard :

-Analyses en laboratoire du sélénium et du soufre;

-Production de tous les tableaux, figures et statistiques;

-Rédaction du contexte géologique, de la description analytique, de la description et de l'interprétation des résultats, ainsi que de la liste de références.

3ième auteur : Wolfgang Maier :

-Critique constructive et conseils sur les parties interprétation et discussion.

4ième auteur : L. Paul Bédard :

-Révision du contenu de l'ensemble du manuscrit.

CHAPITRE IV

CONCENTRATION DU SÉLÉNIUM DANS 26 MATÉRIAUX DE RÉFÉRENCE : NOUVELLES DÉTERMINATIONS ET TENEURS SUGGÉRÉES

Titre du manuscrit :

Selenium concentrations in twenty-six geological reference materials: new determinations and proposed values.

Auteurs :

Dany Savard, L. Paul Bédard & Sarah-Jane Barnes

Source :

Journal of Geostandards and Geoanalytical Research (2009), vol. 33-2 : 249-252.

Résumé :

L'intérêt de déterminer la concentration du sélénium dans les roches augmente parce que cet élément est un outil pour l'exploration des métaux de base et des métaux précieux. Le sélénium est un élément méconnu en géochimie étant donné les nombreuses difficultés à analyser cet élément. Une conséquence de ces difficultés s'exprime par le nombre restreint de matériaux de référence géologique internationaux (MRGI) présentant une teneur certifiée ou assignée. La capacité de la plupart des

laboratoires à déterminer la teneur en sélénium est inadéquate ou inexistante et la « bonne pratique », tel que proposé par Kane et Potts (2007) pour obtenir des valeurs robustes ne peut être appliquée. Pour contrer ce problème, le sélénium a été déterminé par pré-concentration sur fibre de coton thiol suivi de l'analyse par activation neutronique (technique du Se/TCF-INAA) dans 26 MRGI et un matériel de contrôle de la qualité (KPT-1). Ces résultats ont ensuite été utilisés conjointement avec ceux publiés dans la littérature pour évaluer la concentration en sélénium de ces matériaux de référence. Des statistiques fiables ont pu être développées pour 7 MRGI, avec des écart-types relatifs équivalents ou mieux à ceux de la fonction d'Horwitz, et des teneurs fiables (consensus) ont été proposées. Pour 3 MRGI, des résultats dispersés ont mené à des consensus moins fiables et des concentrations suggérées sont présentées. Pour 17 MRGI, un nombre insuffisant de données disponibles ou de larges écart-types ont contraint la proposition de teneurs à valeur informative seulement. (Voir l'annexe D pour le manuscrit original.)

Contribution des auteurs :

1er auteur : Dany Savard :

-Planification du projet;

-Rédaction du corps du manuscrit;

-Analyses en laboratoire du sélénium;

-Rédaction de la description expérimentale de la technique d'analyse;

-Production de tous les tableaux et figures;

-Aide à la rédaction du résumé, de l'introduction, de la discussion et de la conclusion;

-Mise en forme de l'article suivant les critères de l'éditeur.

2ième auteur : L. Paul Bédard :

-Direction du projet;

-Rédaction du résumé;

-Aide à la rédaction de l'ensemble du manuscrit;

-Élaboration de la stratégie statistique.

3ième auteur : Sarah-Jane Barnes :

-Révision de l'ensemble du manuscrit.

CONCLUSION

Ce mémoire de maîtrise en sciences de la Terre est présenté en quatre parties. Chacune des parties a fait l'objet d'une publication scientifique dans des journaux internationaux spécialisés en sciences de la Terre avec comité de lecteurs. Les publications forment un projet d'ensemble qui vise à élargir les connaissances géochimiques du soufre et du sélénium.

Les deux premiers ouvrages scientifiques présentent des techniques d'analyse de quantification pour les matériaux géologiques du sélénium (technique du Se/TCF-INAA, Savard *et al.*, 2006) et du soufre (par spectrométrie infrarouge HORIBA EMIA-220-V, Bédard *et al.*, 2008). La technique du Se/TCF-INAA a de nombreux avantages : l'étape de désorption qui n'est pas nécessaire par INAA, comparativement à l'analyse par absorption atomique munie d'une fournaise au graphite (GF-AAS) et par spectrométrie de masse (ICP-MS); elle consomme moins de temps que la GF-AAS et il n'y a pas d'interférences, comparativement à l'ICP-MS. La technique du soufre permet également la détermination en basse et en hautes teneurs en variant les paramètres d'analyses (masse d'échantillon, température et temps de chauffage). La limite de détection est de 22 µg/g.

La troisième partie présente une application de l'étude du comportement géochimique du soufre et du sélénium dans un gisement magmatique, le complexe du Bushveld en Afrique du Sud (Barnes et *al.*, 2009). L'étude a permis de soulever trois

modèles pour expliquer les basses teneurs en soufre et les relations S-Se-Cu-La observées dans la base du Bushveld, qui est enrichie en éléments du groupe du platine. Le premier modèle suggère que les sulfures qui étaient présents dans l'empilement cristallin aient pu migrer dans les roches encaissantes ou au centre de l'intrusion. Pour sa part, le deuxième modèle suggère que le magma ait été saturé en soufre en profondeur et que, durant le transport, des sulfures aient été emprisonnés dans de petites cavités présentes dans la matrice cristalline. Le troisième modèle, quant à lui, suggère que les roches aient été appauvries en S et en Se à température élevée après la solidification de l'intrusion. Il est impossible d'évaluer pour l'instant lequel de ces modèles est le plus plausible, mais les deux premiers modèles ont une implication importante pour l'exploration de nouvelles ressources. Si l'un de ces modèles s'avère exact, il aura contribué à la découverte de nouvelles ressources associées à l'intrusion telles que le nickel, le cuivre, les éléments du groupe du platine et l'or.

Enfin, la quatrième partie présente une compilation des teneurs en sélénium dans 26 matériaux de références géologiques internationales (MRGI) obtenues à l'UQAC (Savard *et al.*, 2009). Les résultats ont été greffés avec les résultats disponibles dans la littérature et des traitements statistiques ont été réalisés afin de classifier les MRGI selon le degré de consensus des déterminations obtenus. La validation de la qualité des techniques d'analyse est fortifiée par l'analyse de matériaux de référence. Ainsi, ce quatrième ouvrage scientifique est un outil bénéfique pour la communauté scientifique et l'industrie désireuse de développer de nouvelles techniques d'analyse pour le sélénium, pour l'étude scientifique de son comportement géochimique ou pour éventuellement se servir du sélénium comme outil d'exploration.

L'ensemble de ce projet est donc un avancement dans l'étude géochimique du soufre, du sélénium et de leur relation avec d'autres éléments. La compréhension de ces relations conduit vers l'acquisition générale de nouvelles connaissances pour la communauté scientifique et ces connaissances seront notamment bénéfiques à l'industrie pour l'amélioration ou le développement de nouvelles techniques d'exploration.

REMERCIEMENTS

Je tiens à remercier sincèrement mon équipe de supervision interne, madame Sarah-Jane Barnes ainsi que monsieur Paul Bédard pour tout le support, la confiance et la grande latitude qu'ils m'ont accordées tout au long de ce projet. Un grand merci également à monsieur Wolfgang Maier pour les conseils et les contributions intellectuelles. Merci également à madame Sonya Savard pour la correction du français. Les travaux de recherche ont été financés par la Chaire de Recherche Canada en Métallogénie-Magmatique (titulaire: Sarah-Jane Barnes, UQAC).

RÉFÉRENCES

CAWTHORN, R.G. (1999). Platinum-group element mineralization in the Bushveld Complex - a critical reassessment of geochemical models. *South African Journal of Geology*, 102 : 268-281.

DREIBUS, G., PALME, H., SPETTEL, B., ZIPFEL, J. et WANKE, H. (1995). Sulfur and selenium in chondritic meteorites. *Meteoritics* 30 : 439-445.

GOLDSCHMIDT, V.M. (1954). Geochemistry. *Muir, A. Editor, Oxford University Press, London.*

McDONOUGH, W. F. et SUN, S.-S. (1995). The composition of the Earth. *Chemical Geology*, 120 : 223-254.

NALDRETT, A.J., DUKE, J.M., LIGHTFOOT, P.C. et THOMPSON, J.F.H. (1984). Quantitative modeling of the segregation of magmatic sulfides – an exploration guide. *Canadian Institute of Mining, Metallurgy and Petroleum*, 77 : 46-56.

TAYLOR, S. R. et McLENNAN, S. M. (1985). The continental crust: its composition and evolution. *Blackwell, London,* 312p.

ANNEXE A

MANUSCRIT : « SELENIUM AND SULFUR CONCENTRATIONS IN THE BUSHVELD COMPLEX OF SOUTH AFRICA AND IMPLICATIONS FOR FORMATION OF THE PLATINUM-GROUP ELEMENT DEPOSITS ». BARNES *et al.*, 2009.

Miner Deposita (2009) 44:647–663
DOI 10.1007/s00126-009-0237-3

ARTICLE

Selenium and sulfur concentrations in the Bushveld Complex of South Africa and implications for formation of the platinum-group element deposits

Sarah-Jane Barnes · Dany Savard · L. Paul Bédard · Wolfgang D. Maier

Received: 8 January 2009 / Accepted: 9 March 2009 / Published online: 1 April 2009

Abstract We have determined the S, Se, Cu and La contents through a complete stratigraphic section of the Bushveld Complex. The principle aim was to determine which phases controlled these elements. S, Se and Cu show positive correlations, but these elements do not correlate with La. In most cases, the concentration of S, Se and Cu in rocks containing greater than 800 ppm S can be modeled by segregation of a Fe–Ni–Cu sulfide liquid from a fractionating magma. As the magma evolved, Se and Cu were depleted by the continual segregation of sulfide liquid and the S/Se and S/Cu of the rocks increased. The Se/Cu ratio is higher in the more evolved rocks, which suggests that Se has a slightly lower partition coefficient than Cu into sulfide liquid (1,200 versus 1,700). The Lower and lower Critical Zone of the complex contains on average only 99 ppm S. The low S content of these rocks has led some authors to suggest that these rocks do not contain cumulate sulfides, despite the fact that they are moderately enriched in PGE. These samples fall along the same trend as the S-rich samples on the S-versus-Se plot and the S/La and Se/La ratios are greater than the initial magmas suggesting that despite the low S contents cumulate sulfides are present. Three models may be suggested in order to explain the low S content in the Lower and Critical Zone rocks: (a) the sulfides that were present have migrated away from the cumulate pile into the footwall or center of the intrusion; (b) the magma was saturated in sulfides at depth and during transport some sulfides lagged in embayments; (c) the rocks have lost both S and Se at high temperature. The first two models have important implications for exploration.

Keywords Selenium · Sulfur · Platinum-group elements · Merensky Reef · Bushveld Complex · South Africa

Introduction

Selenium is a chalcophile element that has long been used in studying the formation of Ni-sulfide and platinum-group element (PGE) deposits associated with mafic and ultramafic rocks (Eckstrand et al. 1989). High S/Se ratios in Ni-sulfide ore deposits have, in many studies, been taken as evidence that S has been contributed from the country rocks, a process considered to be critical to the formation of many Ni-sulfide ores (e.g. Naldrett et al. 1984; Ripley et al. 2002a, b; Thériault and Barnes 1998). The observation that S/Se ratios are close to chondritic (2,500, Dreibus et al. 1995) in some PGE deposits, e.g. the Main Sulfide Zone of the Great Dyke and the Merensky Reef of the Bushveld Complex, has been used to support a model that the PGE were concentrated by an Fe–Ni–Cu sulfide liquid (hereafter referred to as a sulfide liquid) which separated by liquid immiscibility from the mafic silicate liquid (Barnes et al. 2008; Godel et al. 2007). In reefs where S/Se ratios are subchondritic, e.g. the JM Reef of the Stillwater Complex, the AP and PV Reefs of the Penikat Intrusion and the Platinova Reef of the Skaergaard Intrusion (Andersen 2006; Barnes et al. 2008; Godel and Barnes 2008a, b), it has been suggested that the rocks have experienced S loss. The underlying assumption here, based on studies of sedimentary rocks and

Editorial handling: B. Lehmann

S.-J. Barnes (✉) · D. Savard · L. P. Bédard
Sciences de la Terre, Université du Québec à Chicoutimi,
Chicoutimi, Canada G7H 2B1
e-mail: sjbarnes@uqac.ca

W. D. Maier
Centre for Exploration Targeting, University of Western Australia,
Crawley 6009, WA, Australia

hydrothermal systems, is that S is more mobile than Se (Auclair et al. 1987).

In addition to its use in ore deposits work, the S/Se ratio has also been used to study the behavior of base metal sulfides during partial melting of the mantle (e.g. Guo et al. 1999; Hattori et al. 2002; Lorand et al. 2003). Despite the utility of the ratio, there are few studies on the behavior of Se in crustal rocks. In part, this is due to the very low level at which this element occurs in the crust [the average continental crust contains only 0.050 ppm (Taylor and McLennan 1985)]. In order to determine Se at low levels, we have recently modified an analytical method, consisting of Se pre-concentration on thiol cotton fiber (Marin et al. 2001), and adapted it for instrumental neutron activation analysis (Se/TCF-INAA, Savard et al. 2006). The technique provides low detection limits (~0.006 ppm) and quantitative recovery. The ability to determine Se at low levels offers the opportunity to study a wider range of rocks and processes.

The Bushveld Complex of South Africa contains most of the world's Pt resources (Cawthorn 1999). The role of sulfide liquid in concentrating the PGE into the main PGE deposits (the UG-2 Reef, the Merensky Reef and the Platinova Reef) is much debated. There are essentially three schools of thought. The first suggests that the PGE were precipitated from the magma as platinum-group minerals (e.g. Hiemstra 1979; Tredoux et al. 1995). The second suggests that sulfide liquid segregated from the silicate magma and PGE partitioned into the sulfide liquid. This PGE-rich liquid then settled onto the cumulate pile to form the reefs (e.g. Campbell et al. 1983). The third school of thought suggests that PGE were collected from the cumulate pile by a late magmatic fluid. This fluid rose through the pile to the level of the reefs where it dissolved into the interstitial silicate liquid and precipitated the PGE (e.g. Boudreau and Meurer 1999). In this debate, the critical question is when the Bushveld magma became saturated in sulfide liquid, and whether the initial sulfides were later dissolved and the metals mobilized by late magmatic fluids.

Maier and Barnes (1999) and Barnes and Maier (2002a) found that most of the rocks in the lower part of the intrusion are enriched in PGE. They also noted that many of these rocks have S/Hf and Cu/La ratios higher than the initial magmas and suggested that the magma was saturated in sulfide liquid from the lowest units of the Complex. This argument is based on the idea that if no cumulate sulfides are present, then these elements should all be incompatible and thus the ratios of chalcophile to incompatible elements of the rocks should be the same as that of the parental magma. However, Willmore et al. (2000) argued that insufficient Cu and S are present for the silicate liquid to have been saturated in a sulfide liquid. Cawthorn (2005) was in agreement with this, stating that the Bushveld Complex does not appear to have been sulfide saturated, except at two discrete levels (the Merensky Reef and the Bastard pyroxenite), and he concluded that there is no convincing evidence for sulfur saturation in the Lower and Critical Zones. This argument is based on the premise that if the silicate magma is saturated in sulfide liquid, then the sulfide liquid should be present in the cumulate rocks in cotectic proportions or greater, i.e. the concentrations in the cumulate rocks must equal or exceed the amount needed to saturate the magma in sulfide liquid. In the case of the initial Bushveld magma, this can be calculated to be ~1,200 ppm, using the equation of Li and Ripley (2005), and ~800 ppm, using the Wallace and Carmichael (1992) equation and assuming a pressure of 0.3 GPa and fO_2 at the FMQ buffer. In fact, the amount of S to be expected in the cumulate is a little more complex as will be outlined below but the point that the lower parts of the Complex contain very little S and yet contain PGE enrichment requires some explanation.

One possible way to reconcile the observation of the low S levels and high chalcophile-to-lithophile ratios is that S could have been partially removed from the lower parts of the intrusion. Von Gruenewaldt et al. (1986) and Gain (1985) have suggested that the chromite-rich layers have lost S based on the high Cu/S ratios in these layers. In this case, it is possible that Se would be retained in preference to S.

This work presents Se concentrations in 156 well-characterized samples covering the complete stratigraphy of the ultramafic and mafic layered rocks (the Rustenburg Layered Suite, RLS) of the Bushveld Complex (Maier and Barnes 1998, 1999; Barnes et al. 2004, Godel et al. 2007). Samples will be considered to contain cumulate sulfide if they contain more than 800 ppm S. Therefore, data from these samples will be used to investigate the behavior of Se when the magma is saturated in a sulfide liquid. Observations will then be applied to samples containing less than 800 ppm S to consider the question of whether S has been lost from some parts of the intrusion.

Geology

Geological setting

The Bushveld Complex was emplaced and crystallized at approximately 2,054 Ma (2,054±2.8 Ma, Harmer and Armstrong 2000; 2,054±1.3 Ma Scoats and Friedman 2008) into the supracrustal rocks of the Transvaal Supergroup which is mainly composed of quartzite, sandstone and dolomite with interlayered volcanic andesitic and volcanoclastic sediments (Eriksson et al. 1993). The Complex consists of two main parts, an ultramafic to mafic part known as the Rustenburg Layered Suite (RLS) and a felsic part consisting of granites and granophyres (Fig. 1). The RLS is subdivided into five zones. From the base to the top,

these are the Marginal Zone (discussed in more detail below) as well as the Lower, Critical, Main and Upper Zones. The PGE deposits are found in the Critical Zone of the RLS.

The Marginal Zone

The Marginal Zone is located at the contact between the cumulate rocks and the country rocks and includes dykes and sills found adjacent to the contact. Sharpe (1981) divided the rocks into three groups based on their textures and geochemistry. The Bushveld 1 (B-1) rocks have compositions similar to modern boninites or Archean to Proterozoic siliceous high-Mg basalts (SHMB). Their textures range from quench textures, with elongate pyroxene and plagioclase, to fine-grained equigranular rocks. There is a series of ultramafic sills (UM) in the footwall to the complex, consisting of olivine mesocumulates which have been modeled as a mixture of olivine and B-1 liquid (Sharpe and Hulbert 1985; Davies and Tredoux 1985). The Bushveld 2 and 3 (B-2 and B-3) rocks have compositions similar to tholeiitic basalt and are fine-grained equigranular gabbronorites. Their major element compositions are similar, but they differ in their trace element composition in that the B-2 rocks are richer in all the incompatible elements. The marginal rocks have been used to characterize the parental magmas of the Bushveld (e.g. Cawthorn et al. 1981; Curl 2001; Davies et al. 1980; Davies and Tredoux 1985; Harmer and Sharpe 1985; Sharpe and Hulbert 1985). Se and S have been determined in ten samples from the collection of Harmer and Sharpe (1985) and Sharpe and Hulbert (1985) as well as in three samples from Barnes and Maier (2002b). These samples will be used to estimate the initial magma compositions.

The Union Section stratigraphic boreholes

Most samples were taken from stratigraphic boreholes at Union Section, northwestern Bushveld (Fig. 1). At this locality, the Lower Zone is 1,000 m thick and directly overlies the sedimentary floor rocks. It consists of cyclic units of ultramafic cumulates of dunite, harzburgite and orthopyroxenite (Teigler and Eales 1996). The Critical Zone (1,000 m thick) is subdivided in two sub-Zones on the basis of their composition; the Lower Critical Zone consists of cyclic units of chromitites, harzburgites and orthopyroxenite, whereas the Upper Critical Zone consists of cyclic units of chromitites, orthopyroxenites, norites and anorthosites.

The two main PGE deposits occur at the top of the Upper Critical Zone; the UG-2 Reef (in Upper Group chromitite 2) and the Merensky Reef. As no samples were available for the Merensky Reef from the Union Section boreholes, Se was determined in Merensky Reef samples previously studied by Godel et al. (2007) from the Rustenburg Mine and in the international reference material SARM-7, which is a composite of the Merensky Reef from five different mines (Steele et al. 1975). Selenium has previously been determined in these samples by INAA by Godel et al (2007). In addition, Barnes and Maier (2002a) determined Se in ten Merensky Reef samples from Impala mine. The new results for the reef are similar to the earlier

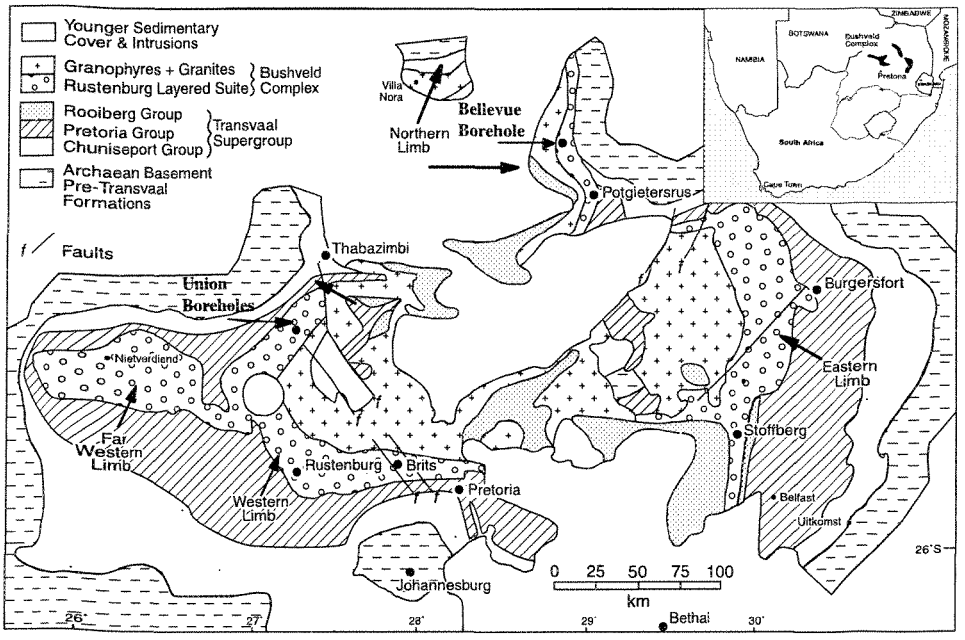

Fig. 1 Geology of the Bushveld Complex and location of the boreholes studied in this work. Map modified after Barnes and Maier (2002b)

results, but more precise, and only the TCF analyses will be used in the current study.

The Main Zone (2,000 m thick) is relatively homogeneous and is composed of norite, gabbronorite and anorthosite. Olivine and chromitite are virtually absent (Mitchell 1990).

The Bellevue stratigraphic borehole

The Bellevue borehole is located on the Northern limb of the complex (Fig. 1). Samples for this study came from the interval between the top of the Main Zone through to the top of the Upper Zone. The Upper Zone is 1,500–2,000 m thick and consists of cyclic units of magnetite, gabbronorite or diorite and anorthosite. Its base is defined as the zone where magnetite becomes a cumulate phase. The lower part of the Upper Zone, known as sub-Zone A, contains cumulate plagioclase, low-Ca pyroxene and magnetite. Overlying this is sub-Zone B, where olivine becomes a cumulate phase, and sub-Zone C, where apatite becomes a cumulate phase. The upper parts of the Upper Zone contain numerous country rock xenoliths (Ashwal et al. 2005; Cawthorn and Street 1994) and the final 100 m consists of granophyre.

Parental magmas

Harmer and Sharpe (1985) showed that the crystallization sequence and trace element composition of the B-1 magma are consistent with it being the parental magma of the Lower Zone. Trace elements and isotopes of the Critical Zone suggest that these rocks formed from a magma that was a mixture of B-1 and B-2 magmas (Kruger 1994; Maier and Barnes 1998; Wilson and Chunnet 2006). The Main Zone is thought to form from the B-3 magma (Sharpe 1981; Maier and Barnes 1998). Sharpe (1981) suggested that the Upper Zone formed from fractionated Critical Zone magma.

Analytical techniques

Selenium determination

A slightly modified version of the Se/TCF-INAA technique described by Savard et al. (2006) was used to determine Se. The first modification was that sample size was reduced from 1 g to 0.9–0.95 g and the quantity of each acid reduced by a factor of 0.75. This modification was introduced so as to allow use of the 50 ml closeable PTFE beakers that fit our digestion block. The second modification was that the pre-cut nanosep centrifugal vials containing the TCF were replaced by 1 ml pipette tips containing TCF with a small cotton ball to keep the TCF in place. Five international reference materials and a blank were determined at the same time as the Bushveld samples. The UQAC results agree with literature values (Table 1), thus the modifications do not appear to have affected the quality of the results. The analytical blank was prepared by placing the reference material BIR-1 in a furnace at 1,000°C overnight to volatilize all Se. Based on the BIR-1 blank, the limits of detection and quantification are 0.007 and 0.021 ppm, respectively. Unfortunately, Se concentrations could not be determined in chromite-rich rocks (e.g. UG-2) because the low-temperature/low-pressure dissolution technique used ($HF–HNO_3–H_2O_2$) does not dissolve all of the chromite.

Sulfur determination

In most of our samples, sulfur had been previously determined by the combustion idometric procedure using a LECO titrator. Recently, analytical methods for low-level S samples have improved and we have re-determined S in many of the samples using high temperature combustion combined with infrared spectrometry using a Horiba 220 V S–C analyzer and the protocol outlined in Bédard et al.

Table 1 Se and S values obtained at UQAC for reference materials and blanks and accepted values for reference materials

Sample	Se (ppm)	±	*n*	Se (ppm)	±	S (ppm)	±	*n*	S (ppm)	±	Reference
	UQAC			Literature		UQAC			Literature		
AN-G	0.046	0.005	3	0.041	0.002	146	5	2	138	6	Terashima and Imai (2000), Okai et al. (2001)
BE-N	0.065	0.004	2	0.061	0.005	310	2	2	304	24	Savard et al. (2006), Bédard et al. (2008)
BIR-1	0.020	0.003	2	0.018	0.003	18	3	2	none		Gladney and Knab (1981)
DR-N	0.098	0.010	2	0.082	0.008	441	12	2	433	15	Marin et al. (2001), Okai et al. (2001)
MRG-1	0.193	0.015	3	0.199	0.010	666	23	3	610	–	Hall et al. (1997), Govindaraju (1994)
Blank	<0.007	0.0023	6	–	–	13	3	8	–	–	

(2008). Sulfur concentrations in five reference materials were also determined along with the Bushveld samples and agree with literature values (Table 1). The detection limit, as defined as 3 sigma on the blank, is 9 ppm. In most cases, the results for the Bushveld samples were comparable to the previously published values. However, in the case of the Upper Zone samples, it was found that most of the previously published values were SO_3 values that were erroneously reported as S values (Barnes et al. 2004). The revised values are indicated with a cross (†) in Table 2.

The whole-rock Cu and La contents and the anorthite content of plagioclase were collected as part of previous studies (Maier and Barnes 1998, 1999; Barnes et al. 2004; Ashwal et al. 2005).

Results

Marginal rocks—parental magmas

The rocks of the Marginal Zone contain 0.006 to 0.182 ppm Se and 40 to 560 ppm S (Table 2). The highest values for both Se and S are found in the B-1 samples (averaging at 0.142 and 496 ppm, respectively). These samples have S/Se ratios broadly similar to the mantle (~3,333; McDonough and Sun 1995). The B-2 and B-3 samples contain less Se and S (averages of 0.0416 and 97 ppm, respectively) but similar S/Se values (3,100).

Three of our B-1 samples (CD001, CD017 and CO114) were the same as those analyzed by Harmer and Sharpe (1985). Their S values covered a wider range than the present values (200–1,200 ppm), but the averages are similar (533±577 versus 465±26 ppm S).

The data of Davies and Tredoux (1985) for both the B-1 and B-2/3 magmas show considerably higher S contents than those of the present study. These authors report averages of 897±300 ppm (n=8) for the B-1 and 287± 312 ppm (n=4) for the B-2/3 magmas. There appears to have been either a calculation error for the average of the B-2/3 magma or an error in the values reported in their raw data, as the average in the table for the B-2/3 samples is actually 526±326 ppm. We believe our S values to be correct, based on the results for the international reference materials and the improved techniques used for S determinations at low levels (Bédard et al. 2008). We respectfully suggest that Davies and Tredoux (1985) overestimated the S concentrations in the marginal rocks because of the limitations of the analytical methods used at the time and the difficulty of determining S at these low concentrations. A similar explanation can be given for the large uncertainty of the S determinations of Harmer and Sharpe (1985). We have determined S in the marginal rocks in a larger sample set and the average results are similar to the ten samples reported here (B-1 average S=396 ppm n=10; B-2/B3 average S=146 ppm n=23, Barnes et al. in preparation).

Samples from the Rustenburg Layered Suite

Within the RLS, Se concentrations decrease from ~0.1 ppm at the base of the intrusion to 0.01 ppm just below the UG-1 chromitite, which occurs in the Upper Critical Zone some 50 m below the Merensky Reef (Table 2, Fig. 2a). Sulfur follows a similar trend decreasing from approximately 300 ppm at the base of the Lower Zone to 30 ppm just below the UG-1 chromite (Table 2 Fig. 2b). The average Se and S contents in rocks from the Lower Zone and Critical Zones below the UG-1 chromitite are 0.03and 99 ppm, respectively, and the average S/Se ratio is similar to mantle at 3,400 (Table 2).

Selenium values increase through the cyclic units immediately underlying the Merensky Reef from 0.024 ppm in the UG-1 pyroxenite to 1–14 ppm in the Merensky Reef and then decrease throughout the Merensky Cyclic unit to 0.07 ppm. In the overlying pyroxenite of the Bastard unit, the Se values rise once again (~0.4 ppm) and then fall throughout the unit. Both S and Cu follow similar trends as Se throughout these units (Table 2 and Fig. 2a and b).

The Main Zone samples from both the Union and Bellevue boreholes generally contain very little Se and S (Table 2, Fig. 2a and b). The concentrations are similar to those of the Lower and Critical Zones below the UG-1 unit (average 0.045 ppm Se and 143 ppm S, S/Se=3,180). Only three samples contain more than 0.1 ppm Se and these also contain more than 200 ppm S. There does not appear to be a systematic variation with either Se or S and stratigraphic height.

In the Upper Zone, Se and S concentrations are generally higher than in the other zones (Fig. 2a and b). The concentration of Se ranges from 0.1 to 10 ppm , with an average of 1.2 ppm for the entire Upper Zone, and the average S content is ~6,000 ppm. Sulfur concentrations in sub-Zones A and B are similar, in the 0.03 to 1 wt.% (average 0.4 wt. %). In contrast, S concentrations in sub-Zone C are generally higher, in the 0.1 to 10 wt.% range (average ~1.2 wt.%). The average S/Se ratio is lower in sub-Zone A (~2,700) than in sub-Zones B and C which average ~7,000.

Interpretation

Modeling sulfide saturation

The samples are meso- to adcumulates of pyroxene, ±oxide, ±plagioclase (Ashwal et al. 2005; Barnes et al. 2004; Godel et al. 2007; Maier and Barnes 1998). The amount of base metal sulfides present varies from <0.1 to 10 modal percent, with the vast majority of samples containing <0.5 modal

Table 2 Whole-rock concentrations of Se, S, Cu, La for rocks from the Bushveld Complex

Sample	Rock type	Zone/unit	Height (km)	Se (ppm)		S (ppm)	Cu (ppm)	La (ppm)	An in Plag	S/Se	S/Cu	Cu/Se
103.88	Diorite	Upper C	6.1461	0.140	†	1,347	34	37.13	41.53	9,621	39.6	243
157.07	Diorite	Upper C	6.0929	0.314	†	1,627	204	53.69	44.98	5,182	8.0	650
269.28	Diorite	Upper C	5.9807	0.768	†	5,647	121	23.43		7,353	46.7	158
269.96	Diorite	Upper C	5.9800	0.418	†	5,776	50	34.71		13,818	115.5	120
272.58	Xenolith	Upper C	5.9774	2.146	†	27,100	530	29.01		12,628	51.1	247
304.72	Diorite	Upper C	5.9453	2.024		12,000	257	162.21		5,929	46.7	127
305.44	Mag layer R	Upper C	5.9446	0.458	†	3,859	93	6.24	54.74	8,426	41.5	203
328.87	Gabbronorite	Upper C	5.9211	9.760		67,900	940	15.17	47.76	6,957	72.2	96
351.13	Gabbronorite	Upper C	5.8989	3.308	†	19,500	398	5.05	48.32	5,895	49.0	120
351.7	Gabbronorite	Upper C	5.8983	1.014	†	6,600	162	6.10	47.02	6,509	40.7	160
352.1	Anorthosite	Upper C	5.8979	0.105	†	1,487	16	7.87		14,162	92.9	152
443.87	Gabbronorite	Upper C	5.8061	0.054	†	332	10	9.68		6,148	33.2	185
559.16	Gabbronorite	Upper C	5.6908	0.825	†	4,840	110	49.97	45.83	5,867	44.0	133
603.67	Mag layer Q	Upper C	5.6463	0.841	†	5,405	152	1.60	50.00	6,427	35.6	181
611.56	Mag layer P	Upper B	5.6384	8.121	†	58,296	1,010	2.12	53.62	7,178	57.7	124
611.76	Mag layer P	Upper B	5.6382	1.303	†	10,158	337	5.79	53.55	7,796	30.1	259
644.8	Mag layer O	Upper B	5.6052	0.300	†	1,599	104	3.63	54.03	5,330	15.4	347
687.3	Gabbronorite	Upper B	5.5627	0.362	†	2,500	110	4.09	48.08	6,906	22.7	304
806.02	Gabbronorite	Upper B	5.4440	0.537	†	4,695	184	3.26	48.27	8,743	25.5	343
830.57	Mag layer M	Upper B	5.4194	0.262	†	1,936	91	1.09	51.19	7,389	21.3	347
830.75	Mag layer M	Upper B	5.4193	0.270	†	1,570	83	2.64		5,815	18.9	307
848.8	Mag layer L	Upper B	5.4012	0.031	†	286	25	0.64	49.08	9,226	11.4	806
882.05	Gabbronorite	Upper B	5.3680	0.058	†	236	28	4.44	53.98	4,069	8.4	483
903.08	Mag layer J	Upper B	5.3469	0.455	†	2,300	292	0.45	56.56	5,055	7.9	642
920.83	Gabbronorite	Upper B	5.3292	1.711	†	5,459	1,210	7.59	56.15	3,191	4.5	707
930.4	Mag layer I	Upper B	5.3196	0.476	†	1,600	345	0.58	56.58	3,361	4.6	725
978	Mag layer II	Upper B	5.2720	0.031	†	212	29	0.66	56.72	6,839	7.3	935
1,002.5	Mag layer H	Upper B	5.2475	0.196	†	774	109	0.81	55.75	3,949	7.1	556
1,028.03	Gabbronorite	Upper A	5.2220	0.046	†	539	18	7.57		11,717	29.9	391
1,048.81	Gabbronorite	Upper A	5.2012	0.120	†	321	79	6.17	55.86	2,675	4.1	658
1,049.26	Gabbronorite	Upper A	5.2007	0.534	†	2,400	179	8.52	56.40	4,494	13.4	335
1,070.95	Gabbronorite	Upper A	5.1791	1.512	†	3,905	1,430	5.57	57.86	2,583	2.7	946
1,144.8	Gabbronorite	Upper A	5.1052	0.120	†	524	56	3.26	56.77	4,367	9.4	467
1,216.3	Gabbronorite	Upper A	5.0337	0.433	†	1,118	341	3.57	56.48	2,582	3.3	788
1,224	Mag layer	Upper A	5.0260	1.330	†	2,068	1,459	1.14		1,555	1.4	1,097
1,279.93	Gabbronorite	Upper A	4.9701	0.596	†	2,000	484	2.02	55.04	3,356	4.1	812
1,316.52	Gabbronorite	Upper A	4.9335	2.276	†	4,913	1,640	1.65	55.56	2,159	3.0	721
1,334.55	Mag layer E	Upper A	4.9155	2.267	†	5,400	1,940	6.46	57.54	2,382	2.8	856
1,374.84	Gabbronorite	Upper A	4.8752	0.444	†	1,723	270	6.29	54.97	3,881	6.4	608
1,382.24	Anorthosite	Upper A	4.8678	0.600	†	1,500	425	8.79	55.61	2,500	3.5	708
1,397.05	Mag layer C	Upper A	4.8530	0.274	†	733	231	0.50	53.23	2,675	3.2	843
1,403.17	Mag layer B	Upper A	4.8468	2.281		11,200	970	2.82	57.87	4,910	11.5	425
1,404.35	Gabbronorite	Upper A	4.8457	2.024	†	5,200	2,150	1.33	55.35	2,569	2.4	1,062
1,483.34	Gabbronorite	Upper A	4.7667	0.245	†	667	194	4.67	60.65	2,722	3.4	792
1,517.08	Anorthosite	Upper A	4.7329	0.095	†	440	49	4.50		4,632	9.0	516
1,520.33	Anorthosite	Upper A	4.7297	4.958	†	8,654	3,500	3.04	61.47	1,745	2.5	706
1,530.27	Gabbronorite	Upper A	4.7197	2.017		1,900	1,647	1.39		942	1.2	817
1,530.47	Gabbronorite	Upper A	4.7195	1.595		1,800	1,320	1.39		1,129	1.4	828

Table 2 (continued)

Sample	Rock type	Zone/unit	Height (km)	Se (ppm)		S (ppm)	Cu (ppm)	La (ppm)	An in Plag	S/Se	S/Cu	Cu/Se
1,534.54	Gabbronorite	Upper A	4.7155	0.662		1,000	808	1.47		1,511	1.2	1,221
1,547.7	Gabbronorite	Upper A	4.7023	0.580	†	625	743	1.34		1,078	0.8	1,281
1,618.43	Gabbronorite	Main	4.6316	0.018	†	54	6	2.31		3,000	9.0	333
1,708.75	Gabbronorite	Main	4.5413	0.053	†	221	30	2.76		4,170	7.4	566
1,745.45	Gabbronorite	Main	4.5045	0.029	†	63	17	1.54		2,172	3.7	586
1,745.45	Gabbronorite	Main	4.5045	0.095	†	492	50	1.54		5,179	9.8	526
1,967.1	Norite	Main	4.2829	0.028	†	90	20	1.30		3,214	4.5	714
1,973.68	Norite	Main	4.2763	0.027	†	97	55	0.30		3,593	1.8	2,037
1,973.78	Anorthosite	Main	4.2762	0.241	†	567	278	0.97		2,353	2.0	1,154
mz7	Gabbro	Main	4.7210	0.029	†	29	30	3.44		1,000	1.0	1,034
mz4	Gabbro	Main	4.5120	0.078	†	23	28	0.00		295	0.8	359
sp11	Gabbro	Main	4.2920	0.017	†	55	27	2.18		3,235	2.0	1,588
a1	Gabbro	Main	4.0319	0.016	†	39	18	2.24		2,438	2.2	1,125
a35	Gabbro	Main	3.8262	0.010	†	30	11	1.88		3,000	2.7	1,100
a65	Gabbro	Main	3.6326	0.033	†	38	12	1.32		1,152	3.2	364
a79	Gabbro	Main	3.5550	0.022	†	97	33	3.32		4,409	2.9	1,500
a106	Gabbro	Main	3.4263	0.025	†	109	17	3.62		4,360	6.4	680
a141	Gabbro	Main	3.2265	0.018	†	55	20	2.53		3,056	2.8	1,111
a168	Gabbro	Main	2.9941	0.017	†	68	22	2.42		4,000	3.1	1,294
a206	Gabbro	Main	2.8224	0.009	†	53	22	3.22		5,889	2.4	2,444
a238	Gabbro	Main	2.6201	0.114	†	280	98	2.23		2,456	2.9	860
a254	Gabbro	Main	2.5550	0.044	†	63	33	2.85		1,432	1.9	750
a255	Gabbro	Main	2.5300	0.023	†	75		0.00		3,261		
a261	Gabbro	Main	2.5150	0.019	†	80		0.00		4,211		
a262	Gabbro	Main	2.4900	0.016	†	63		0.00		3,938		
a271	Gabbro	Main	2.4350	0.019	†	60	27	2.79		3,158	2.2	1,421
a275	Gabbro	Main	2.4000	0.008	†	58		3.48		7,250		
a297	Norite	Main	2.3000	0.063	†	115		0.00		1,825		
a298	Pyroxenite	Main	2.2960	0.210	†	1,066	134	0.77		5,076	8.0	638
a301	Norite	Main	2.2820	0.019	†	58	34	2.58		3,053	1.7	1,789
a315	Norite	Main	2.2000	0.018	†	108		0.00		6,000		
a334	Norite	Main	2.1080	0.022	†	73	22	4.13		3,318	3.3	1,000
ua2	Norite	Critical	2.0820	0.032	†	78	19	4.46		2,438	4.1	594
ua20	Norite	Bastard	2.0320	0.033		180	16	1.59		5,455	11.3	485
ua25	Pyroxenite	Bastard	2.0240	0.451		1,080	216	3.27		2,395	5.0	479
ua31	Anorthosite	Merensky	2.0190	0.067		170	40	2.30		2,537	4.3	597
ua36	Norite	Merensky	2.0100	0.109		260	52	2.55		2,385	5.0	477
ua41	Norite	Merensky	2.0020	0.416		820	151	5.89		1,971	5.4	363
m-4	Melanorite	Merensky	1.9970	4.380		14,542	1,400			3,320	10.4	320
m-3	Melanorite	Merensky	1.9970	3.890		15,848	1,100			4,074	14.4	283
m-2	Melanorite	Merensky	1.9970	3.010		8,007	1,000			2,660	8.0	332
m-1	Melanorite	Merensky	1.9970	14.570		40,271	2,800			2,764	14.4	192
CGM-2	Melanorite	Merensky	1.9970	5.510		14,833	4,300			2,692	3.4	780
GGM-1	Melanorite	Merensky	1.9970	14.320		29,814	3,500			2,082	8.5	244
An	Anorthosite	Merensky	1.9970	1.750		5,924	900			3,385	6.6	514
SARM-7	composite	Merensky	1.9970	1.990	†	4,173	700	4.20		2,097	6.0	352
ua48	Anorthosite	Pseudoreef	1.9940	0.034		70	13	2.66		2,059	5.4	382
ua63	Pyroxenite	UG-2	1.9790	0.058		100	29	3.84		1,724	3.4	500

Table 2 (continued)

Sample	Rock type	Zone/unit	Height (km)	Se (ppm)		S (ppm)	Cu (ppm)	La (ppm)	An in Plag	S/Se	S/Cu	Cu/Se
ua66	Pyroxenite	UG-2	1.9740	0.056		210	33	2.90		3,750	6.4	589
ua70	Harzburgite	UG-2	1.9690	0.061		230	30	2.29		3,770	7.7	492
b235/34	Pyroxenite	UG-1	1.9630	0.024	†	149	23	3.10		6,208	6.5	958
b235/36	Pyroxenite	UG-1	1.9550	0.024	†	105	24	1.90		4,375	4.4	1,000
b235/39	Norite	MG4	1.9470	0.008	†	9	14	1.34		1,125	0.6	1,750
s11	Norite	MG4	1.9000	0.007	†	17	12	1.40		2,429	1.4	1,714
s20	Norite	MG4	1.8450	0.007	†	9	10	1.02		1,286	0.9	1,429
s30	Norite	MG4	1.8000	0.012	†	15	8	0.64		1,250	1.9	667
s40	Pyroxenite	MG4	1.7500	0.010	†	19	13	0.45		1,900	1.5	1,300
s52	Pyroxenite	MG4	1.7000	0.013	†	29	14	0.94		2,231	2.1	1,077
ng3 146.5	Pyroxenite	MG4	1.6668	0.017	†	16	7	0.27		941	2.3	412
ng3 159.4	Pyroxenite	MG3	1.6539	0.029		90	18	1.29		3,103	5.0	621
ng3 176.45	Norite	MG3	1.6368	0.035	†	84	9	1.18		2,400	9.3	257
ng3 194.7	Norite	MG3	1.6186	0.016		50	9	0.88		3,125	5.6	563
ng3 214.25	Pyroxenite	MG2	1.5990	0.022	†	58	13	0.62		2,636	4.5	591
ng3 220.17	Pyroxenite	MG1	1.5931	0.013		50	7	7.52		3,846	7.1	538
ng3 232	Pyroxenite	MG1	1.5813	0.023	†	111	17	2.36		4,826	6.5	739
ng1 25	Pyroxenite	MG1	1.5383	0.044	†	86	18	1.95		1,955	4.8	409
ng1 95.1	Harzburgite	LG7	1.4683	0.016	†	169	7	1.09		10,563	24.1	438
ng1 163.27	Pyroxenite	LG6	1.4000	0.037	†	97	14	2.05		2,622	6.9	378
ng1 233.6	Pyroxenite	LG6	1.3300	0.026	†	88	17	1.45		3,385	5.2	654
ng1 245.25	Pyroxenite	LG6	1.3181	0.013	†	31	8	0.04		2,385	3.9	615
ng1 257.7	Pyroxenite	LG5	1.3056	0.024		80	22	2.27		3,333	3.6	917
ng1 292.3	Pyroxenite	LG5	1.2710	0.009	†	29	12	0.56		3,222	2.4	1,333
ng1 327.45	Pyroxenite	LG5	1.2358	0.026	†	84	18	1.14		3,231	4.7	692
ng1 380.35	Pyroxenite	LG4	1.1830	0.032	†	113	16	2.38		3,531	7.1	500
ng1 421	Pyroxenite	LG4	1.1423	0.052	†	99	18	3.99		1,904	5.5	346
ng1 500.5	Pyroxenite	LG2	1.0628	0.029		50	19	0.00		1,724	2.6	655
ng1 509.8	Harzburgite	LG2	1.0535	0.061	†	120	16	0.68		1,967	7.5	262
ng1 528.5	Pyroxenite	LG1	1.0348	0.022	†	67	17	1.07		3,045	3.9	773
ng1 558.78	Pyroxenite	LG1	1.0045	0.017		60	16	1.52		3,529	3.8	941
ng1 575.35	Pyroxenite	Critical	0.9880	0.017		80	18	1.10		4,706	4.4	1,059
ng1 619.85	Pyroxenite	Critical	0.9435	0.016	†	51	15	4.01		3,188	3.4	938
ng1 670.1	Pyroxenite	Lower	0.8932	0.023	†	142	14	3.22		6,174	10.1	609
ng1 698	Harzburgite	Lower	0.8653	0.027		70	15	1.16		2,593	4.7	556
ng1 773.38	Dunite	Lower	0.7899	0.017	†	25	6	0.03		1,471	4.2	353
ng1 793.8	Dunite	Lower	0.7695	0.007	†	36	16	0.12		5,143	2.3	2,286
ng2 115.25	Pyroxenite	Lower	0.6580		†	23						
ng2 171.5	Pyroxenite	Lower	0.6018	0.028		110	16	1.24		3,929	6.9	571
ng2 253.05	Pyroxenite	Lower	0.5203	0.080	†	168	32	1.88		2,100	5.3	400
ng2 332.25	Pyroxenite	Lower	0.4410	0.083		160	22	2.95		1,928	7.3	265
ng2 373	Pyroxenite	Lower	0.4003	0.036	†	208	22	1.42		5,778	9.5	611
ng2 409.79	Pyroxenite	Lower	0.3635	0.016	†	142		3.29		8,875		
ng2 449.4	Harzburgite	Lower	0.3239	0.079	†	327	29	1.99		4,139	11.3	367
ng2 490.05	Pyroxenite	Lower	0.2833	0.056		320		1.96		5,714		
ng2 557.1	Harzburgite	Lower	0.2162	0.042	†	223	29	1.54		5,310	7.7	690
ng2 626.12	Harzburgite	Lower	0.1472	0.056	†	271	32	1.63		4,839	8.5	571
ng2 678.64	Pyroxenite	Lower	0.0946	0.102	†	270		2.47		2,647		

Table 2 (continued)

Sample	Rock type	Zone/unit	Height (km)	Se (ppm)		S (ppm)	Cu (ppm)	La (ppm)	An in Plag	S/Se	S/Cu	Cu/Se
CD-017	B1-QT	Marginal	0.0000	0.181	†	491	67	15.17		2,713	7.3	370
CD-001	B1-QT	Marginal	0.0000	0.157	†	466	46	19.36		2,968	10.1	293
DI-225	B1-QT	Marginal	0.0000	0.095	†	619	58	20.70		6,516	10.7	611
CO-114	B-1	Marginal	0.0000	0.146	†	439	45	17.44		3,007	9.8	308
DI-204	B-1	Marginal	0.0000	0.131	†	465	47	12.88		3,550	9.9	359
CD-005	B1-UM	Marginal	0.0000	0.143	†	360	52	12.56		2,517	6.9	364
bc-5	B1-UM	Marginal	0.0000	0.073	†	355	32	6.24		4,863	11.0	441
CO-113	B1-UM	Marginal	0.0000	0.072	†	207	23	7.59		2,875	9.0	321
bc-6	B-2	Marginal	0.0000	0.069	†	168	78	15.30		2,435	2.2	1,128
bc-25	B-2	Marginal	0.0000	0.059	†	56	78	15.26		949	0.7	1,319
CO-66	B-2	Marginal	0.0000	0.052	†	165	51	n.d.		3,173	3.2	981
CO-48	B-3	Marginal	0.0000	0.017	†	44	8	3.42		2,588	5.9	441
CO-252	B-3	Marginal	0.0000	0.008	†	53	3	1.78		6,625	17.7	375

† New S value, *Mag* magnetite, *UG* Upper Group unit, *MG* Middle Group unit, *LG* Lower Group unit

percent sulfides. Selenium is known to be a chalcophile element with a high partition coefficient into sulfide (Table 3) and many publications report high Se values in sulfides (e.g. Paktunc et al. 1990). Therefore, one would predict that the bulk of the Se in the rocks is present in the sulfides. Indeed, in situ determination of Se in sulfides from Rustenburg Mine showed this to be the case for the Merensky Reef (Bédard et al. 2007). These sulfides are thought to crystallize from a sulfide liquid which segregated from the silicate liquid by liquid immiscibility. The Se would have partitioned into the sulfide liquid at this time. In detailed studies of the Merensky Reef unit from the

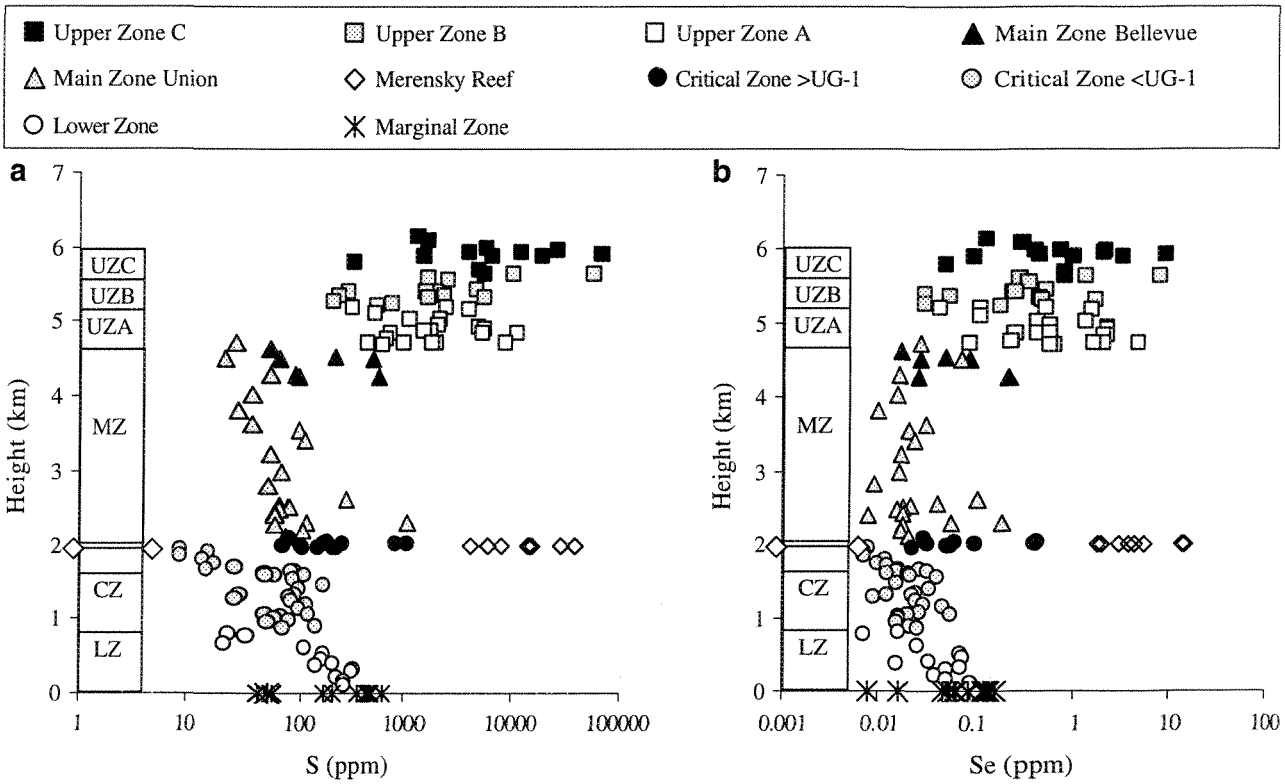

Fig. 2 Variation of S and Se with stratigraphic height in the Bushveld Complex

Table 3 Partition coefficients between silicate and sulfide liquid

Cu	Se	Reference
1,383	1,770	Peach et al. 1990
620–1,513	397–793	Brenan et al. (personal communication 2009)
913–1,006	–	Francis (1990)
250–313	–	Gaetani and Grove (1997)
480–1,303	–	Ripley et al. (2002a, b)
380–1,670	–	Holzheid and Lodders (2001)

Impala and Rustenburg mines, Barnes and Maier (2002a) and Godel et al. (2007) showed that the chalcophile element concentrations, including Se, can be modeled by collection of these elements by a sulfide liquid and accumulation of the liquid on the cumulate pile. The Merensky Reef and Bastard units are relatively S-rich and the presence of cumulate sulfides in these units is plausible. The question in debate is whether cumulate sulfides are present in rocks with low S contents or whether the traces of sulfides found in these rocks represent the crystallization product of the trapped liquid fraction.

Plots of Se versus S, Cu versus S and Se versus Cu show that there is a positive correlation between these elements throughout the RLS (Fig. 3a–c). The data do not, however, form a single trend. The samples from sub-Zones B and C of the Upper Zone have higher S/Se and S/Cu ratios (average ~7,000 and ~34, respectively) than the parental magmas (median ~3,000 and ~9, respectively) and thus form lower trends on S versus Se and Cu plots than the other samples. The change in S/Cu ratios in the Upper Zone was also noted by Harney et al. (1990) and Barnes et al. (2004) who suggested that this trend arises because very little magma was being added to the chamber while sulfide liquid was extracted from the silicate liquid during the formation of sub-Zone A. As a result, the concentration of chalcophile elements decreased in the fractionated magma. The sulfide liquid that segregated from this fractionated magma would be poor in Cu and other chalcophile elements. The magma would be depleted in Se and thus the sulfide liquid that formed would have higher S/Se ratios. This interpretation is supported by the negative correlation between An content of plagioclase (a proxy for fractionation of the magma) and S/Se ratios (Fig. 4).

The plot of Se versus Cu also shows two trends (Fig. 3c). Samples from sub-Zones A and B and the Merensky Unit have higher Cu/Se ratios (660) than samples from sub-Zone C (200). This could occur if the silicate liquid that formed sub-zone C was more depleted (by a factor of ~3) in Cu than Se. If the partition coefficient for Cu between sulfide and silicate liquid were slightly higher than that of Se, then the silicate liquid would have become depleted in Cu relative to Se. The only published study to date where both Se and Cu partition coefficients were estimated (Peach et al. 1990) found that the partition coefficient for Se was slightly higher than that of Cu for sulfide droplets in MORB basalt (Table 3). However, Brenan (personal communication 2009), using experimental work, has found that Cu partition coefficients can be greater than Se (Table 3).

The evolution of the B-1 magma and its cumulates has been modeled using the average B-1 composition and the program PELE (Boudreau and Meurer 1999) V 6.07 (a version of MELTS that allows sulfide liquid saturation). The model used was for fractional crystallization with temperature increments of 20°C. Modeling was stopped when there was 37% liquid left because at this point the An content of the plagioclase in the model is close to that of the most fractionated sections of the Complex (the sub-Zone C of the Upper Zone). As will be outlined below, the partition coefficients used for Se and Cu, 1,200 and 1,700 respectively, were chosen to be within the range reported in the literature (Table 3) and to match the S, Se and Cu distributions in the rocks containing more than 800 ppm S.

The model shows that the magma becomes saturated in sulfide liquid after 16% crystallization, at approximately 600 ppm S, 0.17 ppb Se and 60 ppm Cu (Fig. 5a). The concentrations of S, Se and Cu in the magma fall steadily to 150, 0.03 and 4 ppm as the magma evolves (Fig. 5a).

The compositions of the sulfide liquids in equilibrium with the initial and most fractionated magmas were calculated and tie lines between these magmas and the sulfide liquids are shown on plots of S versus Se and Cu (Fig. 3a and b). The tie line between the least fractionated magma and the sulfide liquid in equilibrium with it passes close to samples from the Merensky Reef, the Critical Zone above the UG-1 and sub-zone A of the Upper Zone. Tie lines between the most fractionated magma and the sulfide liquid in equilibrium pass close to the samples of sub-Zones B and C of the Upper Zone. Thus, most of these rocks can be modeled as containing cumulate sulfides and the composition of the sulfides evolved as the composition of the magma evolved.

An exception to this is a group of five samples mostly located at the base of sub-Zone A of the Upper Zone which have low S/Se ratios (ranging from 942 to 1,745). In a previous study, Barnes et al. (2004) suggested that these samples have lost S, on the basis that they contain corroded

sulfides and that they have whole-rock S/Cu ratios close to 1. The low S/Se ratio of these rocks is in agreement with this interpretation.

Copper can also be modeled in the same fashion using a partition coefficient of 1,700. This is quite a high partition coefficient, but the low Cu concentrations in sub-Zone C cannot be modeled using a lower coefficient. By using these partition coefficients, the low Cu/Se ratio in sub-Zone C can be simulated (Fig. 3c). Modeling in mixing of the B-2 or B-3 magmas does not greatly change the result as the S/Se ratios of these magmas are similar to the B-1 magma.

An alternative possibility to explain the decoupling in chalcophile elements is suggested by the abundance of country rock xenoliths in sub-Zone C of the Upper Zone. It

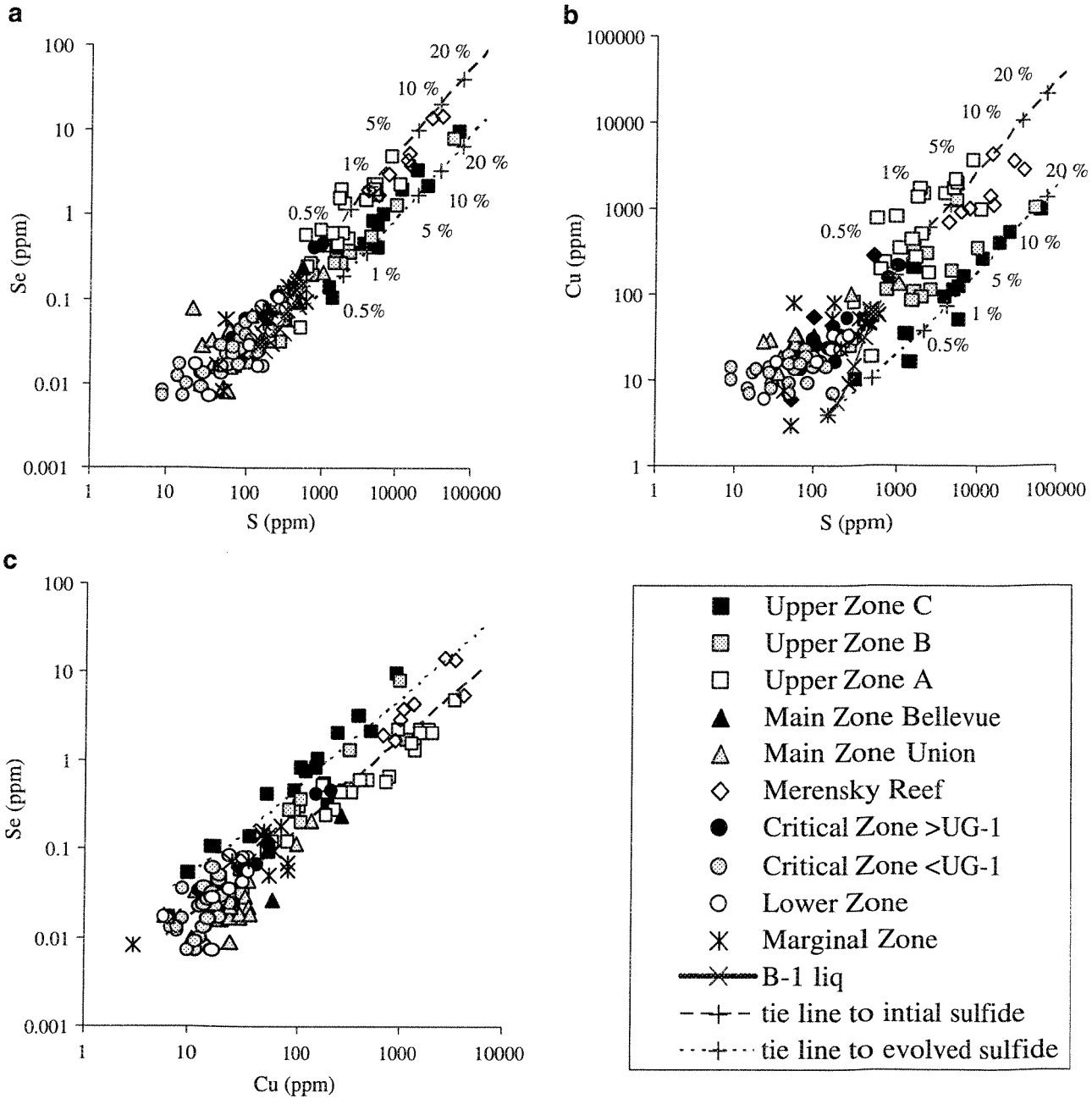

Fig. 3 Plots of **a** Se versus S **b** Cu versus S **c** Cu versus Se, showing that there are positive correlations between these elements. The *heavy dashed lines* are model tie lines between the initial silicate and sulfide liquids. *Light dashed lines* are model tie lines between fractionated silicate and sulfide liquids. Samples containing more than 150 ppm S fall within the model lines indicating that the distribution of these elements can be modeled by sulfide liquid control. The % figures indicate the weight percent sulfide present

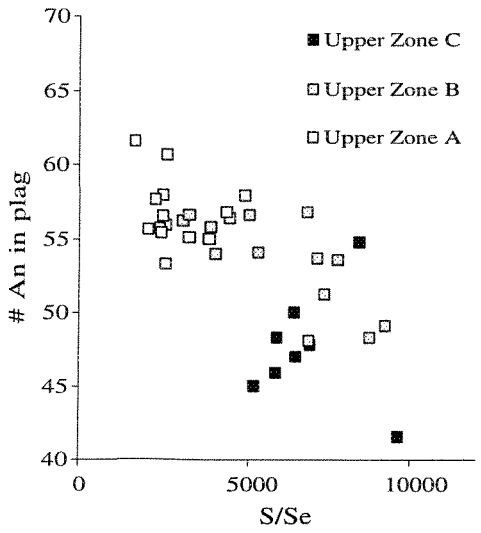

Fig. 4 Plot of S/Se ratio versus An# of the plagioclase in the Upper Zone showing a negative correlation, suggesting that the sulfides formed from fractionated magma were depleted in Se

is possible that the addition of the xenoliths led to saturation of the magma in sulfide liquid, via addition of S, changing the magma composition and raising the fO_2. If the country rock had a slightly lower Cu/Se ratio than the Upper Zone magma, the contaminated magma could have a lower Cu/Se ratio and thus the sulfide liquid that segregated from it would also have a lower Cu/Se ratio. However, we do not believe that this is the correct interpretation as the roof country rocks in the Bellevue area are granitic (Ashwal et al. 2005). They contain very little Cu or Se and thus would not be expected to contribute significant amounts of S, Cu or Se to the magma.

Samples containing less than 800 ppm S

As mentioned in the Introduction, some authors (e.g. Cawthorn 1999) suggest that there is insufficient S and Cu in the Lower and most of the Critical Zone samples for cumulate sulfides to be present. In order to consider how much S should be present in the Lower and Critical Zone samples, the amounts of S present in the model cumulates of the B-1 liquid have been calculated for two cases, the instantaneous cumulate and the average cumulate (Fig. 5b). The concentration in the instantaneous cumulate is calculated as

$$S_{ic} = 330000 * W_{isul}/W_{ic}$$

S_{ic}=S in ppm in the instantaneous cumulate, 330,000= concentration of S expressed in ppm in the sulfide liquid, W_{isul}=the weight percent sulfide liquid segregated in this 20° C interval, W_{ic}=the weight percent of all the cumulate phases that crystallized in this 20°C interval.

The S concentration in the average cumulate after X percent crystallization is calculated as

$$S_{ac} = 330000 * W_{asul}/W_{ac}$$

where S_{ac}=the S content in the average cumulate, W_{asul}=the weight percent sulfide segregated after X percent crystallization, W_{ac}=the weight percent of all cumulate phase that have crystallized after X percent crystallization of the magma.

The instantaneous cumulate assumes that after the cumulate phases form they separate perfectly from the silicate liquid and all the phases remain together. In this case, the amount of S in the cumulate is zero until sulfide saturation occurs. It is highest (~2,400 ppm) just after the silicate liquid becomes saturated in a sulfide liquid and falls off to ~500 ppm once plagioclase comes on the liquidus (Fig. 5b). It is probably unrealistic to assume that the various phases remain together in cotectic proportions. They could be separated by gravity and the sulfide liquid could migrate. Possibly, the average cumulate represents a more realistic model of the cumulates. The average cumulate also contains no S until sulfide saturation. After saturation, the S content increases to approximately 800 ppm when plagioclase comes on the liquidus and then falls to approximately 700 ppm (Fig. 5b).

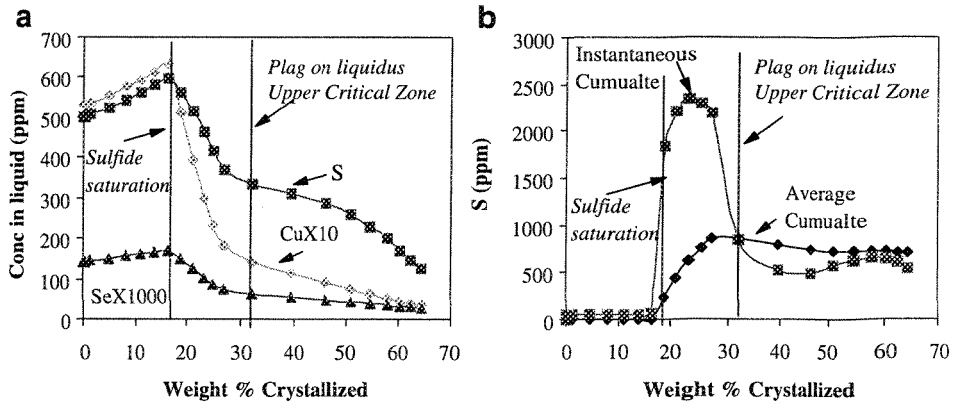

Fig. 5 Plot of weight percent crystallization versus **a** S, Se and Cu content of the liquid, note the fall in the concentration of these elements after sulfide saturation; **b** S concentration of the instantaneous and average cumulate, note the rise in S concentration after sulfide saturation

Plagioclase first becomes a cumulate phase in the upper Critical Zone of the Complex, a few 100 m below the PGE reefs. If the Lower Zone and lower Critical Zone rocks were saturated in a sulfide liquid, then the model requires that the average amount of S in these rocks should be greater than 800 ppm. In fact, on average, the Lower Zone and lower Critical Zone samples contain only 99 ppm suggesting that cumulate sulfides are not present.

On S versus Se and S versus Cu plots, most of the samples containing <800 ppm S plot along the extension of the trend defined by the samples with cumulate sulfides (Fig. 3a and b). These trends could be interpreted to support the model that cumulate sulfide was present in these rocks despite the very low levels of S. However, surprisingly, the accumulation of cumulate sulfide would not radically change the S/Se or S/Cu ratio of a rock. This is because essentially all of the S, Se and Cu partition into the sulfide liquid, thus preserving the ratios observed in the silicate liquid. It could be argued that the correlation of the chalcophile elements in rocks with <800 ppm simply reflects their presence in the trapped liquid component as suggested by Willmore et al. (2000), who based their conclusion on a moderate correlation between Cu and P.

This idea may be tested by considering the chalcophile element to incompatible lithophile element ratios. If both the chalcophile elements and the incompatible elements are present in the trapped liquid fraction, then the S and Se to incompatible element ratios should be similar to that of the magma. La was selected as the incompatible element because it is the incompatible element which has been determined with the greatest precision in most samples. Plots of La versus Se and S (Fig. 6a and b) show that most of the samples with <800 ppm have Se/La and S/La ratios greater than either the B1 or B2/3 magmas suggesting that these samples contain cumulate sulfides despite having <800 ppm S. Plots of S and Se to Zr show similar results.

Discussion

The distribution of Se in most samples from the Upper Zone and from the Merensky and Bastard Units can largely be interpreted by segregation of a sulfide liquid that collected Se and Cu. In the case of the Merensky and Bastard Units, this sulfide liquid also collected PGE. It is notable that the samples from the Merensky Reef unit have S/Se ratios in the 2,000 to 4,000 range and thus do not appear to have lost appreciable amounts of S. In most of the Upper Zone, the concentrations of PGE are very low, thus the sulfide liquid did not collect PGE. Barnes et al. (2004) argued that this is because the Upper Zone magma has been depleted in PGE by the segregation of a PGE-rich sulfide liquid that formed the reefs.

Most samples from the Lower and lower Critical Zone are enriched in PGE and have S/La and Se/La ratios greater than the Bushveld magmas suggesting that some cumulate sulfides were present in these rocks. However, all of the Lower and lower Critical Zone rocks have much less S than model cumulates formed from a B-1 magma saturated in sulfides. This creates an intriguing problem of why these samples have S contents less than model cumulates but more than can be accommodated by the trapped liquid fraction.

We suggest three possible models. In the first model (Fig. 7), the magma was not sulfide saturated when it was emplaced. The magma was emplaced and crystallized silicates and oxides (Fig. 7a). The magma attained sulfide saturation after approximately 17% crystallization and the metals and Se partitioned into the sulfide liquid and collected on the cumulate pile (Fig. 7b). During subsequent magma injections, the sulfide liquid migrated downwards through the cumulate pile along dilatencies as previously proposed for the Merensky Reef (Barnes and Maier 2002a,b; Godel et al. 2006). The dilatencies may have opened up during

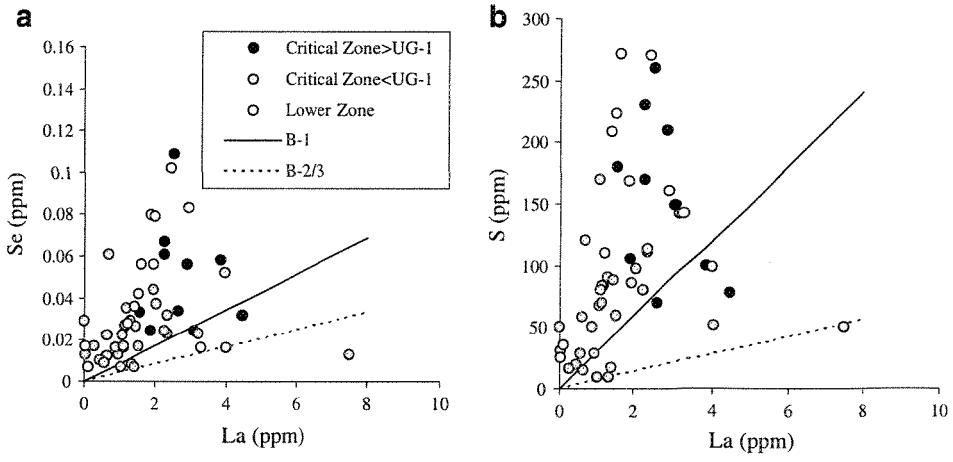

Fig. 6 Plots of S and Se versus La for rocks containing less than 800 ppm S. For most samples, the S/La or Se/La ratios are greater than that of the silicate magma (*solid lines*), suggesting that despite their low S and Se values they contain cumulate sulfide

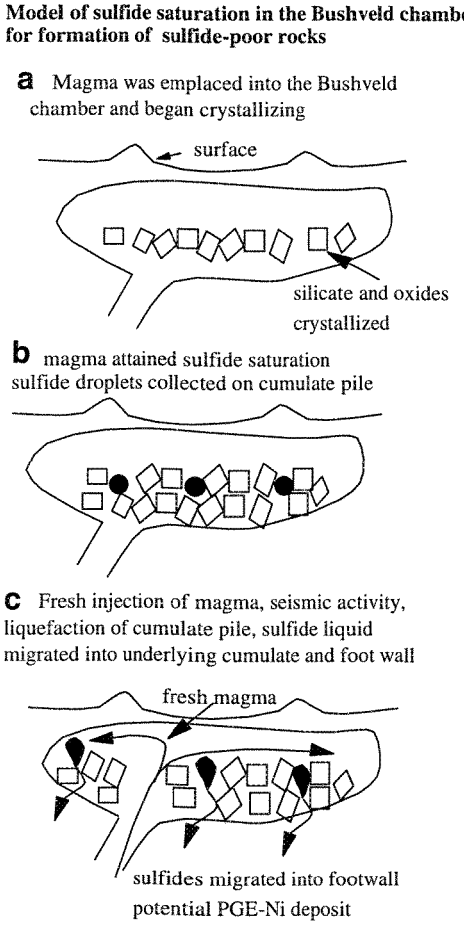

Fig. 7 Model for forming the S-poor PGE-bearing rocks assuming sulfide saturation was attained in the Bushveld magma chamber. Note the leakage of sulfide liquid into the footwall leading to a potential for sulfide mineralization in the footwall

seismic activity associated with each new injection of magma and this seismic activity caused liquefaction of the cumulate pile (Fig. 7c). The migration of the sulfide liquid could result in most of the Lower and Critical Zone rocks having less than model proportions of sulfides. The average S content of the Lower and Critical Zone rocks below the UG-1 is only 99 ppm. Assuming that the magma was saturated at 800 ppm S, this proposal requires that ~90% of the sulfide liquid has migrated away, possibly into the center of the lopolith or into footwall veins. These sulfides would make an interesting exploration target.

In the second model (Fig. 8a–b), the Bushveld magma attained sulfide saturation in a feeder chamber (Fig. 8a). Eales (2002) suggested that magma batches were periodically emplaced into the Bushveld chamber as crystal mush. We suggest that these mushes carried some sulfide droplets (Maier 2005) but the amount present was less than cotectic as some droplets settled out during transport, possibly in embayments (Fig. 8b). In this case, the embayments would represent an interesting target.

The third model suggests that initially sulfides accumulated on the Lower and Critical Zone crystal pile (Fig. 9a). It has long been argued that, during crystallization, the interstitial magma of the Lower and Critical Zone became saturated in a high temperature fluid which rose through the cumulate pile and dissolved sulfides (e.g. Willmore et al. 2000). During the dissolution of the sulfides, some PGE could have formed PGM which remained in situ, accounting for the enrichment of PGE in these zones. It also has the potential to explain the depletion of Pd relative to the other PGE in the Lower and Critical Zones. Experimental work (Peregoedova et al. 2004, 2006) has shown that, during desulfidization, Pd is preferentially partitioned into gas or liquid while the other PGE form alloys or partition into the refractory Fe-rich monosulfide solid solution. The difficulty with this argument is that on average the S/Se ratio of the Lower and lower Critical Zone rocks is close to mantle and

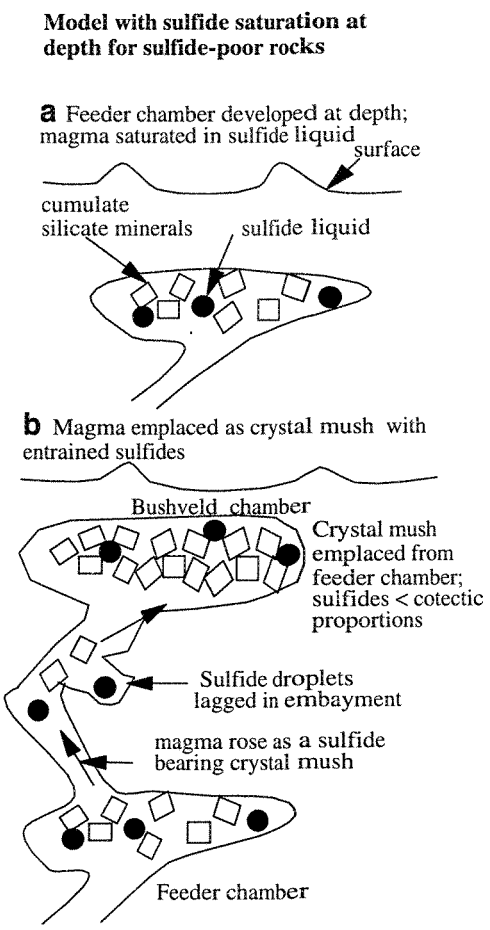

Fig. 8 Model for formation of the S-poor PGE-bearing rocks assuming sulfide saturation occurred at depth. Note the potential for sulfide mineralization in the embayments

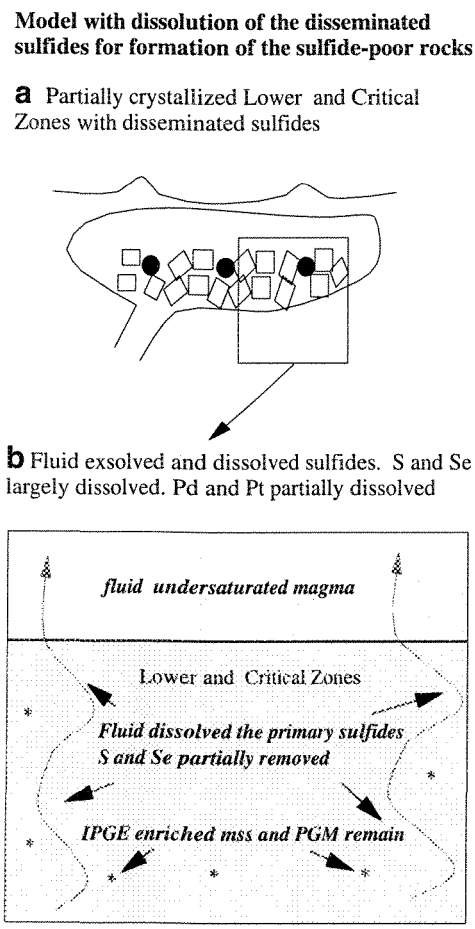

Fig. 9 Model for the formation of the S-poor PGE-bearing rocks by dissolution of S and Se by late magmatic fluid

the initial magma and thus one could suggest that appreciable S lost has not occurred as it is generally assumed that S is more mobile than Se. This premise is based on the idea that S is more readily oxidized than Se and that their mobility increases along with their oxidation state. This is supported by observations of changes in S/Se ratios in weathered rocks, e.g. Dreibus et al. (1995) found lower S/Se ratios in a meteorite affected by weathering. However, if S and Se were volatized at high temperature, then it is possible they not necessarily need to be decoupled. For example, Wulf et al. (1995) heated meteorites above ~1,050°C and found S and Se were equally depleted.

Conclusions

In the Upper Zone and the Merensky and Bastard Units, Se, Cu and S distributions can be modeled by sulfide liquid segregation. In this modeling, partition coefficients of 1,200 and 1,700 were used for Se and Cu, respectively.

Samples from the Lower Zone and Critical Zone rocks below the UG-1 contain less than cotectic proportions of sulfides. However, most of the samples have S/La and Se/La ratios greater than the magma and the samples are generally enriched in PGE. Thus, the rocks appear to contain cumulate sulfides despite their very low S content. Three possible models may be considered. The first model suggests that magma attained sulfide saturation after the emplacement in the Bushveld chamber and some crystallization. The sulfide liquid that collected on the cumulate pile then migrated into the footwall or into the center of the intrusion. The second model suggests that the Bushveld magma was saturated in sulfide liquid in a feeder chamber. The magma that filled the Bushveld chamber was a sulfide droplet-bearing crystal mush and during transport to the Bushveld chamber some sulfide droplets lagged behind in embayments leaving the mush with less than cotectic proportions of sulfides. The third model suggests that originally cumulate sulfides were present in the Lower and Critical Zone samples but both S and Se were remobilized at high temperatures.

We do not have a preferred model at present. It should be noted that the first and second model have important exploration implications as they imply that PGE-bearing sulfides could be present around the Bushveld margins or in the center of the intrusion.

Acknowledgements Jean St-Pierre and Greg Kennedy are thanked for their work at the SLOWPOKE II reactor of the École Polytechnique (Montreal). This research was financed by the Canadian Research Chair in Magmatic Metallogeny. We thank the reviewers, Dr. Steve Barnes, Prof. Ed Ripley and the editor Prof. Lehmann, for their assistance in improving the clarity of the manuscript.

References

Andersen JCO (2006) Postmagmatic sulphur loss in the Skaergaard Intrusion: implications for the formation of the Platinova Reef. Lithos 92:198–221

Ashwal LD, Webb SJ, Knoper MW (2005) Magmatic stratigraphy in the Bushveld Northern Lobe: continuous geophysical and mineralogical data from the 2950 m Bellevue drillcore. S Afr J Geol 108:199–232

Auclair G, Fouquet Y, Bohn M (1987) Distribution of Se in high-temperature hydrothermal sulfides at 13° north, East Pacific Rise. Can Min 25:577–587

Barnes S-J, Maier WD (2002a) Platinum-group element distribution in the Merensky Reef, Impala Mine, Bushveld Complex. J Petrol 43:103–128

Barnes S-J, Maier W D (2002b) Platinum-group element distributions in the Rustenberg Layered Suite of the Bushveld Complex, South Africa. In: LJ Cabri (ed) The Geology, Geochemistry, Mineralogy and Mineral Beneficiation of Platinum-Group Elements. Canadian Institute of Mining, Metallurgy and Petroleum, Special Volume 54, pp 553–580

Barnes S-J, Maier WD, Ashwal LD (2004) Platinum-group element distribution in the Main Zone and Upper Zone of the Bushveld Complex, South Africa. Chem Geol 208:293–317

Barnes S-J, Pritchard HM, Cox RA, Fisher PC, Godel B (2008) The location of the chalcophile and siderophile elements in platinum-group element ore deposits (a textural, microbeam and whole rock geochemical study): Implications for the formation of the deposits. Chem Geol 248:295–317

Bedard L P, Bernard J, Barnes S-J (2007) Searching for selenium: in situ measurement in base metal sulfides. Geochim Cosmochim Acta 71, A71 (abstr)

Bédard LP, Savard D, Barnes S-J (2008) Total sulfur concentration in geological reference materials by elemental infrared analyser. Geostand Geoanal Res 32:203–208

Boudreau AE, Meurer WP (1999) Chromatographic separation of the platinum-group elements, gold, base metals and sulfur during degassing of a compacting and solidifying igneous crystal pile. Contrib Miner Petrol 134:174–185

Campbell IH, Naldrett AJ, Barnes S-J (1983) A model for the origin of the platinum-rich sulphide horizons in the Bushveld and Stillwater Complexes. J Petrol 24:133–165

Cawthorn RG (1999) Platinum-group element mineralization in the Bushveld Complex—a critical reassessment of geochemical models. S Afr J Geol 102:268–281

Cawthorn RG (2005) Contrasting sulphide contents of the Bushveld and Sudbury Igneous Complexes. Miner Depos 40:1–12

Cawthorn RG, Street J (1994) Vertical migration of residual magma in the Upper Zone of the Bushveld Complex. Miner Petrol 51:345–354

Cawthorn RG, Davies G, Clubley-Armstrong A, McCarthy TS (1981) Sills associated with the Bushveld Complex, South Africa: an estimate of the parental magma composition. Lithos 10:1–5

Curl E A (2001) Parental magmas of the Bushveld Complex, South Africa. PhD thesis, Monash University

Davies G, Tredoux M (1985) The Platinum-group element and gold contents of the marginal rocks and sills of the Bushveld Complex. Econ Geol 80:838–848

Davies G, Cawthorn RG, Barton JM, Morton M (1980) Parental magma to the Bushveld Complex. Nat 287:33–35

Dreibus G, Palme H, Spettel B, Zipfel J, Wänke H (1995) Sulfur and selenium in chondritic meteorites. Meteorit 30:439–445

Eales HV (2002) Caveats in defining the magmas parental to the mafic rocks of the Bushveld Complex, and the manner of their emplacement: review and commentary. Miner Mag 66:815–832

Eckstrand O R, Grinenko L N, Krouse H R, Paktunc A D, Schwann P L, Scoates R F (1989) Preliminary data on sulphur isotopes and Se/S ratios, and the source of sulphur in magmatic sulphur in magmatic sulphides from the Fox River Sill, Molson Dykes and Thompson nickel deposits, northern Manitoba. In: Current Research, Part C. Geological Survey of Canada 89–1C, pp 235–242

Eriksson PG, Schweitzer JK, Bosch PJA, Schreiber UM, van Deventer JL, Hatton CJ (1993) The Transvaal sequence: an overview. J Afr Earth Sci 16:25–51

Francis RD (1990) Sulfide globules in midocean ridge basalts (MORB), and the effect of oxygen abundance in Fe–S–O liquids on the ability of those liquids to partition metals from MORB and komatiite magmas. Chem Geol 85:199–213

Gaetani GA, Grove TL (1997) Partitioning of moderately siderophile elements among olivine, silicate melt, and sulfide melt: Constraints on core formation in the Earth and Mars. Geochim Cosmochim Acta 61:1829–1846

Gain SB (1985) The geological setting of the platiniferous UG-2 chromitite layer on the farm Maandagshoek, Eastern Bushveld Complex. Econ Geol 80:925–943

Gladney ES, Knab D (1981) Determination of selenium in twenty geological reference materials by neutron activation and inorganic ion exchange. Geostand Newsl 5:67–69

Godel B, Barnes S-J (2008a) Image analysis and composition of platinum-group minerals in the J-M Reef, Stillwater Complex. Econ Geol 103:637–651

Godel B, Barnes S-J (2008b) Platinum-group elements in sulfide minerals and the whole rock of the J-M Reef (Stillwater Complex): Implication for the formation of the reef. Chem Geol 248:272–294

Godel B, Barnes S-J, Maier WD (2006) 3-D distribution of sulphide minerals in the Merensky Reef (Bushveld Complex, South Africa) and the J-M Reef (Stillwater Complex, USA) and their relationship to microstructures using X-ray computed tomography. J Petrol 47:1853–1872

Godel B, Barnes S-J, Maier WD (2007) Platinum-group elements in sulphide minerals, platinum-group minerals, and whole-rocks of the Merensky Reef (Bushveld Complex, South Africa): Implication for the formation of the Reef. J Petrol 48:1569–1604

Govindaraju K (1994) 1994 compilation of working values and sample description for 383 geostandards. Geostand Newsl 18:1–158

Guo J, Griffin WL, O'Reilly SY (1999) Geochemistry and origin of sulphide minerals in mantle xenoliths; Qilin, southeastern China. J Petrol 40:1125–1149

Hall GEM, MacLaurin AI, Pelchat JC, Gauthier G (1997) Comparison of the techniques of atomic absorption spectrometry and inductively coupled plasma mass spectrometry in the determination of Bi, Se and Te by hydride generation. Chem Geol 137:79–89

Harmer RE, Sharpe MR (1985) Field relations and strontium isotope systematics of the marginal rocks of the eastern Bushveld Complex. Econ Geol 80:813–837

Harmer R E, Armstrong R A (2000) Duration of Bushveld Complex (sensu lato) magmatism: constraints from new SHRIMP zircon chronology. Abstracts and program, Workshop on the Bushveld Complex, Gethane Lodge, Burgersfort, South Africa

Harney DMW, Merkle RKW, Von Gruenewaldt G (1990) Platinum-group element behavior in the lower part of the Upper Zone, Eastern Bushveld Complex—implications for the formation of the Main Magnetite Layer. Econ Geol 85:1777–1789

Hattori KH, Arai S, Clarke DB (2002) Selenium, tellurium, arsenic and antimony contents of primary mantle sulfides. Can Miner 40:637–650

Hiemstra SA (1979) The role of collectors in the formation of the platinum deposits of the Bushveld Complex. Can Miner 17:469–482

Holzheid A, Lodders K (2001) Solubility of copper in silicate melts as function of oxygen and sulfur fugacities, temperature, and silicate composition. Geochim Cosmochim Acta 65:1933–1951

Kruger FJ (1994) The Sr-isotropic stratigraphy of the western Bushveld Complex. S Afr J Geol 97:393–398

Li CS, Ripley EM (2005) Empirical equations to predict the sulfur content of mafic magmas at sulfide saturation and applications to magmatic sulfide deposits. Miner Dep 40:218–230

Lorand JP, Alard O, Luguet A, Keays RR (2003) Sulfur and selenium systematics of the subcontinental lithospheric mantle: inferences from the Massif Central xenolith suite (France). Geochim Cosmochim Acta 67:4137–4151

Maier WD (2005) Platinum-group element (PGE) deposits and occurrences: Mineralization styles, genetic concepts, and exploration criteria. J Afr Earth Sci 41:165–191

Maier WD, Barnes S-J (1998) Concentrations of rare earth elements in silicate rocks of the Lower, Critical and Main Zones of the Bushveld complex. Chem Geol 150:85–103

Maier WD, Barnes S-J (1999) Platinum-group elements in silicate rocks of the Lower, Critical and Main Zones at Union Section, Western Bushveld Complex. J Petrol 40:1647–1671

Marin L, Lhomme J, Carignan J (2001) Determination of selenium concentration in sixty five reference materials for geochemical by GFAAS after separation with thiol cotton. Geostand Newsl 25: 317–324

McDonough WF, Sun S-S (1995) The composition of the Earth. Chem Geol 120:223–253

Mitchell AA (1990) The stratigraphy, petrography and mineralogy of the Main Zone of the northwestern Bushveld Complex. S Afr J Geol 93:818–831

Naldrett AJ, Duke JM, Lightfoot PC, Thompson JFH (1984) Quantitative modeling of the segregation of magmatic sulfides—an exploration guide. Can Inst Miner Meteor Bull 77:46–57

Okai T, Terashima S, Imai N (2001) Determination of total Sulfur in thirty one geochemical reference materials using an inductively coupled plasma-atomic emission spectrometer fitted with a semiconductor photodiode detector. Geostand Geoanal Res 25: 133–136

Paktunc AD, Hulbert LJ, Harris DC (1990) Partitioning of the platinum-group and other trace elements in sulfides from the Bushveld Complex and Canadian occurrences of nickel–copper sulfides. Can Miner 28:475–488

Peach CL, Mathez EA, Keays RR (1990) Sulfide melt–silicate melt distribution coefficients for noble metals and other chalcophile elements as deduced from MORB: implication for partial melting. Geochim Cosmochim Acta 54:3379–3389

Peregoedova A, Barnes S-J, Baker DR (2004) The formation of the Pt–Ir alloys and Cu–Pd rich sulfide melts by partial desulfurization of Fe–Ni–Cu sulfides: results of experiments and implications for natural systems. Chem Geol 208:247–264

Peregoedova A, Barnes S-J, Baker DR (2006) An experimental study of mass transfer of platinum-group elements, gold, nickel and copper in sulfur-dominated vapor at magmatic temperatures. Chemical Geology 235:59–75

Ripley EM, Li C, Shin D (2002a) Paragneiss assimilation in the genesis of magmatic Ni–Cu–Co sulfide mineralization at Voisey's Bay, Labrador: delta S-34, delta C-13, and Se/S evidence. Econ Geol 97:1307–1318

Ripley EM, Brophy JG, Li C (2002b) Copper solubility in a basaltic melt and sulfide liquid/silicate melt partition coefficients of Cu and Fe. Geochim Cosmochim Acta 15:2791–2800

Savard D, Bédard LP, Barnes S-J (2006) TCF selenium preconcentration in geological materials for determination at sub-μg g^{-1} with INAA (Se/TCF-INAA). Talanta 70:566–571

Scoats JS, Friedman RM (2008) Precise age of the platiniferous Merensky reef, Bushveld Complex, South Africa, by U–Pb zircon chemical abrasion ID-TIMS technique. Econ Geol 103:465–471

Sharpe MR (1981) The chronology of magma influxes to the eastern compartment of the Bushveld Complex as exemplified by its marginal border groups. J Geol Soc 138:307–326

Sharpe MR, Hulbert LJ (1985) Ultramafic sills beneath the eastern Bushveld Complex: mobilized suspensions of early Lower Zone cumulates in a parental magma with boninitic affinities. Econ Geol 80:849–871

Steele T W, Levin J, Copelowitz I (1975) The preparation and certification of a reference sample of a precious-metal ore. NIM-Report 1696-04771, The National Institute for Metallurgy, Johannesburg

Taylor SR, McLennan SM (1985) The continental crust; its composition and evolution: an examination of the geochemical record preserved in sedimentary rocks. Blackwell, Oxford

Teigler B, Eales HV (1996) The Lower and Critical Zones of the western limb of the Bushveld Complex as intersected by the Nooitgedacht boreholes. Geol Surv S Afr Bull 111:126

Terashima S, Imai N (2000) Determination of selenium in fifty two geochemical reference materials by hydride generation atomic absorption spectrometry. Geostand Newsl 24:83–86

Thériault R, Barnes S-J (1998) Compositional variations in Cu–Ni–PGE sulfides of the Dunka Road deposit, Duluth Complex, Minnesota: the importance of combined assimilation and magmatic processes. Can Miner 36:869–886

Tredoux M, Lindsay NM, Davies G, McDonald I (1995) The fractionation of platinum-group elements in magmatic systems, with the suggestion of a novel causal mechanism. S Afr J Geol 98:157–167

Von Gruenewaldt G, Hatton CJ, Merkle RKW, Gain SB (1986) Platinum-group element–chromitite associations in the Bushveld Complex. Econ Geol 81:1067–1079

Wallace P, Carmichael ISE (1992) Sulfur in basaltic magmas. Geochim Cosmochim Acta 56:1863–1874

Willmore CC, Boudreau AE, Kruger FJ (2000) The halogen geochemistry of the Bushveld Complex, Republic of South Africa: implications for chalcophiles element distribution in the Lower and Critical Zones. J Petrol 41:1517–1539

Wilson A, Chunnet G (2006) Trace elements and platinum group element distributions and the genesis of the Merensky Reef, Western Bushveld Complex, South Africa. J Petrol 47:2369–2403

Wulf AV, Palme H, Jochum KP (1995) Fractionation of volatile elements in the early solar system: evidence from heating experiments on primitive meteorites. Planet Space Sci 43:451–468

ANNEXE B

MANUSCRIT : « TCF SELENIUM PRECONCENTRATION IN GEOLOGICAL MATERIALS FOR DETERMINATION AT SUB-μg g^{-1} WITH INAA (SE/TCF-INAA) ». SAVARD *et al.*, 2006.

Available online at www.sciencedirect.com
ScienceDirect
Talanta 70 (2006) 566–571
Talanta
www.elsevier.com/locate/talanta

TCF selenium preconcentration in geological materials for determination at sub-$\mu g\,g^{-1}$ with INAA (Se/TCF-INAA)

Dany Savard*, L. Paul Bédard, Sarah-Jane Barnes

Sciences de la Terre, Université du Québec à Chicoutimi, Chicoutimi, Que., Canada G7H 2B1

Received 14 October 2005; received in revised form 10 January 2006; accepted 11 January 2006
Available online 14 February 2006

Abstract

In geological samples, Se concentration ranges from $1 \times 10^{-9}\,g\,g^{-1}$ up to $1 \times 10^{-3}\,g\,g^{-1}$. The analytical difficulty at low concentration ($<1\,\mu g\,g^{-1}$), is one of the main reasons why the geological cycle of Se is poorly known. The analytical method that consisted of preconcentration of Se with thiol cotton fiber (TCF) followed by graphite furnace atomic absorption spectrometry (GFAAS) has been modified by finishing with instrumental neutron activation analysis (INAA). The modified technique involves sample dissolution ($HF–HNO_3–H_2O_2$) and evaporation to dryness at low temperature (55–60 °C) to avoid selenium volatilization. Se^{VI} is converted to Se^{IV} by adding 6 M HCl to the dry residuum and the solution is then heated in a covered boiling bath (95–100 °C). The solution is diluted to obtain 0.6 M HCl and then collected on TCF. The TCF is placed in a polyethylene vial for irradiation in the SLOWPOKE II reactor (Montréal) for 30 s at a neutron flux of $10^{15}\,m^{-2}\,s^{-1}$. The 162 keV peak of ^{77m}Se (half-life 17.36 s) is read for 20 s after a decay of 7 s. The amount of sample to be dissolved is controlled by two competing effects. To obtain low detection limits, a larger amount of sample should be dissolved. On the other hand, the TCF could become saturated with chalcophile elements when large sample is used. Sulfur is a good indicator of the amount of Se and chalcophile elements present. In S poor sample ($<100\,\mu g\,g^{-1}$) 3.0 g of sample was used and the L_D was $\sim 2\,ng\,g^{-1}$. In S high samples (>1.5% S) 0.05 g of sample was used and the L_D was $\sim 120\,ng\,g^{-1}$. The present work also includes suggested Se concentration for eight international geological reference materials (IGRM) that compare favorably with literature values.

Keywords: Selenium determination; Thiol cotton fiber; TCF; Geological analysis references materials; INAA; EPAA

1. Introduction

Selenium is important because it is a pathfinder element in economic geology [1]. It has similar geochemical properties to sulfur, but is slightly less mobile and less volatile. It is also an essential nutrient that becomes toxic at high concentration [2,3] thus it is an important analyte in environmental science [2–8]. Although its environmental cycle is well understood, its geological cycle is almost unknown. The reason for the poorly understood geochemical cycle is in part because precise quantification of this element is a real challenge, especially at low concentrations in geological materials ($<1\,\mu g\,g^{-1}$). Furthermore, the paucity of certified geological reference material makes calibration difficult by any method. Classical INAA analytical methods show a limit of detection too high to be useful for crustal rock analysis [9–11]. ICP-MS is suitable for Se analysis but argyles interferences are numerous and complex [12]. As the selenium abundance is usually low in geological samples, preconcentration is generally necessary, with the added advantage of reducing matrix interferences. The thiol cotton fiber (TCF) originally developed by Nishi et al. [13] for preconcentration of mercury is known today for its affinity with 19 elements [14,15]. TCF is a strong smelling white powder, notably able to collected Se^{IV} from HCl [14,16]. TCF preparation is easy, relatively stable, well known, inexpensive and has been used in some previous works [13–22]. Elements collected on TCF have been analyzed after destruction of TCF with varied instrument such as graphite-furnace atomic absorption (GFAA), ICP-MS and ICP-AES. This work presents development of a method coupling the TCF Se preconcentration with INAA (Se/TCF-INAA). INAA provides some advantages over GFAAS and ICP-MS such as eliminating the desorption step and recalibration, non-destructive, less time consuming than GFAAS and has no interference unlike ICP-MS. Results for geological reference materials AN-G, BE-N, SBC-1,

* Corresponding author. Tel.: +1 418 545 5011; fax: +1 418 545 5012.
E-mail address: ddsavard@uqac.ca (D. Savard).

0039-9140/$ – see front matter © 2006 Elsevier B.V. All rights reserved.
doi:10.1016/j.talanta.2006.01.010

UM-1, WMS-1, QLO-1, BIR-1 and JCh-1 using Se/TCF-INAA technique are compared to published values.

2. Experimental

2.1. Apparatus

1. Closable 50 ml PTFE beaker (Savilex®) is used for the digestion of the rocks samples.
2. A digestion bloc (DigiPrep Jr.; SCP Science) is used for both digestion (60 °C) and reduction steps (95 °C).
3. An adsorption installation (Fig. 1) consisting of a prefiltration 250 ml Millipore funnel (0.45 μm filter) followed by a centrifugal filter device (Pall Life Sciences Nanosep—500 μl, 0.45 μm filter) filled with 0.2 g of TCF to adsorb selenium. The output of the funnel is attached with flexible tubing to the upper part of a centrifugal filter device. The output of the centrifugal device is then attached to flexible tubing and pushed through a perforated cork stopper into an Erlenmeyer flask connected to a vacuum system. The flow rate (1–3 ml min^{-1}) is controlled with a clamp. All instruments are washed in hot aqua regia between each analysis.
4. After the adsorption step, the centrifugal filter device that contains TCF is directly placed into polyethylene capsules (12 mm diameter by 25 mm high) without homogenization, and sealed. Samples are irradiated at the SLOWPOKE II reactor (École Polytechnique, Montréal). The reactor has five internal irradiation sites with a highly reproducible neutron flux of 10^5 m^{-2} s^{-1} [23,24]. The reactor is equipped with the automatic "Rabbit" System.
5. EPAA program is used for peak interpretation of the nuclear decay spectrum [25,26].

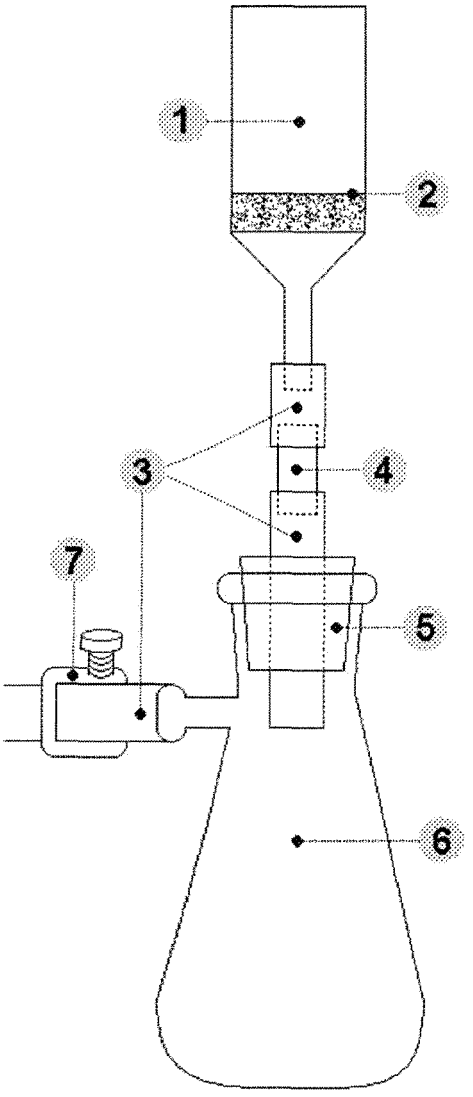

Fig. 1. Installation for the adsorption step: (1) 250 ml Millipore separation funnel; (2) 0.45 μm filter; (3) flexible tubing; (4) centrifugal device (0.45 μm) filled with 0.2 g of TCF; (5) perforated cork stopper; (6) Erlenmeyer flask; (7) flow controller clamp or valve.

2.2. Reagents

2.2.1. Acids

Technical grade hydrogen peroxide (H_2O_2), ACS grade nitric acid (HNO_3) and hydrofluorydric acid (HF) are used for digestion. ACS grade 37% (12 M) hydrochlorydric acid (HCl) is diluted with distilled water to 6.0 M for the reduction step and to 0.6 M for the preconditioning of TCF and for rinsing the instruments.

2.2.2. Standard solution

PlasmaCAL (SCP Science) 1000 μg ml^{-1} (4% HNO_3) Se standard solution diluted with distilled water was used for calibration.

2.3. Making the TCF

Although there are variation in TCF [13–22], the method used in this study is similar to Marin et al. [21]: 10 g of commercial cotton, 53 ml of thioglycollic acid (mercaptoacetic acid), 35 ml of acetic anhydride, 16.5 ml of acetic acid and 0.15 ml of sulfuric acid (H_2SO_4) (all ACS grade) were mixed in an Erlenmeyer flask and placed in a water bath (40 °C) for 4–5 days. The mixture was stirred every day. Then the treated cotton was thoroughly washed with distilled water, dried and pulverized in a domestic coffee grinder to obtain a fine, white, strong smelling powder. The TCF is kept at room temperature in a sealed dark container under vacuum to minimize risk of contamination.

2.4. Procedures

The procedure outlined below assumes that 0.25 g of sample is dissolved. As it will be discussed in Section 3, the optimal amount of sample to be used depends on how much Se and other chalcophile elements are estimated to be present in the rock. If the amount of sample used is adjusted (as described in Section 3) quantity of acids, H_2O and TCF should also be adjusted as indicated in Table 1.

Table 1
Suggested sample and acids weights vs. expected Se concentration based on sulfur content with a S:Se ratio of 3000:1

Sulfur content ($\mu g\,g^{-1}$)	Expected Se concentration range ($\mu g\,g^{-1}$)	Amount of rock sample (g)	HF (ml)	HNO_3 (ml)	H_2O_2 (ml)	HCl 6 M (ml)	Water (ml)	TCF (g)
<100	<0.03	3.0	120	60	12	120	1080	0.4
100–300	0.03–0.1	1.0	40	20	4	40	360	0.2
300–1500	0.1–0.5	0.5	20	10	2	20	180	0.2
1500–15000	0.5–5.0	0.25	10	5	1	10	90	0.2
>15000	>5.0	0.05	10	5	1	10	90	0.4

2.4.1. Digestion of the rock samples

Rock powder was weighed in a 50 ml PTFE beaker then 5 ml of HNO_3, 1 ml of H_2O_2 and 10 ml of HF were successively added to the sample. The beaker was then placed in a digestion block (60 °C) until complete evaporation of acids had occurred. For 1 and 3 g samples, 400 ml Teflon beaker and water bath were used.

2.4.2. Reduction of Se^{VI} to Se^{IV}

In order to reduce Se^{VI} to Se^{IV}, 6 M HCl is added to the dried residuum. The beaker was closed, and samples were heated in the digestion block (95 °C) for 30 min. After cooling to room temperature, the samples were transferred into 500 ml glass beakers and distilled water was added to adjust to 0.6 M HCl.

2.4.3. Pre-filtration

Solutions are pre-filtrated through a 20 μm filter to prevent the obstruction of the 0.45 μm filter mounted on the adsorption installation. The amount of suspension matter varies largely according to the nature of sample (<5% up to about 50% of the initial quantity of sample). Since Se recovery agrees with literature values (see Section 3.6), it has been interpreted that the insoluble residuum were mostly fluorides salts that contain negligible amounts of Se.

2.4.4. Preconditioning the TCF

TCF is preconditioned by passing 10 ml of 0.6 M HCl into the TCF, previously mounted in the adsorption installation. All labware are rinsed before and after the adsorption with 0.6 M HCl solution.

2.4.5. Adsorption of Se on TCF

The 0.6 M HCl solution is poured into the adsorption installation reservoir and flow is adjusted with a clamp to 1–3 ml min^{-1}. After complete filtration, in order to avoid a high background during INAA, 25 ml of distilled water is added to the reservoir in order to leach most of the chlorine absorbed on TCF. This last operation is repeated twice.

2.4.6. Analysis by INAA

The centrifugal device containing the TCF was transferred directly into the 12 mm polyethylene irradiation capsule, without homogenization, and sealed. Se/TCF-INAA does not require the desorption step as in GFAAS or ICP-MS. The TCF was sent to the reactor and irradiated for 30 s (t_i = 30 s). After a decay of 7 s (t_d = 7 s), the spectrum was read for 20 s (t_c = 20 s) on a co-planar detector. Decay peak of ^{77m}Se (161.9 keV) is analyzed with the EPAA program [25,26] to compute Se concentration.

3. Results and discussion

3.1. Calibration

Once a detector has been calibrated, it does not need to be recalibrated for each batch of sample because the neutron flux of the Slowpoke reactor is stable within 1% [23,24]; a notable advantage of INAA over GFAAS and ICP-MS. To establish the initial calibration, different samples of known concentration diluted from standard solution were sent to the reactor. In addition, one Se monitor sample (0.1–1.0 μg) was prepared and sent to the reactor for verification with each batch of sample.

3.2. Blank value

If no rock powder is added to acids, Se recovery could be erratic in some cases [17]. Therefore, a blank was created by first placing a basalt with low Se content (geological reference material BE-N, <0.1 $\mu g\,g^{-1}$ Se) in furnace at 800 °C for 48 h. This process volatilized all Se. The Se content in 3.0 g of this was then determined using the Se/TCF-INAA method. No Se was detected in this sample, indicating Se was present at less then a detection limit of 6 ng, i.e. 2 $ng\,g^{-1}$ in rock concentration equivalent.

3.3. Analytical limits

To estimate the detection limit of neutron activation, Currie's theory (1968) based on background fluctuation is generally used and as been recently modified by De Geer [27]. Three limits were originally outlined by Currie in the 1960 [28]: (1) the critical limit (L_C) defined is the signal present or not, (2) the detection limit (L_D) characterized the measurement process and indicate the sensitivity of the method, (3) the determination limits (L_Q) define the precision good enough for quantitative determination. De Geer [27] developed a model to work with multiple channel analyzer (MCA) and a simple method of limit determination using EPAA program is present here.

To formulate an appropriate L_C, all the irradiations and counting parameter (sample identification code, t_i, t_c, t_d, flux, counting position) must be fed into EPAA program, and the weight of

sample was fixed at 1 g. The chosen area of the signal must be intentionally selected as negative, i.e. background higher than peak, whether a peak is present or not. By doing this, no error from the hidden region below the peak is calculated. Negative peak selection must respect the number of channels at full-width at half maximum height of the original peak (FWHM). When no peak is present, a minimum of three channels (0.5 keV each) was selected in this work instead of a minimum representative area at FWHM. Because left and right background selection should be as wide as possible [27], a minimum of 40 channels was selected in both left and right backgrounds. The EPAA programs compute a negative concentration value and a positive error value. By multiplying the error value by a factor "k" that quantifies the risk of a false signal, the critical limit is obtained (L_C) [27]. For the present work, a 5% risk was chosen which gives a k factor of 1.645. To determine the absolute L_C for Se/TCF-INAA, an average from 56 rock samples (0.05–3.0 g) using the present analysis has been measured and the absolute L_C was estimated to be 3 ng. Consequently, absolute L_D obtained at $2L_C$ and absolute L_Q at $6L_C$ as suggested by De Geer [27] is 6 ng and 18 ng. Uncertainty at L_C and L_D is approximately 60% and 30%. A 10% uncertainty is considered reasonable for L_Q. However, the main factor that affects the absolute L_D is the INAA background fluctuation, while the weight of material used is determinant for the rock concentration equivalent L_D (see Section 3.5).

3.4. Defining EPAA relative error corresponding to limits

Since each sample has its own background fluctuation, determining a relation between EPAA error and the uncertainty is a tool to evaluate if a value is greater than L_Q. Hence, a graph has been plotted with the selenium results in ng and their respective EPAA relative errors obtained from 56 rock samples (cumulative routine analysis and values presented in this work, ranging from 8 ng to 4335 ng Se). A trend line can be draw and Eq. (1) is given as $y = 0.9533x^{-0.6194}$ with a coefficient of correlation of 99.38%. For this exercise, the same samples used to define L_C were used but this time the real peak area was selected and a Se mass (ng) and error (ng) was calculated by EPAA.

From Eq. (1), the EPAA relative errors corresponding to L_C, L_D and L_Q are ~52%, ~34% and ~17%, respectively. In the present work, all value presented respected the L_Q (<17% EPAA relative error). When using 0.25 g of sample the L_Q should be around 72 ng g^{-1}; when using 3.0 g of rock material, L_Q is down to 6 ng g^{-1} and so on: EPAA relative error and different concentration limit based on nominal weight are summarized in Table 2.

3.5. Sample weight and TCF saturation

For many geological samples 0.25 g of powder will produce acceptable Se analysis. However, in samples with low Se content, 0.25 g of sample will not contain sufficient Se to produce a detectable signal. At the other extreme, samples rich in chalcophile elements (including Se) tend to saturate the TCF and the Se is not quantitatively collected. In order to circumvent these problems, it is useful to estimate both the Se and chalcophile element content of the sample and then adjust the sample weight and, proportionally, the amounts of acids and TCF to be used. This is done by considering the S content of the sample (see Table 1).

Table 2
Specific rock equivalent limits L_C, L_D and L_Q for different sample weight based on the absolute L_C (3 ng), L_D (6 ng) and L_Q (18 ng)

Sample weight (g)	L_C (ng g^{-1}) (52%)	L_D (ng g^{-1}) (34%)	L_Q (ng g^{-1}) (17%)
0.05	60	120	360
0.25	12	24	72
0.50	6	12	36
1.00	3	6	18
3.00	1	2	6

Values in parentheses are EPAA relative error %.

Many igneous rocks have a S:Se ratio similar to mantle values of approximately 3000:1 [29,30]. Thus, the S content of the rock may be used to estimate the Se content of the sample and the weight required to produce Se content above the L_Q may be calculated. Because the S:Se ratio can vary largely, the weight used for the samples was increased by a factor of, at least, 1.67 above the absolute L_Q. Consequently, the absolute Se targets range from 30 ng to 1250 ng. Table 1 lists the suggested sample weight for a given S concentration. When the sample weight is increased from 0.25 g, the amount of acids used in the dissolution step needs to be adjusted (see Table 1).

The second point needing consideration is the amount of chalcophile elements present. Sulfur rich samples tend to be rich in chalcophile elements. Multiple elements could saturate the TCF by occupying most of thiol group sites (−SH) rendering Se adsorption on TCF partial. Yu et al. [14,15] discussed TCF saturation. We expected that TCF saturation from geological samples would be made mainly by combined effect of Co, Ni, Cu, Pb and Zn. These elements have affinity with TCF and can be quite abundant in some ores (up to 20 wt% [31]). High concentration of these elements follow sulfur content which, in most cases, reaching up to 35% in some sulfide ore [31]. A good indicator of TCF saturation is the reddish coloration of the TCF. Diminishing the nominal amount of sample to analyze down to 0.05 g combined with larger amount of TCF (0.4 g instead of 0.2 g, see Table 1) reduce risk of TCF saturation. When larger amount of TCF is used, the pre-cut GHP Nanosep MF centrifugal device is too small to contain larger amount of TCF. It can be replaced by a 1 ml pipette tip in which a small cotton ball, thoroughly rinsed with HCl 0.6 M, is used to retain TCF. When selenium content from IGRM WMS-1 was analyzed with 0.25 g of sample and 0.2 g of TCF, a strong reddish coloration of TCF then appeared and saturation was suspected. The Se content found was low (58 μg g^{-1} compared to the accepted value of 108 μg g^{-1} [32]). When the filtrated solution was passed through a second TCF, this latter also show the reddish coloration and analysis confirm the presence of selenium. When 0.4 g of TCF and 0.05 g of WMS-1 were used, saturation was not reached and the Se determined was similar to the accepted value.

Table 3
Detailed results for Se concentration in five geological reference materials analyzed with different weight fixed on the basis of their sulfur content and expected Se concentration

	Sample i.d.				
	AN-G	BE-N	SBC-1	UM-1	WMS-1
S content ($\mu g\,g^{-1}$)	150	300	6400	35000	330000
Se predicted ($\mu g\,g^{-1}$)	0.05	0.10	2.1	11.7	110
Sample weight (g)	1.00	0.50	0.25	0.05	0.05
Determination of individual Se/TCF-INAA values ($\mu g\,g^{-1}$)					
1	0.051	0.054	1.24	10.4	100
2	0.046	0.068	1.18	10.3	140
3	0.048	0.059	1.31	10.8	101
4	0.043	0.063	1.15	9.5	101
5	0.042	0.061	1.16	11.1	112
Average Se ($\mu g\,g^{-1}$)	0.046	0.061	1.21	10.4	111
σ	0.004	0.005	0.07	0.6	17
R.S.D. (%)	9	8	6	6	15
Maximum counting error (%)	<10	<13	<3	<3	<1

3.6. Detailed results for five international geological reference materials (IGRM)

Table 3 presents detailed results obtained for five geological reference materials using different weights as suggested in Table 1. The sulfur content for the SBC-1 was determined in our laboratory and the S content for the other IGRM analyzed is reported in literature [31–33]. Results in Table 3 also demonstrated the reproducibility of the method with low R.S.D. (<10%), except for sample WMS-1, which show high R.S.D. (15%) and this is mainly attributable to a single determination of $140\,\mu g\,g^{-1}$ (see Table 3). High uncertainty also appears in WMS-1 certificate of analysis [32]. This inconsistency could be attributable to "nugget effect" analog to those reported for traces elements [34]. Results are compared with literature values in Table 4.

3.7. Experiment on three IGRM with very low Se contents

To confirm the low concentration determination capacity of the Se/TCF-INAA method, a test has been undertaken on three low sulfur IGRM, thus low Se is expected. BIR-1 sulfur concentration was determined in our laboratory as $60\,\mu g\,g^{-1}$. Sulfur content is $30\,\mu g\,g^{-1}$ for QLO-1 [35] and $4\,\mu g\,g^{-1}$ for JCh-1 [31]. Using a ratio S:Se of 3000:1, selenium should be around $20.0\,ng\,g^{-1}$, $10.0\,ng\,g^{-1}$ and $1.3\,ng\,g^{-1}$ for BIR-1, QLO-1 and JCh-1, respectively. Three grams of these materials have been treated and 0.4 g of TCF was used for Se adsorption to ensure the non-saturation although this reaction was not anticipated. When using 3 g of material, L_Q should be suitable for BIR-1 and QLO-1 analysis (Table 2). For JCh-1, the expected Se ($1.3\,ng\,g^{-1}$) would be near L_D ($2\,ng\,g^{-1}$). Results are given in Table 4 and compare favorably with other literature values. However, selenium concentration found is higher than expected for all three materials (Table 4). Sulfur:selenium ratios in the igneous rocks (BIR-1 and QLO-1) are slightly lower than 3000 at ~2500 and 1500, respectively, but still within reported values for igneous rocks [36,37]. The chert (JCh-1) has a much lower S:Se ratio of 235, which is similar to other quartz rich sediments [37]. Results clearly demonstrate the possibility to quantify precisely very low Se concentration. According to L_D (Table 2) and considering that these low selenium concentrations characterize some

Table 4
Se comparison from this study and Se value from literature

Sample identification	Type (name)							
	Quartz latite (QLO-1)	Chert (JCh-1)	Basalt (BIR-1)	Anorthosite (AN-G)	Basalt (BE-N)	Shale (SBC-1)	Ultramafic (UM-1)	Ore (WMS-1)
This study								
Se	0.016	0.017	0.024	0.046	0.061	1.21	10.4	111
±[a]	0.001	0.001	0.002	0.004	0.005	0.07	0.6	17
n	1	1	1	5	5	5	5	5
Literature values [references]								
[**]	–	–	–	–	–	1.23	–	–
[9]	–	–	–	0.059 ± 0.005	0.133 ± 0.035	–	–	–
[10]	–	–	–	–	–	–	13 ± 3	–
[11]	0.01 ± 0.01	–	0.02 ± 0.01	–	–	–	–	–
[21]	<0.02	–	<0.02	0.045	0.057	–	–	–
[31]	–	–	–	0.06	–	–	–	–
[32]	–	–	–	–	–	–	–	108 ± 17
[35]	0.009–0.011	–	–	–	–	–	–	–
[36]	–	0.0068–0.050	–	–	–	–	–	–
[37]	0.009	–	0.018	–	–	–	13	–
[38]	–	–	–	0.042–0.088	0.063–0.133	–	–	–
[39]	–	–	–	0.041 ± 0.002	0.056 ± 0.004	–	–	–
[40]	–	–	0.016&0.020	–	–	–	–	–

All Se values are given in $\mu g\,g^{-1}$ and uncertainty from literature (±) is given at one standard deviation. [**] S. Wilson (USGS), personal communication.
[a] Given at one standard deviation for multiple analysis ($n > 1$) and INAA counting error of single analysis ($n = 1$).

of the lowest geological material, sample weight from 0.05 g to 1.00 g should be suitable for the Se determination in most type of geological material.

4. Conclusion

Literature shows a paucity of information about the selenium geological cycle. Developing an efficient method for quantifying Se is a key to advance knowledge of the Se geochemical cycle. Se/TCF-INAA technique provides efficient total selenium quantification and show noticeable advantages such as less time consuming than GFAAS, lower detection limit, no major interferences compared with ICP-MS, no hazardous desorption step is required. The Se/TCF-INAA technique has a limit of detection (L_D) of 6 ng g^{-1} when using 1.0 g of geological material and is able to cover large range of Se concentration (from 0.002 μg g^{-1} up to 100 μg g^{-1}). Varying sample weight and amount of TCF give to Se/TCF-INAA technique the flexibility to: (1) diminish risk of TCF saturation, (2) respect low INAA dead time, (3) provide economically affordable results and (4) reach appropriate limit of quantitation. Selenium concentrations from eight IGRM of assorted nature are presented and show agreement with literature values.

Acknowledgements

We would like to sincerely show appreciation to Greg Kennedy and Jean St-Pierre at laboratory SLOWPOKE II (Montréal) who provided advice. Also thanks to Denis Bussières (UQAC), Stephen Wilson (USGS), Luc Marin and Jean Carignan (CRPG) for their precious help and support and Sonya Savard. This study was financed by Canadian Research Chair in Magmatic Metallogeny.

References

[1] R.D. Thériault, S.-J. Barnes, M.J. Severson, Can. J. Earth Sci. 34 (1997) 375.
[2] L. Fishbein, Selenium, in: E. Merian (Ed.), Metals and Their Compounds in the Environment, VCH, Weiheim, 1991, pp. 1153–1179.
[3] L. Wu, Ecotoxicol. Environ. Saf. 57 (2004) 257.
[4] C. Cámara, M.G. Cobo, M.A. Palacios, R. Munoz, O.F.X. Donard, Quality Assurance for Environmental Analysis, Elsevier, 1995, pp. 235–261.
[5] S.J. Fairweather-Tait, J. Anal. Chem. 363 (1999) 536.
[6] R.J. Shamberger, Sci. Total Environ. 17 (1981) 59.
[7] R.M. Olivas, O.F.X. Donard, C. Cámara, P. Quevauviller, Anal. Chim. Acta 286 (1994) 357.
[8] R.S. Ogle, A.W. Knight, Arch. Environ. Contam. Toxicol. 30 (1996) 274.
[9] G. Meyer, Analusis (special ed.) 9–10 (Suppl. 16) (1988) 65.
[10] M.D. Hannington, M.P. Gorton, Geostand. Newslett. 15 (1991) 145.
[11] E.S. Gladney, D. Knab, Geostand. Newslett. 5 (1981) 67.
[12] A.T. Townsend, Anal. Chem. 364 (1999) 521.
[13] S. Nishi, Y. Horimoto, R. Kobayashi, International Symposium of Identification and Measurement of Environmental Pollutants, NRCC, Ottawa, 1971, pp. 202–206.
[14] M. Yu, D. Sun, W. Tian, G. Wang, W. Shen, N. Xu, Anal. Chim. Acta 456 (2002) 147.
[15] M. Yu, G.-Q. Liu, Anal. Chim. Acta 428 (2001) 209.
[16] S. Xiao-Quan, H. Kai-Jing, Talanta 32 (1985) 23.
[17] L. Marin, J. Lhomme, J. Carignan, Talanta 61 (2003) 119.
[18] M.-Q. Yu, G.-Q. Liu, Q. Jin, Talanta 30 (1983) 265.
[19] M. Yu, D. Sun, R. Huang, W. Tian, W. Shen, H. Zhang, N. Xu, Anal. Chim. Acta 479 (2003) 225.
[20] L.-Q. Xu, P. Schramel, Anal. Bioanal. Chem. 342 (1992) 179.
[21] L. Marin, J. Lhomme, J. Carignan, Geostand. Newslett. 25 (2001) 317.
[22] O. Rouxel, J. Ludden, J. Carignan, L. Marin, Y. Fouquet, Geochim. Cosmochim. Acta 66 (2002) 3191.
[23] D.E. Ryan, D.C. Stuart, A. Chattopadhyay, Anal. Chim. Acta 100 (1978) 87.
[24] C. Bergerioux, G. Kennedy, L. Zikovsky, J. Radioanal. Chem. 50 (1979) 229.
[25] G. Kennedy, J. St-Pierre, J. Radioanal. Nuclear Chem. 169 (1993) 471.
[26] G. Kennedy, EPAA Instruction Manual Version 2.20, École Polytechnique, Montréal, 2003 (non-published technical document).
[27] L.-E. De Geer, J. Appl. Radiat. Isotop. 61 (2004) 151.
[28] L.A. Currie, Anal. Chem. 40 (1968) 586.
[29] W.F. McDonough, Encyclopedia of Geochemistry, Kluwer Academic Publishers, Dordrecht, 1998, pp. 151–159.
[30] W.F. McDonough, S.-S. Sun, Chem. Geol. 120 (1995) 223.
[31] K. Govindaraju, Geostand. Newslett. 18 (1994) 1 (special issue).
[32] CCRMP, WMS-1 Certified of Analysis, CANMET (NRCan), 2004.
[33] G.H. Faye, Certified and Provisional Reference Materials Available from the Canada Centre of Mineral and Energy Technology as of 1975, Energy, Mines and Resources, Canada, Ottawa, 1975, p. 38.
[34] P.J. Potts, A Handbook of Silicate Rock Analysis, Blackie Academic & Professional, London, 1987, p. 622.
[35] E.S. Gladney, I. Roelandts, Geostand. Newslett. 12 (1988) 253.
[36] N. Imai, S. Terashima, S. Itoh, A. Ando, Geostand. Newslett. 20 (2) (1996) 165.
[37] P.J. Potts, A.G. Tindle, P.C. Webb, Geochemical Reference Material Compositions, Whittles Publishing, Caithness, 1992, p. 313.
[38] K. Govindaraju, I. Roelandts, Geostand. Newslett. 17 (1993) 227.
[39] S. Terashima, N. Imai, Geostand. Newslett. 24 (2000) 83.
[40] E.S. Gladney, I. Roelandts, Geostand. Newslett. 12 (1988) 63.

ANNEXE C

MANUSCRIT : « TOTAL SULFUR CONCENTRATION IN GEOLOGICAL REFERENCE MATERIALS BY ELEMENTAL INFRARED ANALYSER ». BÉDARD *et al.*, 2008.

Vol. 32 — N° 2 06 08 p. 203–208

GEOSTANDARDS and GEOANALYTICAL RESEARCH

Total Sulfur Concentration in Geological Reference Materials by Elemental Infrared Analyser

L. Paul **Bédard***, Dany **Savard** and Sarah-Jane **Barnes**

Sciences de la Terre, Université du Québec à Chicoutimi, Chicoutimi (Qc) G7H 5Z1, Canada
* Corresponding author. e-mail: pbedard@uqac.ca

Total sulfur is an analyte for which there are few determinations published, despite the fact that it is a very important element (e.g., a major element in most ores, an important gas constituent in global warming, an active participant in acid drainage). Most geological reference materials have very poor quality sulfur results, that is with relative standard deviations (RSD) in the range of 30-50%, even for concentrations over 100 μg g^{-1} S, which compromises their use as calibrators. In order to provide modern results with low RSD, sulfur was determined in twenty-nine geological reference materials with a state-of-the-art elemental S/C analyser using metal chips (certified reference materials with a traceability link) and analytical grade sulfur for high concentration samples. Analytical parameters (sample mass, crucible degassing, calibration strategy, etc.) were optimised by testing. Our results agreed with reference material values provided by issuing bodies. Results for CCRMP SY-2 (129 ± 13 μg g^{-1} S), which has been proposed as a sulfur reference material, were in agreement with the proposed modern value of 122 ± 3.7 μg g^{-1} S.

Keywords: sulfur, infrared analyser, reference materials, CCRMP SY-2.

Le soufre total est un analyte pour lequel il existe très peu de déterminations publiées, bien que cet élément soit très important (par exemple, c'est un élément majeur de la plupart des minerais, un gaz très important dans le problème de réchauffement global et un participant actif au problème des eaux acides). La plupart des matériaux de référence certifiés ont des données sur le soufre de très mauvaise qualité, avec des écart-types relatifs (RSD) de l'ordre de 30 à 50%, même pour des concentrations supérieures à 100 μg g^{-1}, ce qui compromet leur utilisation comme calibrant. Afin de fournir des résultats assortis de très faibles RSD, le soufre a été mesuré dans vingt neuf matériaux de référence certifiés avec un analyseur S/C élémentaire de dernière génération, en utilisant des fragments de métal (matériaux de référence certifiés ayant un lien de traçabilité) et du soufre de qualité analytique pour les échantillons les plus concentrés. Les paramètres analytiques (poids de l'échantillon, dégazage du creuset, stratégie de calibration, etc.) ont été optimisés via une série de tests. Nos résultats sont en bon accord avec les valeurs données pour les matériaux de référence par leurs organismes de certification respectifs. La concentration mesurée (129 ± 13 μg g^{-1} S) pour CCRMP SY-2 qui a été proposé comme matériau de référence pour le soufre, est en accord avec la valeur actuelle de 122 ± 3.7 μg g^{-1} S.

Mots-clés : soufre, analyseur à infra rouge, matériaux de référence, CCRMP SY-2.

Received 27 May 07 — Accepted 17 Sep 07

Sulfur is a geologically important element because it is essential in understanding core/mantle separation, crust evolution, and is present in most metal mineral deposits such as copper, nickel, and the precious metals. In environmental studies, sulfur is a major component of acid mine drainage and an important constituent of volcanic gases, which have major implications for global warming. Thus, its importance in understanding geological processes is very high.

Sulfur is an analyte of relatively high concentration (μg g^{-1} to % m/m) that should be simple to determine

in geological reference materials (RM). However, although sulfur is important, very few determinations are available for geological RMs. In a recent geochemical proficiency test (Potts *et al.* 2005) only twelve out of seventy-one participating laboratories reported results for total sulfur, suggesting that the determination of this analyte is not routine in most laboratories. Furthermore, uncertainties associated with most of the common agreed, accepted or certified values are very large, i.e., 30-35%, suggesting that the quality of determinations that are available is poor. For example, the certificate for BE-N shows 300 ± 150 $\mu g\ g^{-1}$ S, RTS-1 5000 ± 1600 $\mu g\ g^{-1}$ S and SY-4 150 ± 40 $\mu g\ g^{-1}$.

This is surprising since sulfur can be determined by many analytical methods: XRF, atomic absorption spectrometry, combustion/iodometric titration, coulometry, combustion elemental analyser, UV fluorescence, etc. Potentially, it has the advantage of having results contributed by methods that should be independent of each other and so improve the robustness of common agreed values, assuming that instruments are correctly calibrated. Results presented in this contribution are from a state of the art infrared spectrometry carbon-sulfur analyser (HORIBA EMIA 220-V).

Experimental

The HORIBA EMIA 220-V is a latest generation instrument with a programmable high frequency furnace. The plate current control heated the sample in small steps (up to ten) which allowed fine control over sulfur extraction. The sample was placed in a porous crucible with accelerators (Table 1) covering the rock powder. The sample was heated in an O_2 flux by an induction furnace. Volatilised gases were oxidised (S to SO_2) and passed through glass wool in order to filter dust, followed by $Mg(ClO_4)_2$ to dry gases. Gases then flowed to the infrared detector for quantification. Some samples did not fuse entirely, but could be identified easily by the lack of an orange glow in the sample chamber, and the powdery appearance of the sample after fusion, instead of the normal dull grey metallic surface.

Calibration

Two analytical protocols were developed: one for low concentration samples (22 $\mu g\ g^{-1}$ – 10 000 $\mu g\ g^{-1}$ (1% m/m)) and the other for high concentrations (1000 $\mu g\ g^{-1}$ (0.1% m/m) - 50% m/m; sulfides obvious in hand specimen); both protocols overlap in the 1000 – 10 000 $\mu g\ g^{-1}$ (0.1-1% m/m) S range. The JSd-2 reference sample was measured using both calibrations and results agreed within uncertainties (13637 ± 3% versus 13956 ± 4%). Two different protocols were required because the amount and rate of sulfur released differed between low and high sulfur concentration samples although the detector is linear for most of the range. At very high concentrations, a small mass test portion must be used and a slower extraction rate was needed to allow gases time to both react with the O_2 flux to avoid detector saturation, and for water removal in magnesium perchlorate. In order to fully control the calibration, raw counts were extracted from the instrument and a linear calibration curve was defined using a spreadsheet, instead of using the instrument software.

A calibration curve for low concentrations was defined using steel samples (Table 2) because too few geological reference materials have certified S values and traceability links. Such combustion analyses are relatively free of matrix effects, provided carbonate samples are avoided (large amounts of CO and CO_2 released) and/or do not have high structural water contents. Traceability links to certified reference materials are listed in Table 2. The calibration curve (R^2 = 0.99939) was:

Table 1.
Analytical conditions in relation to the matrix

	Silicate rock	Sulfide-rich rock
Accelerators		
Iron	1 g	
Tungsten	2 g	
Tin	0.3 g	
Copper		2 g
Test portion		
Typical mass	0.1-0.3 g	0.05 g

Measurement conditions

Step	Plate current	Time	Plate current	Time
1	0-175 mA	5 s	0-35 mA	20 s
2	175-175 mA	60 s	35-35 mA	20 s
3			50-50 mA	20 s
4			55-55 mA	20 s
5			60-60 mA	20 s
6			70-70 mA	20 s
7			70-75 mA	20 s
8			75-75 mA	20 s
9			85-85 mA	20 s
10			85-200 mA	90 s

Crucibles were heated to 1050 °C for one hour for drying and degassing; accelerators were kept in a dry and dust free area.

Table 2.
Calibration sample list for low concentration determinations and traceability

Reference material	S ($\mu g\ g^{-1}$)	Uncertainties (1s; $\mu g\ g^{-1}$)	Traceable to
LECO #501-510	1340	20	NIST SRM 129c
LECO #501-501 (lot R1030-4)	132	9	NIST SRM 344
LECO #501-501	150	7	
LECO #501-500	228	8	
JSS 155-14	62	1.68	
JSS 150-15	295	5.3	
Ar-958	270	10	NIST SRM: 8j, 14e, 73c, 343a, 367 BAM 228-1, 238-1 JSS 150-14, 155-9
Ar-950	90	10	NIST SRM: 15h, 50c, 101e, 129b, 345a, 368 BAM 079-1 JSS 155-14

Ar = Alpha Resources; BAM = Bureau of Analysed Samples; JSS = Japanese Steel Standard; NIST = National Institute of Standards and Technology.

Table 3.
Contribution from blank in sulfur determination using degassed and non-degassed crucibles (n = 10 determinations)

Material	Crucible	Test portion mass* (g)	S ($\mu g\ g^{-1}$)	s ($\mu g\ g^{-1}$)	RSD (%)
LDI-2	non-degassed	0.5	4510	103	2
LDI-2	degassed	0.5	4660	61	1
Blank	non-degassed	0.5	22	11	50
Blank	degassed	0.5	13	3	23

* Nominal mass.

$$S\ (\mu g\ g^{-1}) = (1.4585 \times -8.82349)\ (\mu g) / (\text{mass of test portion})\ (g) \quad (1)$$

for this particular run. Calibration was performed using fifty-eight calibration points, among which there were twenty-three blanks. Optimal test portion mass was determined by analysing the LDI-2 reference material (OGS) using different sample masses. At 1 g, it was quite clear that the furnace had difficulty in properly fusing the sample as most samples failed (i.e., did not fuse completely as explained in the previous paragraph). At 0.5 g, the number of samples that did not fuse was still large. Reproducibility statistics improved marginally at masses lower than 1 g (RSD was 6% at 1 g and 4% at 0.1–0.5 g). Care had to be taken to avoid using very low test portion masses and so lose representivity. Therefore, typically a test portion of 0.1–0.3 g was used. The instrument did not seem too sensitive to test portion mass within this range (for low sulfur concentration samples).

Another potential variable that it was important to evaluate was the degassing of crucibles. Crucibles can contribute to the blank value because of minute amounts of sulfur within the crucible material or adsorbed on the crucible surface. In order to remove sulfur, crucibles were heated in a muffled furnace at 1050 °C for one hour. Tests (Table 3) showed that the contribution to the blank of unheated crucibles and accelerators was about 22 $\mu g\ g^{-1}$ and about 13 $\mu g\ g^{-1}$ in heated crucibles. Degassing the crucibles approximately halved the relative standard deviation (RSD) of the blank on ten sample replicates and seemed to improve the RSD on unknown samples, although it is not clear that it was statistically significant (see variations in Table 3). The detection limit was 22 $\mu g\ g^{-1}$ (blank + 3s; Table 3).

The high sulfur calibration curve was undertaken using sublimated sulfur (Fisher S594-500) as the calibrator with a mass that varied between 0.0031 and 0.0243 g. This strategy was preferred to using inadequately characterised geological RMs. Metal chips could not be used for this calibration because they did not have sufficient S content to calibrate for sulfide-rich samples. The calibration curve (R^2 = 0.9995) was:

Table 4.
Sulfur results for geological reference materials

	Issuing body	UQAC ($\mu g\ g^{-1}$)	%RSD	Certificate ($\mu g\ g^{-1}$)	%RSD	Alternative values	Ref.
AL-I	GIT-IWG	59	21	85	pv		
AN-G	GIT-IWG	155	11	140	pv		
BE-N	GIT-IWG	304	8	300	pv		
BSK-1	USGS	6100	2	na		6000	W
BX-N	ARNT	115	13	na		160	O
CHR-Pt+	GIT-IWG	467	9	na			
DNC-1	USGS	538	2	na		392	G
DT-N	ARNT	114	16	na		110	O
IF-G	GIT-IWG	702	3	700	pv	724	O
JSD-2	GSJ	13956	4			13146	Go
						13300	I
OKUM	OGS	241	9	200	50		
OU-6	IAGeo	52	11	na		19–115	P
SBC-1	USGS	7440	0.4	na		6000-8000	W
SCo-1	USGS	593	6	630	14		
SDC-1	USGS	609	2	na		650	Go
SDO-1	USGS	54100	3	53500	8	53500 ± 4400	K
						49652 ± 1682	Y
SSAR-1	USGS	2980	0.1	na			
SY-2	CCRMP	129	13	110	na	122 ± 3.7	Gr
						119 ± 5	L
						115 ± 22	M
SY-3	CCRMP	529	5	500			
SU-1	CCRMP	122400	2	na		121000	F
TDB-1	CCRMP	305	1	300	na		
UM-1	CCRMP	37900	1	na		35300	F
UM-2	CCRMP	11070	0.4	9400	na		
UM-4	CCRMP	5370	1	4400	na		
UMT-1	CCRMP	2290	4	2000	na		
WGB-1	CCRMP	188	3	100–300		200	Go
WMG-1	CCRMP	35940	2	37000	5		
WMS-1	CCRMP	313200	2	330000	3	320000	Go
WPR-1	CCRMP	10520	2	9400	6	9000	Go

na = not available; pv is provisional value.
Ref.: W - S. Wilson (personal communication, 2006), O - Okai *et al.* (2001), Go - Govindaraju (1994), I - Imai *et al.* (1996), P - Potts *et al.* (2001) [range of values], K - Kane *et al.* (1990), Y - Yokose *et al.* (2005), Gr - Gros *et al.* (2005), L - Lorand *et al.* (2003), M - Michel and Villemant (2003), F - Faye *et al.* (1973)

$$S\ (\mu g\ g^{-1}) = (1.5874765 \times -7.0868737)\ (\mu g) / (\text{test portion mass})\ (g) \quad (2)$$

The detector saturated at approximately 0.03 g of sulfur. Considering that a massive sulfide has a maximum of 35 to 40% m/m S, test portions had to be kept below 0.08 g in order not to saturate the system. To stay within the optimal range of the detector, a test portion of 0.05 g was used (Table 1).

Results

Determinations were done in triplicate or more (Table 4) and samples that failed to fuse were not included. All UQAC values are within uncertainties of the values available on the certificate (Table 4 and Figure 1) although none are certified. No bias towards high or low values was observed (Figure 1). Two exceptions were WMS-1 and WPR-1, which were respectively 1% too low and 3% (relative percent) too high. Given that the S values on the respective certificates are not certified, these small differences are not considered significant. UQAC values for AL-I were lower than the certificate value, which is provisional based on six determinations that have a computed relative standard deviation of approximately 45%, which would bring it within uncertainties. For samples without S values on their certificates, BSK-1 and DT-N were in agreement with single published values (Table 4). For the samples BX-N, DNC-1 and SDC-1, the UQAC value was in disagreement with a single published value and little argument can be made at this

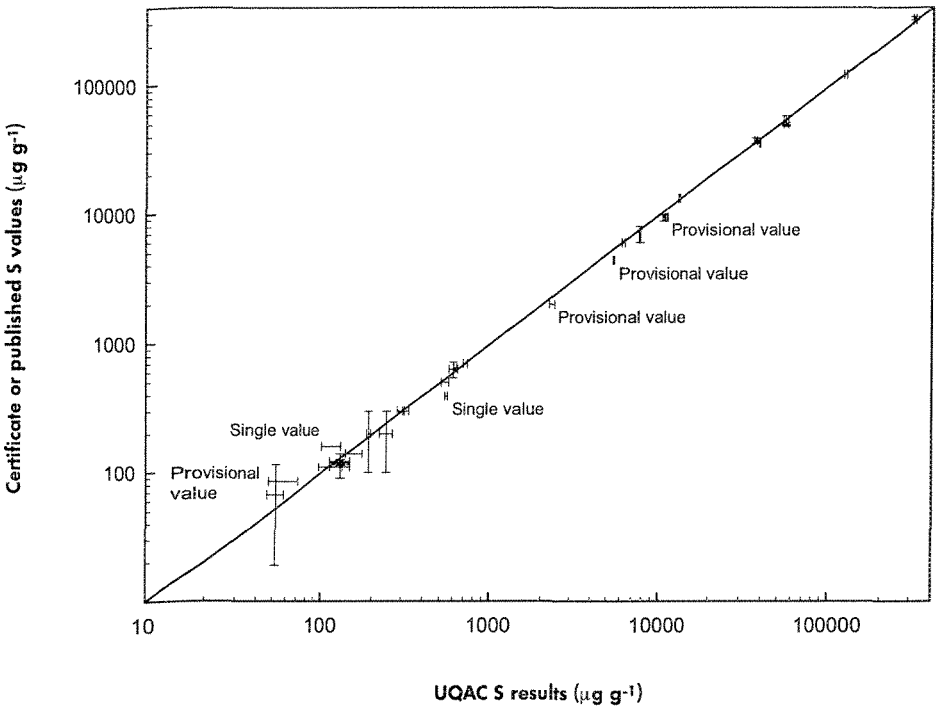

Figure 1. Graph of UQAC sulfur results plotted against certificate or published values (from Table 7) demonstrating the absence of significant bias. Error bars: standard deviation for the x-axis and uncertainty or range of value for the y-axis.

point as to which is the more reliable. JSD-2 was within 4% (including uncertainties) of the two published values (Table 4). Thus, this difference is not considered significant. The UQAC OU-6 value was within the range of those on the original certification (Potts *et al.* 2001). The SBC-1 value was within the range of published values. UM-2 and UM-4 values on the certificate are based on a single determination (Cameron 1975) and it is not clear which value is more reliable. The UQAC value for SY-2 129 ± 13 µg g^{-1} S was in closer agreement with that of Gros *et al.* (2005) (122 ± 3.7 µg g^{-1} S) and the other alternative values in Table 4 than with the certificate value of 110 µg g^{-1} S.

Conclusions

Sulfur is an analyte that needs more attention, as is demonstrated by the lack of agreement between results in proficiency testing and the large coefficient of variation on geological reference materials. New results are presented for twenty-nine geological reference materials by a technique that benefits from an established traceability link.

Acknowledgements

Christophe Morin of Horiba is thanked for his help throughout this project. Financed by the Canadian Research Chair in magmatic metallogeny of S.-J.B.

References

Cameron E.M. (1975)
Three geochemical standards of sulphide-bearing ultramafic rocks: U.M. 1, U.M. 2, U.M. 4. Geological Survey of Canada Paper 71-35, Mineral Science Laboratories (Ottawa, Canada), 15pp.

Faye G.H., Bowman W.S. and Sutarno R. (1973)
Nickel-copper-cobalt ores SU-1 and UM-1: Their characterization and preparation for use as standard reference materials. Mines Branch technical Bulletin TB 177. Mineral Science Division, Mines Branch, Department of Energy, Mines and Resources (Ottawa, Canada), 49pp.

Gladney E.S. and Roelandts I. (1990)
1988 compilation of elemental concentration data for CCRMP reference rock samples SY-2, SY-3 and MRG-1. Geostandards Newsletter, 14, 373-458.

references

Govindaraju K. (1994)
1994 compilation of working values and sample description for 383 geostandards. Geostandards Newsletter, 18 (Special Issue), 158pp.

Gros M., Lorand J.-P. and Bezos A. (2005)
Determination of total sulfur content in the international rock reference material SY-2 and other mafic and ultramafic rocks using an improved scheme of combustion/iodometric titration. Geostandards and Geoanalytical Research, 29, 123-130.

Imai N., Terashima S., Itoh S. and Ando A. (1996)
1996 compilation of analytical data on nine GSJ geochemical reference samples, sedimentary rock series. Geostandards Newsletter, 20, 165-216.

Kane J.S., Arbogast B. and Leventhal J. (1990)
Characterization of Devonian Ohio Shale SDO-1 as a USGS geochemical reference sample. Geostandards Newsletter, 14, 169-196.

Lorand J.-P., Alard O., Luguet A. and Keays R.R. (2003)
Sulphur and selenium systematics of the subcontinental lithospheric mantle: Inferences from the Massif Central xenolith suite (France). Geochimica et Cosmochimica Acta, 67, 4137-4151.

Michel A. and Villemant B. (2003)
Determination of halogens (F, Cl, Br, I) sulfur and water in seventeen geological reference materials. Geostandards Newsletter: The Journal of Geostandards and Geoanalysis, 27, 163-171.

Okai T., Terashima S. and Imai N. (2001)
Determination of total sulfur in thirty one geochemical reference materials using an inductively coupled plasma-atomic emission spectrometer fitted with a semiconductor photodiode detector. Geostandards Newsletter: The Journal of Geostandards and Geoanalysis, 25, 133-136.

Potts P.J., Thompson M., Webb P.C. and Watson J.S. (2001)
GeoPT9 - An international proficiency test of analytical geochemistry laboratories - Report on Round 9 / July 2001 (OU-6 Penrhyn slate). Report of the International Association of Geoanalysts, 33pp.

Potts P.J., Thompson M., Webb P.C. and Wilson S. (2005)
GeoPT16 - An international proficiency test for analytical geochemistry laboratories - Report on Round 16 / February 2005 (Nevada basalt BNV-1). Report of the International Association of Geoanalysts, 33pp.

Yokose H., Lipman P.W. and Kanamatsu T. (2005)
Physical and chemical properties of submarine basaltic rocks from the submarine flanks of the Hawaiian Islands. Marine Geology, 219, 173-193.

ANNEXE D

MANUSCRIT: « SELENIUM CONCENTRATIONS IN TWENTY-SIX GEOLOGICAL REFERENCE MATERIALS: NEW DETERMINATIONS AND PROPOSED VALUES ». SAVARD *ET AL.*, 2009.

Vol. 33 — N° 2 06 09 p. 249–259

GEOSTANDARDS and GEOANALYTICAL RESEARCH

Selenium Concentrations in Twenty-Six Geological Reference Materials: New Determinations and Proposed Values

Dany **Savard***, L. Paul **Bédard** and Sarah-Jane **Barnes**

Sciences de la Terre, Université du Québec à Chicoutimi, 555 boul. Université, Chicoutimi, Québec, Canada G7H 2B1

* Corresponding author. e-mail: ddsavard@uqac.ca

The interest in selenium concentrations in whole rocks is growing, in part because it is a useful tool for base and precious metal exploration. Selenium is often neglected in whole rock geochemistry because of the inability of most laboratories to make reliable determinations of this element. A consequence of these difficulties is a paucity of assigned or certified values for Se in international geological reference materials, so that the "best practice" proposed by Kane and Potts (2007) to obtain robust values for such reference materials cannot be followed. In order to address this problem, we have determined Se by pre-concentration on thiol-cotton fibre followed by INAA (Se/TCF-INAA technique) in twenty-six international geological reference materials, and one quality control material (KPT-1). These values were used, in conjunction with a set of published values, to estimate Se concentrations for these twenty-seven reference samples. Robust statistics were developed for seven of the RMs, with standard deviations equal to or less than precisions calculated using the Horwitz function and so that consensus values could be proposed. For three of the RMs, the presence of outliers gave less robust results, and suggested values are proposed. For seventeen of the RMs, only information values are provided, because either insufficient determinations were available or because large standard deviations of the data were derived.

Keywords: selenium, thiol cotton, INAA, geological reference materials, proposed values, compilation.

Received 06 Jul 08 — Accepted 03 Feb 09

L'intérêt de déterminer la concentration du sélénium dans les roches augmente parce que cet élément est un outil pour l'exploration des métaux de bases et des métaux précieux. Le sélénium est un élément méconnu en géochimie étant donné les nombreuses difficultés à analyser cet élément. Une conséquence de ces difficultés s'exprime par le nombre restreint de matériaux de référence géologique internationaux (MRGI) présentant une teneur certifiée ou assignée. La capacité de la plupart des laboratoires à déterminer le sélénium est inadéquate ou inexistante et la "bonne pratique" telle que proposée par Kane et Potts (2007) pour obtenir des valeurs robustes ne peut être appliquée. Pour contrer ce problème, le sélénium a été déterminé par pré-concentration sur fibre de coton thiol suivi de l'analyse par activation neutronique (technique du Se/TCF-INAA) dans 26 MRGI et un étalon interne (KPT-1) pour le contrôle de la qualité. Nous avons ensuite utilisé ces résultats conjointement à ceux publiés dans la littérature pour évaluer la concentration en sélénium de ces étalons. Des statistiques fiables ont pu être développées pour 7 MRGI avec des écart-types relatifs équivalents ou mieux à ceux de la fonction d'Horwitz et des teneurs fiables (consensus) ont été proposées. Pour 3 MRGI, des résultats dispersés ont mené à des consensus moins fiables et des teneurs suggérées sont présentées. Pour 17 MRGI, un nombre insuffisant de données disponibles ou de larges écart-types ont contraint la proposition de teneurs informatives seulement.

Mots-clés : sélénium, thiol coton, INAA, matériaux de référence géologique, valeurs proposées, compilation.

Selenium has been extensively studied in environmental materials because, although potentially toxic, it is essential in the food chain. In most cases, environmental samples are relatively easy to prepare for analysis (water, organic material) compared to geological samples (silicates and sulfides). Selenium is less mobile than S, especially under oxidising and acidic conditions. Therefore, the S/Se ratio can vary with geological processes, such as weathering and alteration, metamorphism and sulfate formation, thus providing a useful tool for studying these processes (Bethke and Barton 1971, Dreibus *et al.* 1995, Thériault and Barnes 1998, Maier and Barnes 1999, Alirezaei and Cameron 2001, Hattori *et al.* 2002).

Determination of Se in geological samples is difficult because rocks are refractory and resistant to attack by acids. The aggressive techniques used to dissolve rocks can lead to loss of Se by volatilisation at quite low temperatures. In routine analytical techniques (INAA, AAS, XRF), detection limits are higher than the average crustal concentration (~ 50 ng g^{-1} Se, Taylor and McLennan 1995), and in most cases Se cannot be determined by these methods. ICP-MS has a lower detection limit but argide interferences in ICP-MS limit Se determination. The common method of determining Se in the past was hydride generation coupled to atomic absorption spectrometry, but this method appears to have fallen out of favour. Consequently, very few reference materials have certified values for Se. Reference materials with well defined Se contents are essential to facilitate the development of analytical techniques capable of the accurate determination of Se.

Best practice in obtaining values for international geological reference materials is described in Kane and Potts (2007, and references therein). The *International Association of Geoanalysts' protocol* (Kane *et al.* 2003, 2007) proposes that values for geological reference materials should be derived from determinations from at least fifteen laboratories selected by proficiency testing. However, historically, typically between only one and six laboratories have reported results for Se in the IAG's GeoPT proficiency testing scheme (e.g., Webb *et al.* 2006). In circumstances where there is limited ability of most laboratories to adequately determine Se and a limited number of matrix-matched geological reference materials, it is considered justified to use a protocol that does not represent the first choice in terms of best practice, but that will provide useable reference values. Since Se values have been published for many international geological reference materials, we have combined our values with a compilation of literature data as an alternative way of obtaining consensus values that will be useful to the geological community.

Analytical technique

The development of Se pre-concentration using the TCF technique was based on the protocols of Xiao-Quan and Kai-Jing (1985) and Marin *et al.* (2001), and was modified for determinations by INAA by Savard *et al.* (2006). In terms of trueness, INAA has the advantage of being a definitive method. Moreover, it avoids the potential loss of Se by volatilisation associated with wet analytical techniques (i.e., AAS and ICP-MS; Marin *et al.* 2001, Yu *et al.* 2002, Layton-Matthews *et al.* 2006).

The Se/TCF-INAA technique used in the present work is presented in detail in Savard *et al.* (2006) and only a short description is given here. The TCF was prepared as follows: commercial cotton (10 g), mercaptoacetic acid (53 ml), acetic anhydride (35 ml), acetic acid (16.5 ml) and sulfuric acid (0.15 ml) were mixed in a glass beaker, then heated at 40 °C for one week, thoroughly rinsed with distilled water, dried, and the residue was pulverised to a fine powder. Powdered geological material (or when appropriate glass discs that had been pulverised in an agate mortar) was weighed (0.05 g to 1.00 g depending on its expected Se content using a nominal S/Se ratio of 3000) to minimise the risk of saturation of the TCF. Powders were dissolved by mixing with $HF:HNO_3:H_2O_2$ at a ratio of 10:5:1, then heated at 60 °C and evaporated to dryness. Se^{6+} was then reduced to Se^{4+} using 6.0 mol l^{-1} HCl heated at 95 °C in closed vessels for 30 minutes. Solutions were diluted to 0.6 mol l^{-1} with distilled water then passed through TCF mounted in pipette tips at a flow rate of ~ 1 ml min^{-1} to adsorb selectively the Se. The TCF was transferred to a polypropylene capsule and sent to the École Polytechnique SLOWPOKE facility (Montréal) for irradiation. Capsules were irradiated for 30 s, at a flux of 10^{12} $m^{-2}s^{-1}$. After a decay time of 7 s, the samples were counted on a co-axial gamma ray detector for 20 s. The interpretation of spectra was undertaken with the EPAA program (Kennedy 2003). Selenium reference solutions (1000 µg g^{-1}; SCP Science, traceable to NIST SRM 3149) were used for calibration. Detection limits varied with mass of test portion taken for analysis and were equivalent to 6

Table 1.
Se results for this study

Material type	Sample ID	Se ($\mu g\ g^{-1}$)	SD (1*s*)	% RSD	n *
Anorthosite	AN-G	0.046	0.005	10.9	3
Basalt	BE-N	0.070	0.009	12.9	7
Basalt	BIR-1	0.020	0.002	10.0	2
Sediment	BSK-1	4.88	0.23	4.7	6
Bauxite	BX-N	0.174	0.010	5.7	4
Diorite	DR-N	0.100	0.011	11.0	4
Gabbro diorite	KPT-1 **	2.742	0.289	10.5	13
Sediment	MAG-1	1.013	0.080	7.9	6
Gabbro	MRG-1	0.209	0.015	7.2	11
Glass	NIST SRM 610	95.0	5.6	5.9	4
Glass	NIST SRM 612	14.8	0.7	4.7	4
Glass	NIST SRM 614	0.300	0.045	15.0	4
Komatiite	OKUM	0.110	0.035	31.8	4
Platinum ore	SARM-7	1.99	0.19	9.5	3
Shale	SBC-1	1.11	0.09	8.1	6
Shale	SCo-1	0.788	0.160	20.3	13
Shale	SDO-1	1.50	0.09	6.0	6
Shale	SGR-1b	2.93	0.22	7.5	3
Soil	Soil-5	0.357	0.076	21.3	4
River Sediment	SSAR-1	2.08	0.18	8.7	6
Serpentinite	UB-N	0.174	0.058	33.3	3
Ultramafic	UM-1	10.5	0.6	5.7	7
Ultramafic	UMT-1	3.28	0.60	18.3	4
Diabase	W-2	0.091	0.013	14.3	2
Gabbro	WGB-1	0.088	-	-	1
Gabbro	WMG-1	12.2	-	-	1
Altered peridotite	WPR-1	3.4	-	-	1

* Number of individual determinations (UQAC). ** UQAC quality control material.

ng g^{-1} of sample powder. Reproducibility was typically about 10% RSD (Savard *et al.* 2006).

Results and discussion

New Se determinations of twenty-seven reference samples by the TCF-INAA technique are presented in Table 1. Demonstration of method fitness-for-purpose was presented in Savard *et al.* (2006). Single determinations were performed on some reference materials (WGB-1, WMG-1, WPR-1) whilst samples used as quality control materials, KPT-1 and SCo-1, were analysed up to thirteen times. Replicates were not made from aliquots of one sample preparation but always from different rock powders and over a period of many months in different batches. The quality control material KPT-1 was included in every batch. Traceability was ensured by calibration using NIST SRM 3149.

Only original data are presented in the literature compilation (Table 2); results from previous literature compilations were not included to avoid repetition. When Se concentrations were determined using more than two techniques, both set of results are presented (Table 2, e.g., KPT-1 in Webb *et al.* 2006). All uncertainties from published values, when available are expressed as one standard deviation (1*s*) (no matter how these data were originally cited). Average, median, standard deviations, and the target precision using the Horwitz function (Horwitz and Albert 1995) were calculated for all samples with more than three determinations (Table 3). These statistics were computed and are reported in Table 3 for different subsets of the data as follows: (1) for all determinations (lines labelled "All"), (2) for all determinations excluding the highest value (lines labelled "High X"), (3) for all determinations excluding the lowest value (lines labelled "Low X") and (4) for all determinations excluding both the highest and the lowest values (lines labelled "H+L X"). This approach allowed an estimation of the robustness of these statistical parameters by comparing the different values computed. If the results were similar, it is considered that the result is robust. In some samples elimination of end-member outliers dramatically lowered the relative standard deviation, so that the resultant average from the reduced data set might therefore be considered closer to the true value. However, these results are considered to be less robust. The Horwitz

Table 2.
Published Se values for international geochemical reference materials

Reference material (provider)	Se ($\mu g\ g^{-1}$)	SD (1 s)	References	Analytical method †
AN-G (ANRT - CRPG)	0.041	0.002	Terashima and Imai (2000)	HG-AAS
	0.042	0.001	Chan (1985)	HG-AAS
	0.045	0.004	Marin *et al.* (2001)	TCF-GF-AAS
	0.046	0.004	Savard *et al.* (2006)	TCF-INAA
	0.046	0.005	UQAC (this study)	TCF-INAA
	0.053	-	Van der Sloot *et al.* (1982)	HG-INAA
	0.059	-	Meyer (1988)	INAA
	0.06	-	Chan and Baig (1984)	HG-AAS
	0.060	-	Certificate (proposed value)	n.a.
BE-N (ANRT - CRPG)	0.056	0.004	Terashima and Imai (2000)	HG-AAS
	0.057	0.008	Marin *et al.* (2001)	TCF-GF-AAS
	0.061	0.005	Savard *et al.* (2006)	TCF-INAA
	0.063	0.002	Van der Sloot *et al.* (1982)	HG-INAA
	0.070	0.009	UQAC (this study)	TCF-INAA
	0.070	-	Chan and Baig (1984)	HG-AAS
	0.133	-	Meyer (1988)	INAA
BIR-1 (USGS)	0.016	0.001	Van der Sloot *et al.* (1982)	HG-INAA
	0.020	0.010	Gladney and Knab (1981)	INAA
	0.020	0.002	UQAC (This Study)	TCF-INAA
	0.024	-	Savard *et al.* (2006)	TCF-INAA
BSK-1 (USGS)	4.5	0.4	S. Wilson (pers. comm. 2005)	HG-AAS
	4.88	0.23	UQAC (this study)	TCF-INAA
	5.4	-	Korotev (1996)	INAA
BX-N (ANRT - CRPG)	0.08	-	Chan and Baig (1984)	HG-AAS
	0.108	-	Erzinger and Puchelt (1980)	GF-AAS
	0.116	0.004	Terashima and Imai (2000)	HG-AAS
	0.145	0.004	Chan (1985)	HG-AAS
	0.15	0.01	Marin *et al.* (2001)	TCF-GF-AAS
	0.174	0.010	UQAC (this study)	TCF-INAA
	0.183	-	Meyer (1988)	INAA
DR-N (ANRT - CRPG)	0.08	-	Chan and Baig (1984)	HG-AAS
	0.081	-	Van der Sloot *et al.* (1982)	HG-INAA
	0.082	0.003	Terashima and Imai (2000)	HG-AAS
	0.082	0.008	Marin *et al.* (2001)	TCF-GF-AAS
	0.084	-	Erzinger and Puchelt (1980)	GF-AAS
	0.085	0.001	Chan (1985)	HG-AAS
	0.089	-	Meyer (1988)	INAA
	0.0966	0.0013	Kolmer and Raptis (1983)	HG-AAS
	0.100	0.011	UQAC (this study)	TCF-INAA
KPT-1 (UQAC)	0.6	-	Webb *et al.* (2006)	n.a.
	2	-	Webb *et al.* (2006)	n.a.
	2.26	-	Webb *et al.* (2006)	n.a.
	2.5	-	Webb *et al.* (2006)	n.a.
	2.5	-	Webb *et al.* (2006)	n.a.
	2.527	-	Webb *et al.* (2006)	n.a.
	2.7	-	Webb *et al.* (2006	n.a.
	2.742	0.289	UQAC (this study)	TCF-INAA
	2.92	-	Webb *et al.* (2006)	n.a.
	3.1	-	Webb *et al.* (2006)	n.a.
	3.36	-	Webb *et al.* (2006)	n.a.
	3.5	-	Webb *et al.* (2006)	n.a.
	3.8	-	Webb *et al.* (2006)	n.a.
	4	-	Webb *et al.* (2006)	n.a.
	5.3	-	Webb *et al.* (2006)	n.a.

Table 2 (continued).
Published Se values for international geochemical reference materials

Reference material (provider)	Se (μg g^{-1})	SD (1 s)	References	Analytical method †
MAG-1 (USGS)	0.998	0.022	Hall and Pelchat (1997)	HG-ICP-MS
	0.998	0.026	Hall *et al.* (1997)	HG-AAS
	0.998	0.020	Hall *et al.* (1997)	HG-AAS
	1.0	0.1	Wahlberg (1981)	ED-XRF
	1.0	-	Rowe and Steinnes (1977)	INAA
	1.00	-	Van der Sloot *et al.* (1982)	HG-INAA
	1	-	Baedecker *et al.* (1977)	INAA
	1.01	0.05	Marin *et al.* (2001)	TCF-GF-AAS
	1.013	0.080	UQAC (this study)	TCF-INAA
	1.015	0.008	Hall and Pelchat (1997)	HG-ICP-MS
	1.050	0.035	Hall *et al.* (1997)	ICP-MS
	1.11	-	Korotev (1996)	INAA
	1.13	0.04	Gladney and Knab (1981)	INAA
	1.160	0.013	Chan (1985)	HG-AAS
	1.17	-	Chan and Baig (1984)	HG-AAS
	1.308	0.029	Schnepfe and Flanagan (1973)	SF
MRG-1 (CCRMP)	0.19	0.02	Gladney and Knab (1981)	INAA
	0.19	0.01	Imai *et al.* (1984)	HG-AAS
	0.195	0.005	Chan (1985)	HG-AAS
	0.199	0.010	Hall and Pelchat (1997)	HG-ICP-MS
	0.200	-	Chan and Baig (1984)	HG-AAS
	0.200	0.017	Richardson *et al.* (1996)	HG-AAS
	0.209	0.015	UQAC (this study)	TCF-INAA
	0.210	0.010	Marin *et al.* (2001)	TCF-GF-AAS
NIST610 (NBS -NIST)	95.0	5.6	UQAC (this study)	TCF-INAA
	108	4.5	Benjamin *et al.* (1988)	PIXE
	110	6	Rogers *et al.* (1987)	PIXE
	110	-	Fitzpatrick *et al.* (2008)	LA-ICP-MS
	114	7	Rogers *et al.* (1987)	PIXE
	183	16	Rocholl *et al.* (1997)	PIXE
NIST612 (NBS- NIST)	14.8	0.7	UQAC (this study)	TCF-INAA
	20	-	Fitzpatrick *et al.* (2008)	LA-ICP-MS
NIST614 (NBS- NIST)	0.300	0.045	UQAC (this study)	TCF-INAA
OKUM (OGS)	0.110	0.035	UQAC (this study)	TCF-INAA
	0.139	0.005	M. Burnham (pers. comm. 2005)	HG-ICP-MS
SARM-7 (SABS)	1.41	-	Barnes and Maier (2002)	INAA
	1.99	0.19	UQAC (this study)	TCF-INAA
	2.4	-	Korotev (1996)	INAA
SBC-1 (USGS)	1.11	0.09	UQAC (this study)	TCF-INAA
	1.21	0.07	Savard *et al.* (2006)	TCF-INAA
	1.23	0.05	S. Wilson (pers. comm. 2005)	HG-AAS
SCo-1 (USGS)	0.7	-	Wahlberg (1981)	ED-XRF
	0.780	0.017	Hall *et al.* (1997)	HG-AAS
	0.788	0.160	UQAC (this study)	TCF-INAA
	0.80	0.04	Gladney and Knab (1981)	INAA
	0.82	-	Chan and Baig (1984)	HG-AAS
	0.82	-	Korotev (1996)	INAA
	0.823	0.046	Hall and Pelchat (1997)	HG-ICP-MS
	0.832	0.045	Hall *et al.* (1997)	HG-AAS
	0.839	0.028	Hall *et al.* (1997)	ICP-MS
	0.861	0.035	Hall and Pelchat (1997)	HG-ICP-MS
	0.89	0.03	Marin *et al.* (2001)	TCF-GF-AAS
	0.907	0.078	Schnepfe and Flanagan (1973)	SF
	0.930	0.000	Chan (1985)	HG-AAS
	0.983	0.068	Van der Sloot *et al.* (1982)	HG-INAA

Table 2 (continued).
Published Se values for international geochemical reference materials

Reference material (provider)	Se (μg g^{-1})	SD (1 s)	References	Analytical method †
SDO-1 (USGS)	1.50	0.08	UQAC (this study)	TCF-INAA
	1.72	-	Korotev (1996)	INAA
	1.89	0.11	Marin *et al.* (2001)	TCF-GF-AAS
	1.9-6.3	-	Certificate (range)	n.a.
SGR-1 (USGS)	2.93	0.22	UQAC (This Study, SGR-1b)	TCF-INAA
	3.25	0.21	Rowe and Steinnes (1977)	INAA
	3.3	0.2	Baedecker *et al.* (1977)	INAA
	3.377	0.184	Van der Sloot *et al.* (1982)	HG-INAA
	3.5	0.1	Gladney and Knab (1981)	INAA
	3.520	0.102	Hall *et al.* (1997)	HG-AAS
	3.6	0.15	Wahlberg (1981)	ED-XRF
	3.610	0.131	Hall and Pelchat (1997)	HG-ICP-MS
	3.652	0.120	Hall *et al.* (1997)	ICP-MS
	3.67	0.13	Marin *et al.* (2001)	TCF-GF-AAS
	3.69	0.23	Schnepfe and Flanagan (1973)	SF
	4.0	-	Korotev (1996)	INAA
	3.5	-	Certificate (recommended value)	n.a.
SOIL-5 (IAEA)	0.22	-	Van der Sloot *et al.* (1982)	HG-INAA
	0.339	-	Erzinger and Puchelt (1980)	GF-AAS
	0.357	0.076	UQAC (this study)	TCF-INAA
	1.28	0.49	Dybczynski *et al.* (1979)	INAA
	1.81	0.88	Dybczynski *et al.* (1979)	XRF
	1.3	-	Certificate (information)	n.a.
SSAR-1 (USGS)	2.08	0.18	UQAC (this study)	TCF-INAA
	2.36	0.01	S. Wilson (pers. comm. 2005)	HG-AAS
UB-N (ANRT - CRPG)	0.101	-	Erzinger and Puchelt (1980)	GF-AAS
	0.106	0.006	Kolmer and Raptis (1983)	HG-AAS
	0.110	-	Chan and Baig (1984)	HG-AAS
	0.112	0.003	Terashima and Imai (2000)	HG-AAS
	0.12	-	Van der Sloot *et al.* (1982)	HG-INAA
	0.125	0.003	Chan (1985)	HG-AAS
	0.130	0.009	Marin *et al.* (2001)	TCF-GF-AAS
	0.135	-	Meyer (1988)	INAA
	0.174	0.058	UQAC (this study)	TCF-INAA
UM-1 (CCRMP)	10.4	0.6	Savard *et al.* (2006)	TCF-INAA
	10.5	0.6	UQAC (this study)	TCF-INAA
	13.0	3.0	Hannington and Gorton (1991)	INAA
UMT-1 (CCRMP)	3.28	0.60	UQAC (this study)	TCF-INAA
	4.80	0.23	Constantin (2006)	INAA
W-2 (USGS)	0.091	0.013	UQAC (this study)	TCF-INAA
	0.10	0.02	Gladney and Knab (1981)	INAA
	0.103	0.024	Van der Sloot *et al.* (1982)	HG-INAA
WGB-1 (CCRMP)	0.088	-	UQAC (this study)	TCF-INAA
	0.1-0.8	-	Certificate (informational range)	n.a.
WMG-1 (CCRMP)	12.2	-	UQAC (this study)	TCF-INAA
	13.8	0.7	Constantin (2006)	INAA
	15.0	3.0	Certificate (provisional value)	n.a.
WPR-1 (CCRMP)	3.4	-	UQAC (this study)	TCF-INAA
	4	1	Certificate (provisional value)	n.a.

† HG = hydride generation; TCF = thiol cotton fibre; GF = graphite furnace; SF = Spectrofluorimetry.

Table 3.
Statistical treatment of data

	Data §	Se (μg g^{-1})	SD (1s)	% RSD	Median	Hwz	SD / Hwz
AN-G (n = 8)	All	0.049	0.007	14.3	0.046	0.006	1.17
	High X	0.047	0.006	12.8	0.046	0.006	1.00
	Low X	0.050	0.007	14.0	0.046	0.006	1.17
	H+L X	0.049	0.006	12.2	0.046	0.006	1.00
BE-N (n = 7)	All	0.073	0.027	37.0	0.063	0.009	3.00
	High X	0.063	0.006	9.5	0.062	0.008	0.75
	Low X	0.076	0.029	38.2	0.067	0.009	3.22
	H+L X	0.064	0.006	9.4	0.063	0.008	0.75
BIR-1 (n = 4)	All	0.020	0.003	15.0	0.020	0.003	1.00
	High X	0.019	0.002	10.5	0.020	0.003	0.67
	Low X	0.021	0.002	9.5	0.020	0.003	0.67
	H+L X	0.020	0.003	15.0	0.020	0.003	1.00
BX-N (n = 7)	All	0.137	0.037	27.0	0.145	0.015	2.47
	High X	0.129	0.034	26.4	0.131	0.014	2.43
	Low X	0.146	0.030	20.5	0.148	0.016	1.88
	H+L X	0.139	0.027	19.4	0.145	0.015	1.80
DR-N (n = 9)	All	0.087	0.007	8.0	0.085	0.010	0.70
	High X	0.085	0.005	5.9	0.084	0.010	0.50
	Low X	0.087	0.007	8.0	0.085	0.010	0.70
	H+L X	0.086	0.006	7.0	0.085	0.010	0.60
KPT-1 (n = 15)	All	2.93	1.01	34.5	2.74	0.20	5.08
	High X	2.75	0.82	29.8	2.72	0.19	4.34
	Low X	3.09	0.83	26.9	2.83	0.21	3.97
	H+L X	2.92	0.58	19.9	2.74	0.20	2.91
MAG-1 (n = 16)	All	1.060	0.091	8.6	1.012	0.084	1.08
	High X	1.043	0.064	6.1	1.010	0.083	0.77
	Low X	1.064	0.092	8.6	1.013	0.084	1.10
	H+L X	1.047	0.066	6.3	1.012	0.083	0.80
MRG-1 (n = 8)	All	0.199	0.008	4.0	0.200	0.020	0.40
	High X	0.198	0.007	3.5	0.199	0.020	0.35
	Low X	0.200	0.007	3.5	0.200	0.020	0.35
	H+L X	0.199	0.006	3.0	0.200	0.020	0.30
NIST SRM 610 (n = 6)	All	120.0	31.5	26.3	110	4.7	6.70
	High X	107.4	7.3	6.8	110	4.2	1.74
	Low X	125.0	32.5	26.0	110	4.8	6.77
	H+L X	110.5	2.5	2.3	110	4.4	0.57
SCo-1 (n = 14)	All	0.841	0.071	8.4	0.828	0.069	1.03
	High X	0.830	0.060	7.2	0.823	0.068	0.88
	Low X	0.852	0.060	7.0	0.832	0.070	0.86
	H+L X	0.841	0.047	5.6	0.828	0.069	0.68
SGR-1 (n = 12)	All	3.51	0.27	7.7	3.56	0.23	1.16
	High X	3.46	0.23	6.7	3.52	0.23	1.01
	Low X	3.56	0.21	5.9	3.60	0.24	0.89
	H+L X	3.52	0.16	4.5	3.56	0.23	0.68
Soil-5 (n = 5)	All	0.80	0.71	88.0	0.36	0.07	10.70
	High X	0.55	0.49	89.3	0.35	0.05	10.23
	Low X	0.95	0.72	76.3	0.82	0.08	9.51
	H+L X	0.66	0.54	81.4	0.36	0.06	9.59
UB-N (n = 9)	All	0.124	0.022	17.7	0.120	0.014	1.57
	High X	0.117	0.012	10.3	0.116	0.013	0.92
	Low X	0.127	0.022	17.3	0.123	0.014	1.57
	H+L X	0.120	0.011	9.2	0.120	0.013	0.85

§ = "High X" = data treatment excluding the highest value; "Low X" = data treatment excluding the lowest value; "H+L X" = data treatment excluding both the highest and the lowest values; "AVG" = average; SD = Standard deviation; "Hwz" = Target precision calculated using Horwitz function.

Table 4.
Consensus, suggested and information values, and comparison with the literature

Sample	Se (μg g^{-1})	SD (1s)	% RSD	Selected data - stat	n ‡	Se (μg g^{-1}) Govindaraju (1994)
Consensus (most robust statistics)						
AN-G (ANRT-CRPG)	0.049	0.007	14.3	All AVG +/- StdDev	8	0.06
BIR-1 (USGS)	0.020	0.003	15.0	All AVG +/- StdDev	4	< 0.018
DR-N (ANRT-CRPG)	0.087	0.007	8.0	All AVG +/- StdDev	9	n.a.
MAG-1 (USGS)	1.060	0.091	8.6	All AVG +/- StdDev	16	1.16
MRG-1 (CCRMP)	0.199	0.008	4.0	All AVG +/- StdDev	8	0.194
SCo-1 (USGS)	0.841	0.071	8.4	All AVG +/- StdDev	14	0.89
SGR-1 (USGS)	3.51	0.27	7.7	All AVG +/- StdDev	12	3.5
Suggested (less robust statistics)						
BE-N (ANRT-CRPG)	0.063	0.006	9.5	High X AVG +/- StdDev	6	n.a.
NIST SRM 610	110.5	2.5	2.3	H+L X AVG +/- StdDev	4	n.a.
UB-N (ANRT-CRPG)	0.117	0.012	10.3	High X AVG +/- StdDev	8	n.a.
Information (insufficient data or large variations)						
BSK-1 (USGS)	4.93	0.45	9.1	All AVG +/- StdDev	3	n.a.
BX-N (ARNT-CRPG)	0.137	0.037	27.0	All AVG +/- StdDev	7	n.a.
KPT-1 (UQAC)	2.92	0.58	19.9	H+L X AVG +/- StdDev	13	n.a.
NIST SRM 612	17.4	3.7	21.3	All AVG +/- StdDev	2	n.a.
NIST SRM 614	0.30	0.05	16.7	This study	1	n.a.
OKUM (OGS)	0.125	0.021	16.8	All AVG +/- StdDev	2	n.a.
SARM-7 (SABS)	1.93	0.50	25.9	All AVG +/- StdDev	3	n.a.
SBC-1 (USGS)	1.18	0.06	5.1	All AVG +/- StdDev	3	n.a.
SDO-1 (USGS)	1.70	0.20	11.8	All AVG +/- StdDev	3	n.a.
SOIL-5 (IAEA)	0.80	0.71	88.8	All AVG +/- StdDev	5	1
SSAR-1 (USGS)	2.22	0.20	9.0	All AVG +/- StdDev	2	n.a.
UM-1 (CCRMP)	10.5	0.10	1.0	All AVG +/- StdDev	3	n.a.
UMT-1 (CCRMP)	4.04	1.07	26.5	All AVG +/- StdDev	2	n.a.
W-2 (USGS)	0.098	0.006	6.1	All AVG +/- StdDev	3	n.a.
WGB-1 (CCRMP)	0.088	-	-	This study	1	n.a.
WMG-1 (CCRMP)	13.0	1.2	9.2	All AVG +/- StdDev	2	n.a.
WPR-1 (CCRMP)	3.4	-	-	This study	1	n.a.

‡ Number of values used for statistics.

function is an empirical model that can be used for estimating the target pecision in group determinations. The expected relative standard deviation (% RSD) is calculated as $2C^{(-0.1505)}$, where "C" is the concentration of the analyte expressed as a decimal fraction (Horwitz and Albert 1995). Thompson *et al.* (1996) used a slightly modified Horwitz function for pure geochemistry ($0.01\,C^{0.8495}$). The Horwitz function used in the present work provides an estimation of the standard deviation at the 1s level. When assessing the results presented in this work, if the calculated standard deviation was smaller than the Horwitz function value and the average and median were close in value, then a *consensus* value was proposed (Table 4). For samples where the standard deviation exceeded the Horwitz function, *suggested* values were proposed. Finally, for samples where less than four determinations were available, the average is provided as an *information* value. The "consensus", "suggested" and "information" terminology is designed to give an overall assessment of the degree of confidence in the respective values.

Results for the reference materials AN-G, BIR-1, DR-N, MAG-1, MRG-1, SCo-1 and SGR-1 gave average and median values that were within one standard deviation, the magnitude of which was similar to or smaller than those predicted by the Horwitz function (Table 3). Thus, for these RMs, because of the perceived robustness of the statistical data, the average and standard deviation of all values were designated *consensus* values (Table 4). For BE-N, NIST SRM 610 and UB-N, the standard deviation approached the Horwitz function when the data set was trimmed. For these RMs, the trimmed values are *suggested* values. For BX-N and KPT-1 the average and median were similar, and trimming the data set did not greatly change the results. However, since the respective standard deviations were larger than those predicted by the Horwitz function, only *information* values could be proposed. For SOIL-5,

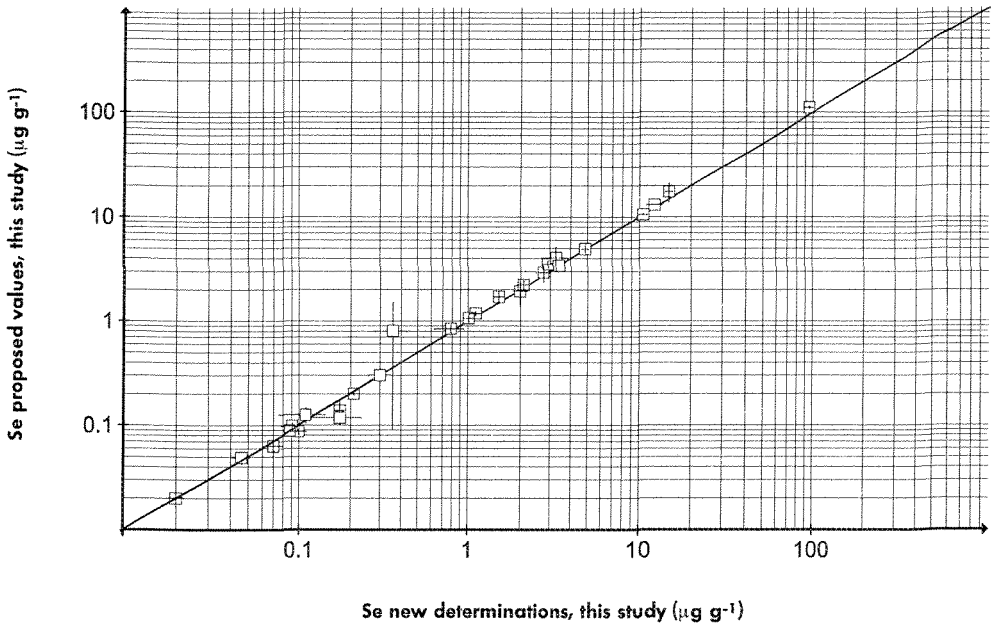

Figure 1. Comparison of new Se determinations provided in this study with proposed values (this study). Uncertainties are shown at the 1s level.

the average, median and standard deviations changed significantly if one high or low determination was trimmed from the data set. In fact, the results for this sample had a bivariant distribution and thus an information value is presented.

The new results (labelled UQAC) are in good agreement with previously published results (Table 2) as they are within one standard deviation of the *proposed* values (Figure 1). For two *consensus* values (DR-N and MRG-1, Table 4) the UQAC values were in the upper range, in agreement with recent results (Marin *et al.* 2001) and older neutron activation results (Meyer 1988) probably because Se is an analyte that is easily lost by volatilisation in many protocols that involved acid dissolution. A similar argument can be made for the UQAC results for BX-N and UB-N, which were in the upper range of results that may have been affected by Se volatilisation losses. The exception is sample SGR-1, which was determined on a different split (SGR-1b) than the original results (SGR-1). In addition, the high oil content of this petroleum- and carbonate-rich shale may have caused unforeseen analytical problems in the present study. For NIST SRM 610, the UQAC value was the lowest (but still within one standard deviation of the proposed value with its own standard deviation) but since there are so few independent determinations (n = 6, Table 2), it is unclear what is the most probable Se concentration for NIST SRM 610.

Conclusions

A capability of determining the total Se content of geological materials is useful because Se is a trace element in sulfide mineralisation, and is important in some platinum-group element mineralisation studies. Accurate characterisation of Se in international geological reference materials is essential to contribute to the development of analytical techniques for Se measurement to allow determinations of the appropriate quality to be made. It is proposed that geological reference materials of various matrices (AN-G (anorthosite), BIR-1 (basalt), DR-N (diorite), MAG-1 (sediment), MRG-1 (gabbro), SCo-1 (shale), and SGR-1 (shale)) can be used for assessing the calibration of Se and for quality control, whereas BE-N, NIST SRM 610 and UB-N should be used with caution. Additional analyses of other geological reference materials are needed in order to develop and increase our geochemical knowledge of selenium. In particular, results for sulfide and chromite-rich materials would be valuable.

Acknowledgements

Greg Kennedy and Jean St-Pierre are thanked for their help at the SLOWPOKE reactor. We would also

like to thank Marcus Burnham (OGS) and Steve Wilson (USGS) for providing their unpublished results. Julie Fredette and the anonymous reviewers are also thanked for their constructive comments. This study was financed by the Canadian Research Chair in Magmatic Metallogeny held by S.-J. Barnes.

References

Alirezaei S. and Cameron E.M. (2001)
Variations of sulphur isotopes in metamorphic rocks from Bamble Sector, southern Norway: A laser probe study. Chemical Geology, 181, 23-45.

Baedecker P.A., Rowe J.J. and Steinnes E. (1977)
Application of epithermal neutron activation in multielement analysis of silicate rocks employing both coaxial Ge(Li) and low energy photon detector systems. Journal of Radioanalytical Chemistry, 40, 115-146.

Barnes S.-J. and Maier W.D. (2002)
Platinum-group elements and microstructures of normal Merensky Reef from Impala Platinum Mines, Bushveld complex. Journal of Petrology, 43, 103-128.

Benjamin T.M., Duffy C.J. and Rodgers P.S.Z. (1988)
Geochemical utilisation of nuclear microprobes. Nuclear Instruments and Methods in Physics Research, B30, 454-458.

Bethke P.M. and Barton P.B. (1971)
Distribution of some minor elements between coexisting sulfide minerals. Economic Geology, 66, 140-163.

Chan C.C.Y. (1985)
Semi automated method for determination of selenium in geological materials using a flow injection analysis technique. Analytical Chemistry, 57, 1482-1485.

Chan C.C.Y. and Baig M.W.A. (1984)
Semi-automated method for determination of selenium in rocks. Analytical Letters, 17, 143-155.

Constantin M. (2006)
Determination of Au, Ir and thirty-two other elements in twelve geochemical reference materials by instrumental neutron activation analysis. Journal of Radioanalytical and Nuclear Chemistry, 267, 407-414.

Dreibus G., Palme H., Spettel B., Zipfel J. and Wanke H. (1995)
Sulfur and selenium in chondritic meteorites. Meteoritics, 30, 439-445.

Dybczynski R., Tugsavul A. and Suschny O. (1979)
Soil-5, a new IAEA certified reference material for trace element determinations. Geostandards Newsletter, 3, 61-87.

Erzinger J. and Puchelt H. (1980)
Determination of selenium in geological reference samples using flameless atomic absorption spectrometry. Geostandards Newsletter, 4, 13-16.

Fitzpatrick A.J., Kyser T.K., Chipley D. and Beauchemin D. (2008)
Fabrication of solid calibration standards by a sol-gel process and use in laser ablation ICPMS. Journal of Analytical Atomic Spectrometry, 23, 244-248.

Gladney E.S. and Knab D. (1981)
Determination of selenium in twenty geological reference materials by neutron activation and inorganic ion exchange. Geostandards Newsletter, 5, 67-69.

Govindaraju K. (1994)
1994 compilation of working values and sample description for 383 geostandards. Geostandards Newsletter, 18 (Special Issue), 158pp.

Hall G.E.M., MacLaurin A.I., Pelchat J.C. and Gauthier G. (1997)
Comparison of the techniques of atomic absorption spectrometry and inductively coupled plasma mass spectrometry in the determination of Bi, Se and Te by hydride generation. Chemical Geology, 137, 79-89.

Hall G.E.M. and Pelchat J.-C. (1997)
Determination of As, Bi, Sb, Se and Te in fifty five reference materials by hydride generation ICP-MS. Geostandards Newsletter: The Journal of Geostandards and Geoanalysis, 21, 85-91.

Hannington M.D. and Gorton M.P. (1991)
Analysis of sulfides for gold and associated trace metals by direct neutron activation with a low-flux reactor. Geostandards Newsletter, 15, 145-154.

Hattori K.H., Arai S. and Clarke D.B. (2002)
Selenium, tellurium, arsenic and antimony contents of primary mantle sulfides. The Canadian Mineralogist, 40, 637-650.

Horwitz W. and Albert R. (1995)
Precision in analytical measurements: Expected values and consequences in geochemical analyses. Fresenius' Journal of Analytical Chemistry, 351, 507-511.

Imai N., Terashima S. and Ando A. (1984)
Determination of selenium in twenty-eight geological reference materials by atomic absorption spectrometry. Geostandards Newsletter, 8, 39-41.

Kane J.S. and Potts P.J. (2007)
ISO best practices in reference material certification and use in geoanalysis. Geostandards and Geoanalytical Research, 31, 361-378.

Kane J.S., Potts P.J., Meisel T. and Wiedenbeck M. (2007)
International Association of Geoanalysts' protocol for the certification of geological and environmental reference materials: A supplement. Geostandards and Geoanalytical Research, 31, 285-288.

Kane J.S., Potts P.J., Wiedenbeck M., Carignan J. and Wilson S. (2003)
International Association of Geoanalysts' protocol for the certification of geological and environmental reference materials. Geostandards Newsletter The Journal of Geostandards and Geoanalysis, 27, 227-244.

references

Kennedy G. (2003)
EPAA instruction manual (version 2.20). Unpublished technical document, École Polytechnique (Montréal), 24pp.

Kolmer H.W. and Raptis S.E. (1983)
Selenium content of geochemical reference samples determined by a simple method at ng g^{-1} level. Geostandards Newsletter, 7, 315-318.

Korotev R.L. (1996)
A self-consistent compilation of elemental concentration data for 93 geochemical reference samples. Geostandards Newsletter, 20, 217-245.

Layton-Matthews D., Leybourne M.L., Peter J.M. and Scott S.D. (2006)
Determination of selenium isotopic ratios by continuous-hydride-generation dynamic-reaction-cell inductively coupled plasma-mass spectrometry. Journal of Analytical Atomic Spectrometry, 21, 41-49.

Maier W.D. and Barnes S.-J. (1999)
The origin of Cu sulfide deposits in the Curaçá Valley, Bahia, Brazil: Evidence from Cu, Ni, Se and platinum-group element concentrations. Economic Geology, 94, 165-183.

Marin L., Lhomme J. and Carignan J. (2001)
Determination of selenium concentration in sixty five reference materials for geochemical by GFAAS after separation with thiol cotton. Geostandards Newsletter: The Journal of Geostandards and Geoanalysis, 25, 317-324.

Meyer G. (1988)
Dosage non-destructif du sélénium dans les roches par activation neutronique et spectrométrie de coïncidence. Analusis, 16 (sup. to 9-10), 65-68.

Richardson J.M., Lightfoot P.C. and de Souza H. (1996)
Current geoscience laboratories geoanalytical programs and their quality assurance underpinnings. Geostandards Newsletter, 20, 141-156.

Rocholl A.B.E., Simon K., Jochum K.P., Bruhn F., Gehann R., Kramar U., Luecke W., Molzahn M., Pernicka E., Seufert M., Spettel B. and Stummeier J. (1997)
Chemical characterisation of NIST silicate glass certified reference material SRM 610 by ICP-MS, TIMS, LIMS, SSMS, INAA, AAS and PIXE. Geostandards Newsletter: The Journal of Geostandards and Geoanalysis, 21, 101-114.

Rogers P.S.Z., Duffy C.J. and Benjamin T.M. (1987)
Accuracy of standardless nuclear microprobe trace element analyses. Nuclear Instruments and Methods in Physics Research, B22, 133-137.

Rowe J.J. and Steinnes E. (1977)
Determination of 22 minor and trace elements in new USGS standard rocks by instrumental activation analysis with epithermal neutrons. Journal of Research of U.S. Geological Survey, 5, 397-402.

Savard D., Bédard L.P. and Barnes S.-J. (2006)
TCF selenium preconcentration in geological materials for determination at sub-μg g^{-1} with INAA (Se/TCF-INAA). Talanta, 70, 566-571.

Schnepfe M.M. and Flanagan F.J. (1973)
The selenium content of U.S.G.S. standard rocks. Chemical Geology, 12, 77-80.

Taylor S.R. and McLennan S.M. (1995)
The geochemical evolution of the continental crust. Reviews of Geophysics, 33, 241-265.

Terashima S. and Imai N. (2000)
Determination of selenium in fifty two geochemical reference materials by hydride generation atomic absorption spectrometry. Geostandards Newsletter, 24, 83-86.

Thériault R.D. and Barnes S.-J. (1998)
Compositional variations in Cu-Ni-PGE sulfides of the Dunka Road deposit, Duluth Complex, Minnesota: The importance of combined assimilation and magmatic processes. The Canadian Mineralogist, 36, 869-886.

Thompson M., Potts P.J. and Webb P.C. (1996)
GeoPT1. International proficiency test for analytical geochemistry laboratories - report on round 1 (July 1996). Geostandards Newsletter, 20, 295-325.

Van Der Sloot H.A., Hoede D., Klinkers TH.J.L. and Das H.A. (1982)
The determination of arsenic, selenium and antimony in rocks, sediments, fly ash and slag. Journal of Radioanalytical Chemistry, 71, 463-478.

Wahlberg J.S. (1981)
Determination of selenium at trace levels in geologic material by energy-dispersive X-ray fluorescence spectrometry. Chemical Geology, 33, 155-161.

Webb P.C., Thompson M., Potts P.J. and Bédard L.P. (2006)
GEOPT-18 - An international proficiency test for analytical geochemistry laboratories - report on round 18 / Jan 2006 (Quartz diorite, KPT-1). International Association of Geoanalysts report.

Xiao-Quan S. and Kai-Jing H. (1985)
Matrix modification for determination of selenium in geological samples by graphite-furnace atomic-absorption spectrometry after preseparation with thiol cotton fiber. Talanta, 32, 23-26.

Yu M., Sun D., Tian W., Wang G., Shen W. and Xu N. (2002)
Systematic studies on adsorption of trace elements Pt, Pd, Au, Se, Te, As, Hg, Sb on thiol cotton fiber. Analytica Acta, 456, 147-155.